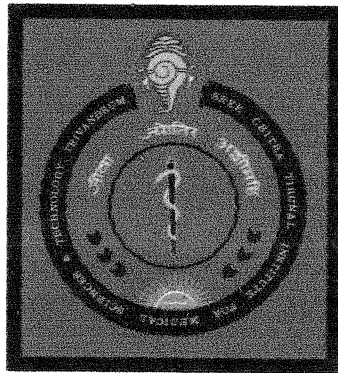


27
DMNR 0

**SREE CHITRA TIRUNAL INSTITUTE
FOR
MEDICAL SCIENCES AND TECHNOLOGY
THIRUVANANTHAPURAM**



PROJECT REPORT

NAME : SANDEEP KUMAR BURATHOKI

PROGRAMME : D.M NEUROIMAGING AND INTERVENTIONAL
NEURORADIOLOGY

**MONTH & YEAR
OF SUBMISSION :** NOVEMBER 2006



SCTIMST HOSPITAL COMPLEX LIBRARY
276
DMNR 01

**SREE CHITRA TIRUNAL INSTITUTE
FOR
MEDICAL SCIENCES AND TECHNOLOGY
THIRUVANANTHAPURAM**



PROJECT REPORT

TITLE OF THE PROJECT:

***“ENDOVASCULAR TREATMENT OF CEREBRAL AVMs :
PROSPECTIVE MR STUDY PRE AND POST EMBOLISATION”***

NAME : SANDEEP KUMAR BURATHOKI

PROGRAMME : D.M NEUROIMAGING AND INTERVENTIONAL
NEURORADIOLOGY

**MONTH & YEAR
OF SUBMISSION :** NOVEMBER 2006



CERTIFICATE

I, Dr. Sandeep Burathoki, hereby declare that I have actually carried out the project 'Endovascular Treatment of Cerebral AVMs : A Prospective MR Study Pre and Post Embolisation' independently under supervision and guidance in the institution.

Thiruvananthapuram

November 2006

Signature. 

Dr.Sandeep Burathoki

Forwarded :

Dr. Sandeep Burathoki carried out the above-mentioned project in the Department of Imaging Sciences & Interventional Radiology, SCTIMST, Thiruvananthapuram.

Signature. 

Prof.A.K.Gupta
Head of the Department of Imaging
Sciences & Interventional Radiology
(IS&IR), SCTIMST,
Thiruvananthapuram.

ACKNOWLEDGEMENTS

I am grateful to Dr. A.K. Gupta, Professor and Head of Department of Imaging Sciences and Interventional Radiology, without whom this would not have been possible. His vision and guidance at every step of the study were of great help in enabling me to complete this study. I am very much indebted to him for his help.

I sincerely thank Dr. T.R. Kapilamoorthy, Additional Professor, Dr. C. Kesavadas and Dr. Bejoy Thomas, Associate Professors, Dr. T. Krishnamoorthy and Dr. N.K. Bodhey, Assistant Professors of ISIR for their constant help, constructive criticism and encouragement during the entire study.

I also sincerely thank my colleagues Dr. Hima Pendarkar, S.Somasundaram, Dr. Raja Shaikh, Dr. Aravinda, Dr. AL.Periakaruppan and Dr. Amith Aslamkhan for their help and constant support in carrying out the study.

I am grateful to our ISIR technologists including Mr. Hari Kumar, Mr. Alex Jose, Mr. Johnson, Mrs. Geetha, Nishad, Geo, Lalitha, Munavar, Rupesh and Ambily for their wholehearted support and help to conduct this study.

I acknowledge the constant support, encouragement and love from my parents throughout the residency programme.

**ENDOVASCULAR TREATMENT OF
CEREBRAL AVMs :
A PROSPECTIVE MR STUDY PRE
AND POST EMBOLISATION**

CONTENTS

	Pages
INTRODUCTION	1
AIMS OF STUDY	4
REVIEW OF LITERATURE	5
MATERIALS AND METHODS	35
RESULTS	62
DISCUSSION	92
CONCLUSION	106
REFERENCES	107

Introduction

INTRODUCTION

Cerebral arteriovenous malformations (AVMs) are congenital lesion with a prevalence of 0.06%–0.11% and an incidence of 0.0013% – 0.01% (1-3). The AVM nidus contains high flow; low resistance transnidal arterio-venous shunts stealing blood form adjacent brain tissue causing local cerebral arterial hypotension. The altered hemodynamic in intranidal and perinidal region can be of clinical consequence and may determine endovascular or surgical out come.

AVM can affect brain function by mass effect, hemodynamic changes (e.g. Steal phenomenon, ischaemia, venous hypertension etc), irritative effect and consequences of hemorrhage. Intracranial hemorrhage and epilepsy, the most important manifestations of AVM, are seen in 52%–71% and 23%–40% of cases, respectively (4-6). The AVMs carry a risk of initial hemorrhage of ≈2% to 3% per year (68,69,70) with an associated neurological morbidity of 20% to 30% and mortality of 10% to 30% with each bleed. One of the main indications of treatment is prophylaxis of hemorrhage in future. Treatment modalities include endovascular techniques, microsurgery or stereotactic radiotherapy (focused radiation). Often multimodality therapy is being performed with an aim of eradicating an AVM.

Other symptoms, such as headache and transient ischemic attacks, have been reported (6).

Clinically, the progressive or fluctuating neurological defects that occur in 4-12% of patients with AVM are attributed partly to the steal phenomenon. Furthermore, hyperperfusion injury following AVM surgery has been attributed to normal pressure breakdown due to loss of autoregulation in the region of ischaemia secondary to steal phenomenon.

Conventional MR imaging has a very important role in determining the size and exact location of the AVMs and therefore in grading the AVMs, and in predicting the clinical outcome of the treatment. The hemodynamic alteration caused by AVMs has been studied by injected Xe-133 or Kr-85 (13,14), inhaled Xe-133 CT (15,18,19,24) or by PET (32), SPECT (17) and Doppler sonography (26,38).

MR Perfusion imaging provides a non-invasive, simple and fast objective method to study the perfusion of brain and various brain pathologies. Recently, MR perfusion is being used for studying the hemodynamic changes occurring before and after the treatment of AVMs (34,35).

This study was planned to study the hemodynamic changes induced by AVMs in immediate perinidal and remote brain parenchyma and the hemodynamic and structural changes in the AVM and adjacent brain parenchyma after embolisation.

Aims of study

AIMS OF THE STUDY

1. To study the hemodynamic alterations in the perinidal and remote brain parenchyma ipsilateral and contralateral to the cerebral AVMs.
2. To study the effect of embolisation on hemodynamics of AVM, on adjacent brain parenchyma and remote parenchyma.
3. Association of angioarchitecture with AVM obliteration after embolisation and post embolisation complication.
4. Study the long-term follow up.

Review of Literature

REVIEW OF LITERATURE

The abnormality (arteriovenous malformation) is a 'malformation' (it is not neoplastic, and therefore not an 'angioma'), the constituent vessels may be anywhere on the morphological spectrum between arteries and veins (the safest generalization being 'arteriovenous'). AVMs are tangled anastomoses of blood vessels of varying calibre in which arteriovenous shunting occurs in a central nidus (Latin *nidus*, nest), which is the area towards which multiple feeding arteries converge, and from which enlarged veins drain. Thus, AVMs of the brain are congenital cerebrovascular anomalous lesions, composed of a network of channels interposed between feeding arteries and draining veins, without any direct shunt.

In macroscopic pathology (47,48,49), brain AVMs are composed of:

- (a) Clustered and abnormally muscularised feeding arteries which may also show changes such as duplication or destruction of the elastica, fibrosis of the media, and focal thinning of the wall.
- (b) Arterialized veins of varying size and wall thickness.
- (c) Structurally ambiguous vessels formed solely of fibrous tissue or displaying both arterial and venous characteristics.

Feeding arteries:

There are usually several tortuous, branching, high flow arterial vessels of varying calibre and wall thickness that supply the central nidus where arteriovenous shunting occurs through one or more fistulae. These afferent vessels are typically recruited from more than one intracranial branch of the internal carotid and/or vertebrobasilar systems, and occasionally from branches of the external carotid or vertebral arteries through transdural anastomoses (51). The high flow, low resistance shunt of an AVM may recruit collateral supply from surrounding vascular territories, sometimes called 'angiomatic change'. Chronic high blood flow in the feeding cause stenotic and/or dilated arterial 'angiopathy' due to endothelial thickening and intimal hyperplasia (52), which may resemble the angiographic appearance of moyamoya disease (53). The arterial feeders may terminate in the nidus, continue to supply brain beyond the nidus (giving 'en passage' supply) or arise indirectly from an artery in close proximity to the nidus.

Nidus:

Nidus is the area towards which multiple feeding arteries converge and from which enlarged veins drain. The AVM nidus either can be a tumor like well circumscribed (**Compact nidus**) or can

consist of sparse, diffuse abnormal network of AV channels spread within normal brain parenchyma (**Diffuse nidus**) (46).

Draining veins

One or more dilated veins originate deep within the AVM nidus, and reach its surface acquiring tributaries along the way to drain, directly or via collateral pathways, into the superficial and/or deep venous systems. Through the loss of the normal resistance to flow in the capillary bed, the arteriovenous shunt transmits arterial pressure to the compliant venous system, causing venous hypertension. The draining veins are often anomalous due to haemodynamic stresses causing stenosis, ectasia and varix formation (54).

INDICATION FOR AVM TREATMENT:

1. The main reason to treat cerebral AVMs is the prophylaxis against spontaneous intracranial hemorrhage.
2. Symptomatic AVM, presented with hemorrhage, seizures, neurological deterioration, and severe headache.
3. Large AVMs presenting with progressive neurological deficit secondary to high flow or venous hypertension, the aim of

treatment is to reduce the flow across the AVM, with an aim to minimize or halt symptom progression.

Intracranial hemorrhage is the most common presenting symptom accounting for nearly 30 - 82 % of cases (60). Overall risk of initial hemorrhage of \approx 2% to 3% per year (62,63,64,65,66,67,68,69,70) with an associated neurological morbidity of 20% to 30% and mortality of 10% to 30% with each bleed. Ruptured AVM had a 6 % risk of rebleeding in first year after hemorrhage and 2% thereafter (71).

If one assumes an annual hemorrhage risk among people with previously unruptured AVMs of \approx 2% to 4% per year, the lifetime risk of intracranial hemorrhage in a person with an AVM is approximated by the following formula (72,73) :

Lifetime risk (%) = $105 - \text{the patient's age in years}$

The risk of recurrent hemorrhage may be even higher in the first year after the second hemorrhage and has been reported to be 25% during that year (74). Each bleeding episode is estimated to be associated with 10% mortality and 30% to 50% morbidity.

Therefore, a young person with a malformation has a substantial cumulative risk of hemorrhage and attendant morbidity

throughout the rest of his or her life and warrants a treatment for hemorrhage in future.

EPIDIOMOLOGY AND NATURAL HISTORY OF AVMs :

In order to make an educated decision regarding therapy, a thorough understanding of the natural history is needed. Treatment decisions for patients with brain arteriovenous malformations (AVMs) should be based on natural course risk estimates weighed against outcome data from invasive intervention.

The incidence and prevalence of intracranial vascular malformations are not known with certainty, although there are data available from autopsy series and limited population-based studies. Autopsy data suggest that there is an overall frequency of detection of AVMs in $\approx 4.3\%$ of the population (55,56). AVMs have an incidence of ~ 1 per 100 000 per year in unselected populations, and a point prevalence in adults of ~ 18 per 100 000 (1 in approximately every 5500 adults) (58).

AVMs account for between 1 and 2% of all strokes, but may be $\sim 4\%$ of strokes in young adults. AVMs are identified in $\sim 9\%$ of people presenting with SAH, and are the cause of $\sim 4\%$ of all primary intracerebral hematomas (PICHs), but as many as one-third of primary

intracerebral hemorrhage in young adults. AVMs are far less common causes of first presentations with unprovoked seizures (1%), and of people presenting with headaches in the absence of any neurological signs (0.3%) (50).

AVMs are typically dynamic, i.e. they undergo continuous subtle anatomic and hemodynamic changes. A cerebral AVM becomes clinically evident when host's capacity to effectively compensate has reached its threshold. Cerebral AVMs are often symptomatic in young adults, typically before the age of 40 (57).

Most common clinical presentation of brain AVM is intracranial hemorrhage with a frequency of 30-82 % (60). Hemorrhage of brain AVMs are subarachnoid hemorrhage (30%), parenchymal (23%), intraventricular (16%) and in combined locations in 31 % of cases (59). The available natural history studies indicate an overall risk of initial hemorrhage of \approx 2% to 3% per year (62,63,64,65,66,67,68,69,70) with an associated neurological morbidity of 20% to 30% and mortality of 10% to 30% with each bleed. Ruptured AVM had a 6 % risk of rebleeding in first year after hemorrhage and 2 % thereafter (71). The risk of recurrent hemorrhage may be even higher in the first year after the second hemorrhage and has been reported to be 25% during that year (74).

The next most common presentation is seizure, which occurs in 16 - 53 % of cases with a mean of 34% (60). Seizures can be either focal or generalized and may be an indicator of the location of the lesion. Cortical AVMs are more often associated with seizures. Chronic headache is the initial symptom in 7 – 48 % (mean: 31 %) of cases (60). Focal neurological deficit without hemorrhage are initial symptom in 1- 40 % of patients. The focal neurological deficit encountered in patients harboring brain AVMs may be progressive, stable, or reversible. Reversible focal neurologic defecits are questionable regarding their mechanism, since a post-ictal etiology cannot be ruled out. The progression of neurologic deficit can be due to steal phenomenon, venous hypertension, or mass effect (61).

TREATMENT OF CEREBRAL AVMs:

The lesion can be monitored expectantly with the understanding that the patient would have some risk of hemorrhage or other neurological symptoms such as seizures or focal deficit.

Alternatively, intervention can be undertaken with the goal of complete AVM obliteration, because subtotal therapy does not confer protection from hemorrhage. A multidisciplinary team composed of an Interventional Neuroradiologist, neurologist, neurosurgeon and radiotherapist should take any treatment decision.

At present, there are 4 major treatment options available for patients with an AVM of the brain :

1. Endovascular
2. Surgery
3. Stereotactic Radiotherapy
4. Combination of any of these modalities

Management strategies include single or combined therapy applying microsurgery, endovascular techniques, or stereotactic radiotherapy (focused radiation). AVMs are often treated by more than one treatment modality. Multimodality therapy should be performed with an aim of eradicating an AVM.

This occurs in one of two fashions. It is done as either a planned maneuver, typically with embolisation followed by surgical resection or radiotherapy, or as an unplanned maneuver where one treatment modality fails and a second treatment modality is necessary to obliterate the AVM. This can occur in situations such as residual AVM after subtotal surgical resection or resection of an AVM after incomplete radiotherapy.

Depending on the size, location, and angioarchitecture of the AVM, complete obliteration of the malformation requires a combined therapeutic approach.

1. AVM EMBOLISATION:

The goal of endovascular embolisation is the permanent and complete obliteration of the AVM nidus and the restoration of normal cerebral blood flow.

Current indications for embolisation are :

1. Curative embolisation:

1. Embolisation alone
2. Presurgical embolisation
3. Embolisation before Stereotactic radiotherapy

2. Palliative embolisation:

1. To reduce the flow across large AVMs (nonsurgical or nonradiosurgical AVMs) presenting with progressive neurological deficit secondary to high flow or venous hypertension with an aim to minimize or halt symptom progression.

2. Embolization of a pseudoaneurysm.

EMBOLISATION ALONE AS A CURATIVE MODALITY :

Despite that cyanoacrylate embolisation is the most effective technique for endovascular embolisation, endovascular cure of an AVM is considered unusual if not rare. Complete obliteration rates after embolization alone have been reported to be between 5 and 18% in the majority of series (75).

Valavanis and Yasargil (76) and **Yu and colleagues (77)** recently reported the highest rates of complete obliteration (40.8% in 387 patients and 60% in 10 patients, respectively) for AVMs selected for curative embolisation. Embolisation of AVMs as a sole therapeutic modality is usually only achieved in small lesions fed by no more than 4 arterial pedicles (78).

An attempt at curative embolisation is only justified in AVMs of relatively simple angioarchitecture, with endovascularly accessible feeding arteries located in deep and/or critical areas of the brain, where surgery would carry an unacceptable risk of morbidity or where the patient's associated medical comorbidities would make open surgery excessively risky.

Presurgical Embolisation :

Preoperative embolisation of AVMs has become part of the treatment for many AVMs, especially larger lesions (79,80,81,82) and this is the most important role of embolisation.

The goals of presurgical embolisation are:

1. To decrease the nidus size of the AVM,
2. To attempt to occlude deep, surgically inaccessible or deep arterial feeding vessels such as the anterior/posterior perforating vessels, choroidal vessels, or posterior cerebral vessels to facilitate surgical excision.
3. To occlude intranidal aneurysms and
4. To occlude high-flow fistulas.

Embolisation can convert high Spetzler-Martin grade lesions to lower-grade lesions and reduce blood flow to AVM nidus, and thereby diminishing blood loss, reducing surgical times and reducing surgical morbidity and mortality.

Furthermore, a progressive, staged reduction of arteriovenous shunting with endovascular embolisation may result in gradual restoration of normal cerebral perfusion and vascular reactivity,

reducing the potential for perioperative complications of brain swelling and hemorrhage (“*perfusion breakthrough*”) with very large high-flow AVMs.

The decision to perform embolisation of an AVM should take into consideration Spetzler-Martin grade as well as the combined surgical and endovascular risk for a particular patient. In general, Spetzler-Martin grade II or III lesions may be embolised before surgery or radiosurgery. Grade IV or V lesions should not be embolised unless this is to be done in conjunction with other treatment modalities (surgery or radiotherapy) for the goal of complete cure. The only exception to this may be in a patient with a grade IV or V lesion with venous outflow obstruction, in whom embolisation is used to reduce arterial inflow to control edema, or in a patient with true "steal," in whom embolisation is used to relieve the amount of shunt through the AVM.

STEREOTACTIC RADIOTHERAPY:-

Stereotactic radiotherapy has become an important treatment technique for the management of cerebral AVMs. The purpose of radiotherapy is to irradiate the blood vessels of the AVM to cause progressive luminal obliteration and thereby prevent hemorrhage. Involution of the irradiated mass is the final stage of the healing

response, as well as the final stage of inflammation (83). At that time, the AVM vessels are occluded and AVM volume is reduced. With focused radiation, the dose of radiation to brain tissue surrounding the Stereotactic radiotherapy AVM can be minimized.

Stereotactic radiotherapy is most appropriate for patients with small AVMs, especially when such AVMs are located in eloquent brain locations. Lesions most effectively treated with Stereotactic radiotherapy have volumes $<10\text{-cm}^3$ or maximum diameter $<3\text{ cm}$ (84,85,86). Endovascular therapy has 3 potential goals when used before Stereotactic radiotherapy intervention for AVMs (87, 88, 89):

1. To decrease target size to $<3\text{ cm}$ in diameter, because smaller volumes have a higher cure rate with less morbidity;
2. To eradicate angiographic predictors of hemorrhage, such as intranidal aneurysms or venous aneurysms; and
3. To attempt to reduce symptoms related to venous hypertension.

Stereotactic radiotherapy can be considered in lesions thought to be at high risk from a surgical or endovascular standpoint. The overall efficacy of Stereotactic radiotherapy is higher for small lesions, and therefore, this modality may be considered as a primary treatment for

smaller as opposed to larger lesions. However, size is not the only factor in the final determination of treatment. The exact location, patient age, symptoms, and angiographic anatomy must be considered in this decision process. For small, surgically accessible lesions (Spetzler-Martin grade I or II), surgery has fewer risks than Stereotactic radiotherapy. Stereotactic radiotherapy may be considered in larger lesions (Spetzler-Martin grade II through V) only if the overall goal is complete obliteration of the lesion. Partial treatment of a larger lesion with Stereotactic radiotherapy or embolisation subjects the patient to the risks of the procedure without eliminating the risk of hemorrhage.

Palliative Embolisation:

Regarding the issue of palliative or partial embolisation, the important question is whether partial embolisation alone alters the natural history of an AVM with reference to its risk of bleeding in the future.

Kwon et al (91) followed up on 27 patients harboring AVMs larger than 4 cm that were located in eloquent cortex (Spetzler–Martin Grade III), which were believed to be inoperable. Eleven patients underwent embolisation; following this procedure, 27.3% of the patients had deterioration in their conditions, and 45.5% experienced

hemorrhage. These results were compared with those in 16 patients who underwent medical treatment only; 31% of the patients who only received medical treatment had deterioration in their conditions, and 25% experienced hemorrhage. Similarly, a review of the Barrow Neurological Institute's experience with Grades IV and V AVMs showed a 1% annual bleeding rate in patients treated conservatively compared with a 10.4% rate in patients whose AVMs were treated partially; because of these results, clinicians at that center have recommended conservative treatment without embolisation for most Grades IV and V AVMs (90). Palliative embolisation of AVMs does not appear to improve clinical results when compared with conservative treatment of AVMs believed to be inoperable; therefore, it seems unjustified to place these patients at the significant risk of embolisation unless the latter has a reasonable chance of resulting in complete obliteration of the AVM.

Palliative embolisation may be recommended for patients who have large, inoperable cortical and subcortical AVMs and in patients presenting with seizures resistant to medical management or with progressive neurological deficit thought to be secondary to venous hypertension and/or arterial steal (92,93,94). Partial embolisation may be successful in reversing these signs and symptoms; however, it is usually only temporary, because collaterals develop rapidly, reducing

the effectiveness of such therapy. Palliative embolisation should be used as part of a strategy aimed at staged AVM obliteration, to treat a specific AVM-associated feature (eg, associated aneurysm), or to reverse a specific symptom. There is no evidence that partial AVM embolisation alters long-term hemorrhagic risk, and as such, it is not recommended as a broad treatment strategy for AVMs.

Hemodynamic of AVMs

Cerebral blood flow is directly proportional to arterial pressure and inversely proportional to cerebrovascular resistance, while cerebrovascular resistance is related to the internal diameter of the vascular bed. Local changes in vascular diameter result in exponential changes in resistance and therefore in flow.

AVMs are functionally low resistance shunt with a disproportionate flow will be directed toward the AVM nidus, bypassing the normal capillary vascular bed in brain parenchyma. Thus, AVMs can be considered as “*vascular sponge*” which consume large volume of blood, depriving the brain of normal circulation. This phenomenon has been termed as “*intracerebral steal*”.

The mechanism by which an AVM can alter CBF locally or in distant areas of the brain can be grouped into two general categories:

- 1) decreased flow reserve and
- 2) decreased flow demand.

The mechanism causing decreased flow reserve is probably due to altered perfusion gradients in higher resistance vasculature that supplies normal parenchyma. In the normal situation, cerebral arteries exhibit autoregulation and perfusion remains relatively constant despite wide changes in mean arterial pressure. The minimum mean arterial blood pressure that allows autoregulation to remain intact is approximately 50-60 mm Hg (20). The normal brain parenchyma surrounding the brain AVM is subjected to the chronic vascular steal and mean arterial pressure in normal nutrient vessels may be below the minimum needed for autoregulation (21,22). The relative deficiency of the blood flow cause maximum dilatation of the cerebral resistance vessels in an attempt to increase local CBF. After a long period of dilation, the vessels became a tonic and can loose the capacity for normal autoregulation (“**stress relaxation phenomenon**”). These vessels are dilated as much as they can be, and any further decrease in perfusion pressure will actually cause a decrease in blood flow. This lack of response to pressure change (non-autoregulation) of the major feeding vessels of the AVM cause the flow across the AVM to depend upon the systemic blood pressure,

and therefore may decrease during hypotension or increase in hypertensive state. **Pertuist** et al. (36) used technetium-99 to measure blood volume in brains of normal individuals and in patients with AVMs during normotension and hypotension. They demonstrated that patients with AVMs continued to have autoregulation in normal brain, however perfusion of the AVM was dependent only on the systemic blood pressure. Similarly, there may be poor vascular reactivity to CO₂ in the adjacent brain and they cannot augment CBF in response to acetazolamide challenge. Such abnormal reactivity reflects a decompensation in the ability of the microcirculation to respond to hemodynamic disturbance induced by shunt.

Alternatively, AVMs may decrease flow to normal brain parenchyma by decreasing demand for flow because of either neuronal loss or decreased neuronal metabolic activity. **Gereon R. Fink** (32) studied metabolic and hemodynamic effects of cerebral AVMs in 14 patients using PET. They observed significant reduction of CMRGLc (Cerebral Metabolic glucose metabolism), GEF (Glucose extraction fraction), CMRO₂ (Cerebral Oxygen metabolism) and OEF (Oxygen extraction fraction) in low-flow perifocal regions. The CMR was also significantly reduced in low flow perifocal tissues, indicating that CMRGLc was more severely depressed than CMRO₂. The CBV was significantly increased in both low and high flow

perifocal regions. The tissue metabolism was decreased in perifocal regions showing the most severe hypoperfusion. This observed perifocal tissues dysfunction may be explained best as a state of chronic damage perhaps related to neuronal loss consequent to diapedetic bleeding or significant ischaemia. **Yamada & Conjocar** et al (37) have demonstrated that there is a decrease in the number of mitochondria in glia and neurons around the areas surrounding the AVM. This decrease may represent either chronic hypoxia with a decreased capacity to produce energy or decreased energy consumption. So that the balance between supply and demand remains constant. Pathological examination has shown areas of gliosis around the AVMs. These perinidal loss of afferent or efferent axons can cause cell body loss or decreased cell body activity in remote cortical or subcortical regions owing to loss of association fibers between these areas (“ *intracerebral diaschisis*”) and therefore , can affect blood flow demand far removed from the AVM (20,23).

The first suggestion of such vascular steal phenomenon occurred following the recognition of preferential blood flow towards AVM during angiography and non-visualization of vessel in a normal area of the cerebrum.

Initial attempts to assess the hemodynamic alteration caused by AVMs focused on the actual shunt flow by using inert gas diffusion with injected Xe-133 or Kr-85 (13,14) and inhaled Xe-133 (15). CBF values measured as total flow by the nitrous oxide or radioactive krypton inhalation methods have been reported to be 2 to 4.4 times higher in the hemisphere with the AVM, compared to normal values. **Fiendel et al** (16) reported red cerebral veins observed during operation in AVM patients. Later, with the use of fluorescein angiography and diffusible and nondiffusible radiotracers, they reported improved blood flow in uninvolved regions of the brain after ligation of the main vessels feeding a temporal lobe AVM, providing evidence of "cerebral steal".

Homan et al (17) used Xe-133 SPECT to show "steal areas" in eight of 11 AVM patients who were compared with a group of normal controls. These regions, however, appeared to be randomly located in the contralateral and ipsilateral hemispheres and in areas of arterial supply that were not related to the AVM. **Marks et al** (18) studied 21 patients of AVMs with stable Xe-CT and found a significant decrease in CBF in the ipsilateral cortical gray matter adjacent to the AVM relative to the corresponding contralateral cortex.

Tarr RW et al (24), studied CBF in 13 AVM patients using Xenon CT before and after acetazolamide challenge. The authors found 26 % decreased vascular reserve in near site and 15 % decreased vascular reserve in far site regions. In addition, 27 % of near site areas and 17 % of far site areas with a normal CBF on baseline study showed decreased augmentation on the postacetazolamide study, indicating decreased vascular reserve demand for blood flow rather than lowered flow reserve. Sixteen % of all parenchymal areas showed decreased CBF on the baseline examination but normal augmentation on the postacetazolamide study, suggesting a relatively decreased

They classify CBF patterns in following groups:

Pattern I: Normal preacetazolamide CBF (> 35 ml/100g/min) and normal augmentation (> 10 %) of CBF after acetazolamide administration.

Pattern II: Normal preacetazolamide CBF (> 35 ml/100g/min) and decreased augmentation ($< 10\%$) of postacetazolamide CBF.

Pattern III: Low preacetazolamide CBF (>35 ml/100g/min) and decreased augmentation($<10\%$)of postacetazolamide CBF.

Pattern IV: **Low** preacetazolamide CBF (<35 ml/100g/min) and normal augmentation($>10\%$) of postacetazolamide CBF.

HEMODYNAMIC CHANGES AFTER SURGICAL OR ENDOVASCULAR INTERVENTION :

Intraoperative vascular pressure measurements were performed with either direct puncture or Doppler sonography. The pressure recording from the feeding arteries at the entrance of the AVM were significantly below systemic arterial blood pressure, with a mean pressure ranging between 15 and 56 mm Hg (25). On temporary occlusion, the stump pressure rapidly rose to a mean pressure of 76 mm Hg, resulting in a concomitant rapid increase in cortical artery perfusion pressure. Before surgical excision of the AVM, the pressure in the draining vein(s) were also elevated with a mean pressure of 50 mm Hg; after excision of the malformation the venous pressure decreases to 0-2 mm Hg. The drop of venous pressure contributes further to the increase in normal tissue perfusion after embolization and/or resection of the AVM.

Hassler and Steinmetz (38) studied local hemodynamics during operations for cerebral AVMs, using microvascular Doppler sonography and intravascular pressure recordings. Doppler sonographic examinations of blood flow velocity and CO₂ reactivity in vessels supplying brain and/or the AVMs were performed. The response to PaCO₂ changes in the feeder arteries was almost

abolished; Velocities only slightly increased with hypercapnia and remain stable in hypocapnia. Feeders reveal slightly abnormal spectra with high diastolic and end-diastolic velocities. Following removal of AVMs, the feeder vessels showed that flow velocities in former AVM feeders are considerably reduced with often-undetectable diastolic values indicating a sharp increase in arteriolar resistance. Intravascular mean pressures in the feeding branches increased from 45 - 61.8 % (baseline) to 52.3 % to 90 % of the mean systemic arterial blood pressure after the AVM excision. The previously impaired hypocapnic vasomotor responses of the feeder arteries immediately normalized following AVM removal (25).

Norlen G (41) observed that the dilated feeding arteries supplying AVM return to their normal size after 3 weeks of excision of the AVM. Similarly, displacement of watershed zones and reversal or at least partial correction of angiographic steal has been demonstrated during follow up angiography after embolization or surgery (42,43).

Takashi Okabe et al (19), studied 16 patients of cerebral AVMs with stable xenon (Xe-CT CBF) CT scanning and were compared to Xe-133 inhalation using external probes. Five patients were studied before and after the total excision of AVMs.

The mean CBF values in AVM patients were significantly reduced in adjacent gray matter around the AVM. After successful excision of the AVM, mean CBF values for gray matter were significantly improved to the normal in the hemisphere formerly containing the AVMs.

CLINICAL IMPACT OF CEREBRAL STEAL:

There are different viewpoints concerning the clinical impact of this steal.

The hemorrhagic complications of AVMs are well known, but the physiologic and clinical consequences of hemodynamic disturbances resulting from a high flow shunt are less well understood. Many of the complications of AVMs including seizures, progressive neurological defects, and intellectual – emotions determinations are attributed to a “steal phenomenon”(15,16,18,25).

Using transcranial Doppler ultrasonography of brain AVM, **Mast** et al (26) found no evidence of correlation between steal and focal neurological deficits. **Young** et al (27) observed that the distributions of oxygen supply and nutritive capillary flow to the cortex surrounding brain AVMs were almost identical to that in normal cortex (i.e., no evidence of cerebral hypoperfusion was found in brain AVMs).

Using a microspectrophotometer to study AVM relevant cortical oxygen saturation, Meyer et al (28) found that the reduction of cerebral perfusion pressure in brain-nutritive branches of arterial feeding arteries did not cause lowered tissue oxygenation in most patients. Compensating mechanisms, therefore, counteract the reduced perfusion pressure. Arteriolar dilatation might be one of the mechanisms but seemingly not to the extent of a maximum cerebrovascular resistance reduction (29). An increased capillary density as a structural adaptation might be another plausible compensation (30). It was hypothesized that erythrocytic capillary recruitment, as defined by Kuschinsky and Paulson (31), might also play an independent role for the adaptation.

Gereon R. Fink (32) studied metabolic and hemodynamic effects of cerebral AVMs in 14 patients using PET. They observed significant reduction of CMRGLc, GEF, CMRO₂ and OEF in low-flow perifocal regions. The tissue metabolism was decreased in perifocal regions showing the most severe hypoperfusion. This observed perifocal tissue dysfunction may be explained best as a state of chronic damage perhaps related to neuronal loss consequent to diapedetic bleeding or significant ischaemia. Therefore, the clinically claimed steal phenomenon such as progressive focal neurological deficits or impairment of higher cognitive functions

might, also, be a consequence of neuronal dedifferentiation and diaschitic phenomena in distant or even contralateral regions of the brain.

ACUTE POST EMBOLISATION HEMORRHAGE (APEH)

Acute post embolization hemorrhage (APEH) is the most frequent and the most neurologically devastating complication of embolization;

APEH can be due to:

1. Occlusion of the draining vein with glue.
2. Delayed venous thrombosis.
3. Normal Pressure perfusion break through
4. Intranidal aneurysm rupture.
5. Vessel wall tearing during micro catheter retrieval

Inadvertent embolisation with sudden complete occlusion of the vein by embolic material is probably the most frequent cause of APEH. **Deruty et al** (39) reported five cases of APEH in 40 patients (12.5 %) in the week after embolization. In 4 of these 5 cases occlusion of the main venous drainage was demonstrated. Continued inflow into the malformation with impaired out flow is a very high-

risk situation for rupture and hemorrhage, partial occlusion of the draining vein with glue, associated with decreased arterial flow, may favour further complete venous thrombosis and hemorrhage.

Picard et al.(97) did a recent review of the literature and presented the largest series ever published on APEH. In 18 series of brain AVM embolization in which, cases of spontaneous APEH were reported there were 58 (4.8%) APEH among 1206 patients. These series involved very different embolization techniques and embolic materials (pellets, IBCA, silk suture, PVA, NBCA). Considering only series with glue embolization, there were 31 (8.2) APEH in 379 patients (98,99). **Picard** et al (97) reported a series of 564 patients with brain AVMs; 492 (87%) were treated with intranidal injection in a total of 1569 procedures, with a mean embolization of three pedicles per procedure. The rate of APEH was 1 % per embolization (15/1569) and 3% per patient (15/492). Out of these 15 patients, 4 patients were asymptomatic and hemorrhage was detected incidentally.

NORMAL PERFUSION PRESSURE BREAK THROUGH (NPPB) :

Another implication of intracerebral steal phenomenon is - *Normal perfusion pressure breakthrough* (NPPB). The concept of normal perfusion pressure break through (NPPB) was first described by **Spetzler** et al (33), who assessed that the normal brain parenchyma

surrounding the AVM is subjected to the chronic vascular steal phenomenon by the AVM and disturbed vascular auto regulation. The acute reduction of flow after resection of an AVM, re-establishes a normal flow in the surrounding brain; the lack of autoregulation results in disruption of local capillary beds and produces subsequent brain edema or hemorrhage. There is experimental evidence of the theory that vasomotor regulation can be seriously impaired due to the long period of arteriole inactivity (25).

Sekhan LH et al. (30) surgically created arteriovenous fistula (carotid-jugular fistula) in the rats and experimentally created chronic cerebral hypoperfusion with a reduction in CBF of between 25-to 50%. They observed increased capillary density and absent astrocytic foot process in the CA1 pyramidal cell region of the hippocampus and believe that a structural accompaniment to the hemodynamic changes that occur in brain in the vicinity of cerebral AVM made them prone to mechanical weakness and instability following the increase in perfusion pressure that occurs in adjacent brain parenchyma after AVM excision.

Al-Rodhan et al. (45) suggested that "*occlusive hyperemia*" might be the actual pathophysiological process explaining post-operative hemorrhage and brain edema that might otherwise be

described as normal perfusion pressure break through in AVM patients. The basis of occlusive hyperemia is obstruction of the venous outflow system of adjacent brain parenchyma, with subsequent passive hyperemia and engorgement.

Regardless of whether arterial autoregulatory override (i.e. NPPB) or venous occlusion is responsible for the pathological process, both are manifested by capillary rupture and breakdown of the blood-brain barrier.

Folkow et al (40) showed an adaptive structural change of the resistance vessels in chronically hypotensive beds with medial hypertrophy, loss of contractile strength, and decreased resistance and greatly increased lumina in arterioles of chronically underperfused vascular beds in animal models. The maximal contractile strength and steepness of the resistance curve were decreased.

Recently, effects of the endovascular and radiosurgical treatment on hemodynamics of AVMs were studied and a favourable outcome was observed in term of reduction of arteriovenous shunting and cerebral steal.

Wan-Yuo Guo et al. (34), studied 19 patients with AVM with MR perfusion imaging performed in before and after radiosurgery. They demonstrated Postradiosurgical, nidal rCBV and rCBF ratios

gradually decreased to 1.0, whereas rMTT ratios gradually increased to 1.0; anterior and posterior immediate perinidal rCBV and rCBF ratios decreased, indicating reversal of steal toward normal perfusion. AVM nidus volumes were observed to be decreasing after radiosurgery on follow up imaging.

Cronqvist et al. (35) studied 21 patients of AVMs with perfusion MR before and after embolization. Seventeen perfusion MR imagings (85%) were abnormal with increased rCBF and rCBV at the site of the AVMs before embolization. No major differences were noted between rCBF and rCBV patterns in other areas of the ipsilateral parenchyma versus the contralateral hemisphere, with 2 exceptions. MTT did not reveal any obvious hemodynamic disturbances in 18/20 MR imagings (90%). The final MR imaging revealed decreased AVM size and perfusion disturbances in all treated AVMs. Decreases in rCBF and rCBV within and around the AVM were found after 19/40 procedures while rCBF and rCBV remained unchanged after equal number of procedures i.e., 19/40 procedures.

Materials & Methods

MATERIAL AND METHOD

Subjects: -

This prospective study was done between 01 January 2004 to 31 September 2006.

All patient were referred with clinical and imaging diagnosis of Cerebral AVM.

All patients were referred to department Imaging Sciences and Interventional Radiology, (IS & IR), SCTIMST, Trivandrum, Kerala, India, for endovascular treatment of AVM.

A total of 15 patients were included in the study.

Two patients were excluded form the data analysis; one had right transverse-sigmoid sinus DAVF and other had a large postoperative MCA territory infarct, ipsilateral to the temporal AVM, after an emergency evacuation of intracranial hematoma, three month prior to the referral to the hospital.

Thirteen patients (10 male, 3 female) of cerebral arteriovenous malformation (AVMs) were prospectively studied with conventional MR imaging as well DWI and MR perfusion study.

Ten patients underwent 25 endovascular procedures and 3 patients underwent surgical excision of the AVMs.

Eight patients were imaged before and after the AVM embolization.

A total of 24 MR perfusion studies carried out in 15 patients. One patient who underwent 2 settings of AVM embolisation was imaged before and after each setting of embolisation.

The mean age of the patients was 29 years (range from 15 to 48 years).

All patients were symptomatic at presentation. Most commonly patients presented with partial seizures (6 patients) followed by intraparenchymal bleed (4 patients), chronic headache (3 patients) and LOC with speech arrest (1 patient).

At the time of presentation, two patients had neurological deficit; one patient had residual right hemiparesis due to previous intracranial bleed and another patient with AVM in left visual cortex, had right homonymous superior quadrantanopia.

Inclusion criteria:

1. Compact nidus AVM
2. AVMs, previously never embolised.
3. AVMs previously never bled.
4. AVMs previously not treated (surgical, radiotherapy or endovascular)

Exclusion Criteria:-

1. Diffuse AVMs
2. AVM patients with stroke.
3. Infratentorial AVMs.
4. Dural arteriovenous malformation.
5. Multiple AVMs.

AVM GRADING (SPETZLER MARTIN GRADING)

AVMs were graded according to the Spetzler Martin grading (96).

The **Spetzler and Martin** (1986) classification (96) was established to grade AVMs according to their degree of surgical difficulty and the risk of surgical morbidity and mortality. To assign

an AVM grade, the size, the venous drainage, and the eloquence of the adjacent brain are determined from angiography, computed tomography, and MR imaging. A numerical value is assigned for each of the categories:

SIZE: The sizes of the AVMs were determined (excluding the feeding arteries and draining veins) by correlating the measurements from the corresponding digital subtraction angiography (DSA) and the MR imaging.

Small (< 3 cm) : 1; Medium (3-6 cm) : 2 ; Large (>6 cm) : 3

ELOQUENCE: Eloquent areas include superficial cortical areas (primary motor, sensory, visual & language areas) and deep eloquent areas (hypothalamus, thalamus, brainstem & cerebellar peduncles).

Non-eloquent :0; Eloquent: 1

PATTERN OF VENOUS DRAINAGE :

Superficial : 0 ; Deep : 1

The grade of AVMs is obtained by summing up the points assigned for each category.

GRADE OF AVM = SIZE + ELOQUENCE + VENOUS DRAINAGE

AVM Characteristics

AVM	No. of Cases
1. SITE	Eloquent - 4
	Non-eloquent - 10
2. Venous Drainage	Deep - 3
	Superficial - 10
	Both - 1
3. AVM GRADE	Grade I - 4
	Grade II - 4
	Grade III - 4
	Grade IV - 1

Table 1 : AVM Characteristics

Case/Age /Sex	Clinical Presentation	Site	Size (APxWxHcm)	Venous Drainage	Grade
1/37yrs/M	Headache	Left parietal	4.2 x 3.4 x 3.7	Deep	III
2/29yrs/F	Speech Arrest	Left Insular	4.3 x 3.8 x 2.5	Superficial	II
3/15yrs/F	Seizure	Left Premotor	2.3 x 1.3 x 2.4	Superficial	I
4/27yrs/M	Seizure	Left Temporal	3.8 x 2 x 2.5	Deep	III
5/2yrs/M	thalamic bleed	Left thalamus	1.4 x 1.3 x 1.7	Deep	III
6/4yrs/M	Headache	Left Occipital	5 x 3.3 x 3.8	Superficial	IV
7/24yrs/M	Seizure	Left frontal	1.9 x 1.5 x 1.7	Superficial	I
8/31yrs/F	Seizure	Left temporal	3.3 x 2.6 x 4	Superficial	II
9/36yrs/M	Seizure	Left temporal	4.6 x 3.5 x 3.2	Superficial + Deep	III
10/23yrs/M	Seizure	Right Premotor	4 x 3.5 x 2.8	Superficial	II
11/23yrs/M	ICH	Right Fusiform gyrus	1.35 x 1.3x2	Superficial	I
12/46yrs/M	ICH	Left Precuneus	3.4 x 2.3 x 2.5	Superficial	III
13/48 yrs/M	Seizures	Right Sensory motor cortex	2.5 x 2.4 x 2.3	Superficial	II

MR Examinations

All patients underwent MR Imaging including standard routine sequences for brain imaging as well as diffusion weighted imaging and perfusion MR imaging, before the embolization. Embolization was electively planned two or three days later. Diagnostic cerebral angiogram and embolization were done in the same setting in all patients except one patient.

Eight patients underwent MR study after embolization, using same MR imaging protocols.

All examinations were conducted with a 1.5 T whole-body MR unit ,Magnetom (Magnetome Avanto, Tim 76X18 SQ Engine, Siemens medical system, Erlangen, Germany) with high-performance gradients (master gradients), with a maximum slew rate of 200 mT/m/msec and a maximum strength 45 mT/m. A standard transmit-receive birdcage head coil was used.

MR Protocol: -

Following sequences were performed before and after the procedure:

- SE T1W: Axials
- FSE T2W: Axials, Coronals and Sagittals

- FLAIR: Axials
- DWI & ADC Maps
- Dynamic Susceptible Contrast (DSC) Perfusion Imaging

The MR examination began with the acquisition of anatomic images of the whole brain by using dual echo intermediate (PD) and T2-weighted fast spin echo sequences, spin echo T1-weighted and FLAIR sequences. This sequences were being followed by DWI and perfusion imaging.

SEQUENCE PARAMETERS :

T2-weighted sequences:

Sections, 20; Thickness, 5 mm; Slice gap, 1.5 mm; Field of view, 230 mm;

Matrix, 256 x 256. Repetition time msec/Echo times (TEs) msec/NEX, 3,800/22, 90/1;

Flip angle, 150°; turbo factor of 5 and bandwidth of 130 Hz/pix.

T1-weighted sequences:

Sections, 20; Thickness, 5 mm; Slice gap, 1.5 mm; Field of view, 230 mm;

Matrix, 256 x 256. Repetition time(TR) msec/Echo times (TEs) msec/NEX, 735/14/1;

Flip angle, 70° and bandwidth of 86 Hz/pix.

FLAIR sequences:

Sections, 20; Thickness, 5 mm; Slice gap, 1.5 mm; Field of view, 230 mm;

Matrix, 256 x 256. Repetition time (TR) /Echo times (TEs) /Inversion time(TI), 900/108/2500 msec; flip angle, 150°; turbo factor of 21 and bandwidth of 130 Hz/pix.

Diffusion weighted imaging:

Transverse DWI was performed by using a SE echo-planar imaging (EPI) technique with diffusion-encoding gradients applied in 3 orthogonal directions (section, read, and phase) with 3 *b* values (0, 500, and 1000 s/mm²). The parameters used were :

TR/TE, 3100/96 msec; NEX, 3; number of slices, 20; slice thickness/gap, 5/1.5 mm; FOV, 230 mm; matrix size, 128 x 128 matrix; band width of 1502 Hz/pix and EPI factor of 128. Mean apparent diffusion coefficient (ADC) maps, based on the 3 individual gradient directions, were calculated.

Dynamic susceptibility-weighted contrast-enhanced MR imaging. —

Perfusion MR imaging was performed using by using dynamic susceptibility contrast MR imaging based on rapid gradient-echo single shot EPI echo-planar imaging technique, with an echo-planar imaging factor of 128, and a bandwidth per pixel, or BW_{pix} , of 1502 Hz. The imaging parameters were:

TR/TE, 1460/43; NEX, 1; flip angle, 90° ; slice thickness/ slice gap, 5 / 1.5 mm; FOV, 230 mm; and matrix, 256 x 256.

Before injecting contrast, 14 X 60 baseline images were obtained then 15 ml of contrast agent, gadoteric acid (Dotarem; Guerbet, France) was injected intravenously via an antecubital 18-gauge cannula by using a MR-compatible power injector (*Spectris; Medrad, Volkach, Germany*) at a flow rate of 5 mL/sec. Total 13 sections and 60 measurements per section were obtained so that a total of 960 dynamic images per perfusion study was acquired for analysis; total acquisition time was 1.33 seconds. Motion artifacts were prevented with fixation of the patient's head in the 12-channel head matrix coil with a vacuum cushion.

At least one section was positioned at the level of the middle cerebral artery to obtain the arterial input function; after a 90° excitation pulse, a GRE echo-planar MR image was acquired first.

Following a 180° section-selective refocusing pulse, a spin-echo echo-planar MR image of the same section was recorded. The TE for the GRE and spin-echo MR images was 35 and 105 msec, respectively.

Processing of dynamic MR images.—

All perfusion imaging data were transferred to a workstation Leonardo (Perfusion Software Package, *syngo*, Siemens Medical Systems) and the perfusion data were converted into concentration-time curves with the assumption that the change in relaxivity, calculated as $\Delta R2^* = \Delta(1/T2^*)$, is proportional to the time-dependent contrast medium concentration, calculated as $\Delta R2^*(t) = k[CA]$, where t is time, k is a field-strength- and pulse sequence-specific constant, and $[CA]$ represents the concentration of the contrast agent. Dynamic susceptibility-weighted contrast-enhanced MR images were postprocessed by using singular value decomposition and deconvolution as described by Ostergaard et al (7). Measured signals, $S(t)$, were converted to relative concentration time courses, $c(t)$, in a voxel-by-voxel manner by using the mean baseline signal, S_0 , with the following equation:

$$c(t) = -1/TE \ln[S(t)/S_0]. \quad (3)$$

$S(t)$: Measured signals, $c(t)$: relative concentration time courses, S_0 : mean baseline signal.

The arterial input function was determined in a section that contained large arteries (preferably the middle cerebral artery in plane). The arterial input function was determined from an artery in the Sylvian fissure contralateral to the AVM. The arteries component indicated in-plane major branches of cerebral arteries and AVM nidus. The arteries components were used as a mask to produce an averaged arterial signal intensity-time curve and arterial input function (i.e., an averaged concentration-time curve of arterial area). Tracer concentration-time curves can then be analyzed to determine various tissue hemodynamic parameters, such as tissue blood volume, blood flow, transit time, and bolus arrival time. Cerebral blood volume refers to the volume of blood in a given region of brain tissue, commonly measured in milliliters per 100 g of brain tissue. Cerebral blood flow refers to the volume of blood per unit time passing through a given region of brain tissue, commonly measured in milliliter per minute per 100 g of brain tissue. Mean transit time refers to the average time it takes blood to pass through a given region of brain tissue, commonly measured in seconds.

Based on residue detection in indicator dilution theory, the relative cerebral blood volume (rCBV) in a voxel is proportional to the area under the concentration-time curve in a voxel (8,9). The relative cerebral blood flow (rCBF) was computed by means of the singular value deconvolution method (10). The relative mean transient time (rMTT) of contrast agent particles was defined as the ratio between rCBV and rCBF according to the central volume principle (11,12). Assuming high maximum signal decay, short arrival time, and small full width at half maximum, we identified candidate voxels by using an automated algorithm. The arterial input function voxels were then selected manually. Singular value decomposition of the triangular matrix filled with the arterial input function was performed, and deconvolution of all voxel time courses of all sections was performed by using thresholds between 5% and 15% for the singular values, depending on the contrast-to-noise ratio of the measurement. Relative CBF, relative CBV, and mean transit time maps were generated voxel by voxel from the maximum of the deconvolved function, numerical integration of $c(t)$, and the ratio of relative CBV to relative CBF, respectively.

CBV calculated from the area under the curve; and CBF index, equal to CBV/apparent MTT. These maps do not afford quantitative assessment of brain hemodynamics but provide indicators of

hemodynamic disturbances. They can be interpreted visually or semiquantitatively by calculating the ratio or difference between the values in an ROI placed in the abnormal area and a mirror ROI placed in the contralateral area considered as a normal reference.

Data Analysis :

ROI-based quantitative analysis of perfusion variables. —

The largest nidal section was chosen for calculation of hemodynamic parameters. The measurement was based on the assumption that the image section having the largest nidal diameter represented the most significant section for AVM hemodynamic alterations.

The areas in the vicinity of the AVM nidus defined as the ROIs (region of interest) for perfusion measurement and their homologous ROIs in the contralateral hemisphere as the intrasubject control. ROI of 5 pixels were placed manually on AVM target sections as follows:

N: AVM nidus;

IPN: Immediately perinidal region within 1 cm on the AVM nidus. Immediate perinidal region is divided into immediate anterior and immediate posterior perinidal regions.

R: Remote, brain parenchyma > 1 cm to the nidus.

Whenever possible, remote areas were taken in anterior as well as posterior to the AVM nidus, however, in case where AVM had involved the frontal lobe, occipital lobe was taken as remote area and similarly, if the AVM had involved occipital lobe, frontal lobe was taken as remote area. If it is not possible to select ROI in the same selected plane then, remote ROI was chosen in the one section above or below the chosen target section. If both the anterior and posterior ROIs measurements are decreasing or increasing together, then average of both the measurements were taken; otherwise both were noted down separately.

Similar ROIs in the contralateral hemisphere (N1, IPN1, and R1) served as internal references. Perfusion ratios of ROI-ROI1 were defined.

Perfusion map relative cerebral blood volume (rCBV), cerebral blood flow (rCBF), and mean transient time (rMTT) were assessed.

Relative rCBF and rCBV maps were color coded after normalization to the relative rCBF and rCBV values of the contralateral normal brain parenchyma.

Abnormally high nidus rCBV and rCBF ratios and low nidus rMTT ratios indicated high flow transnidus shunts in AVMs. Abnormal rCBV and rCBF ratios in immediate and remote areas indicated brain perfusion disturbance of the hemisphere secondary to the steal phenomenon.

Patient management :

The entire patients were selectively planned for endovascular treatment of the cerebral AVMs. Patients were admitted one to three days prior to the day of embolisation. All the patients were investigated with routine hemogram, blood coagulation profile, HIV-HBsAg status and cardiac status. CT scans head (plain) and MRI brain was done as a baseline structural imaging and also to know the size of the AVM nidus and exact site (eloquence).

Preoperative clinical assessment includes and detailed neurological examination and visual field charting.

Anticonvulsant medication (Tab Eption 100 mg three times a day) was used only in-patient who have had previous seizures or intracerebral hematoma or subarachnoid hemorrhage.

Patient preparation:

Patients were kept nil per orally after midnight except for the antiepileptic drug that was allowed to take in the morning. Premedication included Tab Diazepam (0.1 – 0.2 mg/kg) 90 minutes before and Inj. Glycolpyrolate (0.2 mg intramuscular) half an hour before shifting the patient to the cath lab.

Procedure:

All patients were catheterized in the Cath lab to monitor urine output and also avoid urinary retention.

All cases were done under general anesthesia.

Once the patient was on the table, blood pressure cuff, ECG leads, oxygen saturation finger pad was connected and continuous monitoring of vitals and oxygen saturation was done.

Induction of anesthesia was done by titration of propofol and fentanyl and/or midazolam intravenous infusion. Bolus dose of muscle relaxant was given at the time of the induction (Pancuronium, 8 mg intravenously). General anesthesia was maintained with inhalation agents (Isoflurane and/or Propofol) and muscle relaxant (Pancuronium , 1-2 mg every 90 minutes) was given intermittently. Intraarterial systemic blood pressure monitoring was done throughout

the procedure and during controlled hypotension at the time of glue injection. Continuous bispectral index (BIS) monitoring was done for very rigid control of depth of sedation.

A GE uniplanar Digital Subtraction Angiography unit [GE Advantex system, DLX LCV, Milwaukee, Illinois, USA] was used for all DSA and interventions. A nonionic, low-osmolar contrast agent (240 mg/mL Omnipaque, Amersham Health [GE Health Care, Oslo, Norway]) was used in all procedures. Right common femoral artery was punctured and 7F short sheath (Avanti+, Cordis, Miami, USA) was placed using seldingers technique.

After placing the sheath, 7000 to 10,000U of loading dose of heparin (70 – 100U/kg) was given as bolus through the sheath and then the systemic heparinization was maintained to keep APTT 2 to 3 times normal by repeating heparin 1000 U every hour. The flush solution for syringes was heparinized, and the guiding catheter was connected to a continuous flush of heparinised NaCl solution.

Preprocedure diagnostic angiogram was done using 4F vertebral glide (Terumo, Tokyo, Japan). Bilateral selective internal carotids and vertebral injection in three standard projections (Anterioposterior, oblique and lateral views)were obtained. Additional views were obtained at varying angles to study the angioarctecture of the AVM

and to separately identify the feeding vessels from the adjacent nidus and draining veins.

For the AVM embolisation, 90cm long 7F guiding sheath (Launcher, Medtronic, Minneapolis, USA) was kept at CCA or distal vertebral artery of the involved site and then flow guided microcatheter was taken over the stela in ICA or vertebral and was allowed to propagate in the feeder. Embolisation was carried out intranidally. The microcatheters used were the Spinnaker Elite 1.5 or 1.8 F (Boston Scientific, Target, CA, USA) / Ultraflow 1.5–1.8 F (MicroTherapeutics [MTI], Irvine, Calif) or Magic 1.2 or 1.5 F (Balt Extrusion, Montmorency, France). The Trascend 0.10" (Boston Scientific, Target, CA, USA) and the Agility 0.10" (Boston Scientific, Target, CA, USA) were the most frequently used microwires. Flow guided microcatheters (Spinnaker Elite 1.5 or 1.8 F) over stela was taken upto the tip of the guiding catheter and then stela was removed and microcatheter was gently pushed to the desired feeder artery and was taken as distal as possible. In case microcatheter was not propagating a microguidewire was used for selective catheterization of the feeder artery.

Selective catheterization of the feeder artery was achieved by one of the following maneuvers.

1. Flushing the microcatheter with pure saline or diluted contrast with different pressure using 1ml luerlock syringe.
2. Raising the systemic blood pressure.

3. Temporary manually compressing the contralateral cervical ICA to increase the flow across Acom and to facilitate selective catheterization of ACA.
4. By using micro-guidewire (Transcend 0.010" or agility 0.010") to provide more stiffness and increase pushability.

Most commonly N-Butyl-2 cyanoacrylate (Histoacryl, Braun, Melsungen, Germany and Nectacryl, Nectar, AP, INDIA) was used for embolisation. Lipodol (Guerbet, Aulnay, Sous Bois, France) was used for making optimal concentration of the glue (from 17 to 80%) and also for imparting the visualization of the glue. For glue injection, best projection was selected to separate the feeder artery, nidus and draining vein and to visualize the tip of the micro catheter then test injection was performed to judge the rate of blood flow across the AVM nidus and thereafter to decide the glue concentration.

More concentrated glue was used in following conditions:

- (1) High flow AVMs and macro-AVFs, with a risk of escape of glue to the venous side, occluding the venous drainage.
- (2) When the security distance from the tip of the micro catheter to normal arteries is short.
- (3) When the origin of a vein, which should not be occluded, is very close to the catheter tip.

Glue injection was carried out under DSA mode, on road map and occasionally under fluoroscopy. The glue was injected very slowly to avoid the formation of multiple little drops of glue exiting to rapidly and spreading quickly in the veins. In case of high flow AVMs and macro-AVFs, high concentration of glue (50 – 80%) was injected under control hypotension. Control hypotension (Mean BP of 50 -600 mm of Hg) was achieved most commonly by Sodium Nitroprusside infusion (SNP, @ 1-5 mic. /Kg/min) and the aim behind it is to produce vasodilatation of normal brain (where the autoregulation is intact), while diverging the blood away from the malformation and slowing the flow through the nidus, thus allowing better filling of the nidus.

At the end of the injection the guiding catheter was pulled down into the aorta and then microcatheter was withdrawn inside the guiding catheter and both were taken out of the sheath together. Then check angiogram was done to see the percentage reduction of nidus size, reduction in AV shunt and venous drainage pattern. Depending upon the number of primary feeding arteries, size of the nidus, venous drainage, location of the AVM etc., one or multiple feeder arteries were embolized in the same setting with an aim of achieving maximum nidus reduction without increasing the risk of normal perfusion pressure breakdown.

Liquid polymer Onyx (EV3; MTI) was used in 3 cases; Other embolic agents used were absolute alcohol (7 patients), PVA particles

for dural feeders in of mixed – pial dural AVM (in one patient) and in one case, 11 coils were deployed in the venous sac to reduce the flow in arteriovenous fistula and followed by embolization of the feeder using 80% glue.

Table 2 : ENDOVASCULAR PROCEDURE:

Case	No. of Feeders Embolised	No. of Microcatheter Used	Embolic Agent
1	5	4 SPK	NBCA + Alcohol (12m)
2	7	5 SPK + 1.MTI	NBCA + ONYX
3	1	1	Alcohol (20ml)
4	2	1 SPK	Alcohol (27ml)
5	1	1 SPK + 1 Magic	NBCA + Alcohol (3ml)
6	5	3 SPK	NBCA + Alcohol + PVA
7	2	1 SPK	Alcohol (12ml)
8	1	1 MTI + 1 SPK	Onyx
9	1	4 SPK	NBCA + Alcohol
10	1	1 SPK+ 1 EXCEL	11GDC Coils + NBCA (80%)

Table 3 : Percentage Nidus Occlusion

Case No	Nidus Occlusion (%)	No. of Settings
1	70-90%; AVF Occluded	2
2	80-90%	2
3	No Significant reduction	1
4	80% AV Shunt, Markedly reduced	1
5	50-60%	1
6	40%	1
7	40/50%	1
8	50%	1
9	50-60%	1
10.	50-60%; AVF Occluded	1

Table 4 : Histoacryl Concentration Chart

No.	Concentration	Histoacryl	Lipidol
1	15%	0.5ml	2.8ml
2	17%	0.5ml	2.4ml
3	20%	0.5ml	2ml
4	22%	0.5ml	1.7ml
5	25%	0.5ml	1.5ml
6	33%	0.5ml	1.0ml
7	40%	1.0ml	1.5ml
8	50%	0.5ml	0.5ml
9	60%	1.5ml	1ml
10	66%	1ml	1ml
11	75%	1.5ml	0.5ml
12	80%	2ml	0.5ml

POSTPROCEDURE MANAGEMENT :

All except one patients were extubated on the table after the procedure. Reversal of general anesthesia was achieved by withdrawing the inhalation agents and Inj. Glycopyrolate (0.4 mg) and Neostigmine (2.5 – 3 mg) intravenously. No fresh neurological deficit was noted in any of patient. One patient, who had intraprocedural bleed in the brain due to feeding artery rupture, was not extubated only after 24 hours of the procedure. All patients were shifted to neurointensive care unit and kept for 24 to 48 hours after the procedure and remained hospitalized for another 3–6 days before discharge.

Intraarterial BP, Heart rate and Oxygen saturation was monitored continuously.

Postprocedure, the blood pressure was kept below the baseline BP (Systolic BP of 110-120 mm Hg) using infusion of Sodium Nitroprusside (@ 1-3 mic/Kg/min) or NTG (@1-5 mic./Kg/min) for 24 to 48 hours.

All patients were administered steroids (Inj. Dexamethasone, 4 mg three times a day) and Mannitol (75-100 ml twice daily, 0.25-1 gm/Kg) intravenously for 2 days after the embolizations . Neurological examination was performed regularly

Adverse Events Noted during the Endovascular Procedure

Of the 10 patients undergoing embolization of cerebral AVM , two patient had intraprocedural complication.

One patient had feeder artery rupture while pulling out the microcatheter at the end of onyx injection immediately, the feeder artery was recatherized with spinnaker elite 1.5F and the ruptured feeder artery was sealed with 20 % NBCA. Immediate CT scan showed left temporal hematoma; patient was electively ventilated for 24 hours and extubation after 24 hours, neurological exmination show no fresh defecit, however patient complained of mild paresthesia in right side of face which subsided spontaneously within few days.

Another patient with left premotor AVM, had mild right hemiparesis (power grade 4/5) with mild right facial paresis and had motor aphasia after alcohol embolization. CT scan after 48 hours and MRI after 10 day showed moderate perinidal vasogenic edema. Patient was managed conservatively with antiedema measures, physiotherapy and speech therapy. At the time of discharge, the patient was almost completely recovered except for the mild difficulty in performing finer activity by right hand and had mild decrease in word output.

Rest of the patients was neurologically intact after the procedure.

Results

RESULTS

Patients and clinical presentation:-

A total of 15 patients were included in the study. Two patients were excluded from the data analysis, one with right transverse-sigmoid sinus DAVF and another patient with left temporal AVM who had large ipsilateral MCA territory stroke at the time of presentation (the patient had suffered the stroke after hematoma evacuation, before being referred for embolisation).

Thirteen patients (10male, 3 female) of cerebral arteriovenous malformation (AVMs) were prospectively studied with conventional MR imaging as well DWI and MR perfusion study. Ten patients underwent 25 endovascular procedures and 3 patients underwent surgical excision of the AVMs. Eight patients were imaged before and after the AVM embolization. A total of 24 MR perfusion studies carried out in 15 patients. One patient who underwent 2 setting of AVM embolisation was imaged before and after each setting of embolisation.

The mean age of the patients was 29 years (range from 15 year to 48yr).

All patients were symptomatic at presentation. Most commonly patients prescribed with partial seizures (6 patients) followed by intra parenchymal bleed (4 patients), chronic headache (3 patients) and LOC with speech arrest (1 patient).

At the time of presentation, two patients had neurological deficit; one patient had residual right hemiparesis due to previous intracranial bleed and another patient with AVM in left visual cortex, had right homonymous superior quadrantanopia.

AVM CHARACTERISTICS:

Location: All cerebral AVMs were located in supratentorium; 4 AVMs were present in eloquent areas (2 AVMs in visual cortex, 1 thalamic and 1 in sensory-motor cortex), 10 were in non-eloquent areas (4 temporal lobe, 1 insular, 3 frontal, 1 occipital and 1 parietal lobe).

Venous drainage : Venous drainage was most commonly to superficial venous system via dilated, ectatic cortical veins (10 patients), followed by deep venous system in 3 patients and in one patient the AVM nidus was draining in both deep and superficial venous system.

GRADE (Spetzler Martin Grading) : Four patients were of grade III, 4 patients were of grade II, 3 patients are of grade I and 1 patient was of grade IV.

CONVENTIONAL AND DIFFUSION WEIGHTED MR

IMAGING :

(A) BASELINE MR IMAGING (PRE INTERVENTION) :

The AVM nidus was noted as network of flow voids with adjacent dilated ectatic flow voids converging to deep or superficial venous system. Flow of the voids shows hyperintensity signal intensity on T1W suggestive of slow venous flow.

The AVM nidus per se was hypointense on FLAIR.

Perinidal focal area of hyperintensity on FLAIR sequences suggestive of gliosis is noted in 4 cases.

Except for one AVM, none of the AVM shows any mass effect before treatment.

On DWI, the AVM nidus was profoundly hypo intense on DWI and hyper intense on ADC map. Veins were seen as hypointense rounded or linear structures within the hyperintensity on ADC map. Large venous sac was hypointense on both DWI and ADC maps. Baseline DWI did not reveal recent ischemia in any of the patients.

(B) POSTEMBOLIZATION MR IMAGING:

Out of 13 patients with cerebral AVM, 10 patients underwent endovascular treatment.

Eight of them were imaged after the embolization. The time gap between the embolization and MR study was from 2 day to 1 month.

Posttreatment MR imagings were abnormal in all patients.

Of the 8 patients who were studied after the embolization, 5 of them showed diffuse nidus hyperintensity on FLAIR sequences suggestive of nidus thrombosis. Only glue (NBCA / Onyx) was used in 4 of patients, absolute alcohol alone in 4 patients and combined alcohol and glue in 3 patients.

All of the patients, who were embolized with glue, show focal and linear hyperintensity on T1W and T2W sequences suggestive of glue cast.

Absolute alcohol as the only embolic agent in 3 patients; 2 of them show moderate perinidal vasogenic edema. The probable explanation is alcohol reflux into the proximal branches or the feeder might be supplying the normal territory (Enpassent feeder), but

alcohol extravasation should cause, cytotoxic edema instead of vasogenic edema but since the imaging study was done on 10 day after the procedures, therefore vasogenic edema rather than cytotoxic edema was observed. Another possible explanation to account for the perinidal hyperintensity is progressive nidal-perinidal and draining vein thrombosis but none of these 2 patients show any nidal hyperintensity on FLAIR suggesting any nidal thrombosis. Also in 2 cases where, nidal hyperintensity as well as draining vein thrombosis was noted after 2nd day of glue (NBCA) embolization, both cases did not show any vasogenic edema, instead both cases show focal immediate peri nidal restriction on DWI suggestive of cytotoxic edema which is most likely due to ischaemic infarct or rarely due to venous thrombosis. Venous thrombosis rarely can cause cytotoxic edema instead of vasogenic edema.

In 2 cases multiple focal hyper intensities were noted within the nidus in DWI suggestive of intranidal thrombosis.

Table 5 : New Findings in postembolization MR Imaging:

Case 1	<ul style="list-style-type: none">➤ Perinidal ischaemic infarcts➤ Venous sac thrombosis
Case 2	<ul style="list-style-type: none">➤ Perinidal ischaemic infarct➤ Draining vein thrombosis➤ Mass Effect.
Case 3	<ul style="list-style-type: none">➤ Peri nidal vasogenic edema➤ Focal bleed in peri nidal region.➤ Mass effect.
Case 4	<ul style="list-style-type: none">➤ Perinidal vasogenic edema➤ Perinidal focal bleed➤ Embolic infarct left motor cortex➤ Mass effect
Case 5	<ul style="list-style-type: none">➤ Infarct in splenium
Case 6	<ul style="list-style-type: none">➤ Focal areas of restriction / hyper intensities within nidus suggestive of nidal thrombosis
Case 7	<ul style="list-style-type: none">➤ Focal areas of restriction/hyper intensities within nidus suggestive of nidal thrombosis.➤ Embolic infarct left sensory cortex

MR PERFUSION STUDY

Baseline MR perfusion study

Thirteen patients of cerebral AVMs underwent pretreatment MR perfusion study. All MR imagings were abnormal with increased rCBF and rCBV at the site of the AVM nidus as well as along the pathway of the draining veins. The extent of rCBF and rCBV increase within each patient was almost always approximately similar.

The rCBV color map is overestimating the extent of the AVM nidus. It may be difficult to select ROI without any inclusion of adjacent nidus or draining vein.

PERFUSION IN IMMEDIATE PERINIDAL AND REMOTE REGION:

All of the cerebral AVMs show hemodynamic alterations adjacent to the nidus (immediate perinidal region). The most common hemodynamic alteration in immediate perinidal region was decrease perfusion (Low rCBV and rCBF), occurring in nearly 70% of the cases (9/13 patients). In 3 patients, immediate perfusion (rCBV and rCBF) was high, whereas one patient had increase perfusion in immediate perinidal region and decrease in posterior perinidal region.

rMTT did not reveal any obvious hemodynamic disturbances in immediate perinidal region in 7 patients (68%).

Five patients show decreased immediate perinidal rCBV that increased to 1 after embolization in 3 patients. Similarly, in 6 patients immediate perinidal rMTT was reduced and it increased to 1 in 3 patients after embolization.

In 4 patients, rCBV, r CBF and r MTT all were decreased in immediate perinidal region; which could be due to steal effect rather than due to permanent changes like gliosis in the perinidal brain tissue.

On the other hand, 38 % of the patients (5 out of 13 patients) show no perfusion abnormality in remote brain parenchyma, all of them had smaller AVM nidus (< 3cm) with only mild to moderate arterio-venous shunting. Three patients had low perfusion and 4 patients had increased perfusion in remote areas.

PERFUSION IN AVM NIDUS (rCBV, rCBF AND r MTT):

Both rCBV and rCBF were invariably increased within the nidus although; frequently increase in rCBF is more than the increase in rCBV so that rMTT is more frequently reduced (r MTT <1) within the nidus.

Infact, increase in intranidal rCBV and rCBF with decrease rMTT less than 1 is suggestive of intranidal arteriovenous shunting and was noted in 9 cases.

Out of these 9 cases, 6 patients showed reduction of rCBV and rCBF after embolization and rMTT increased to 1 suggestive of reduction in intranidal arteriovenous shunting. This finding is well confirmed in postembolization final check angiogram.

In 4 patients intranidal r MTT was normal.

Following patterns of perfusion abnormality noted in the hemisphere ipsilateral to the AVM:

Pattern I: Low perfusion in immediate and normal perfusion in remote perinidal regions.

Pattern II: Low perfusion in immediate as well as in remote perinidal region.

Pattern III: Low perfusion in immediate perinidal region and high perfusion in remote areas.

Pattern IV: High perfusion in immediate perinidal region with high perfusion in remote region.

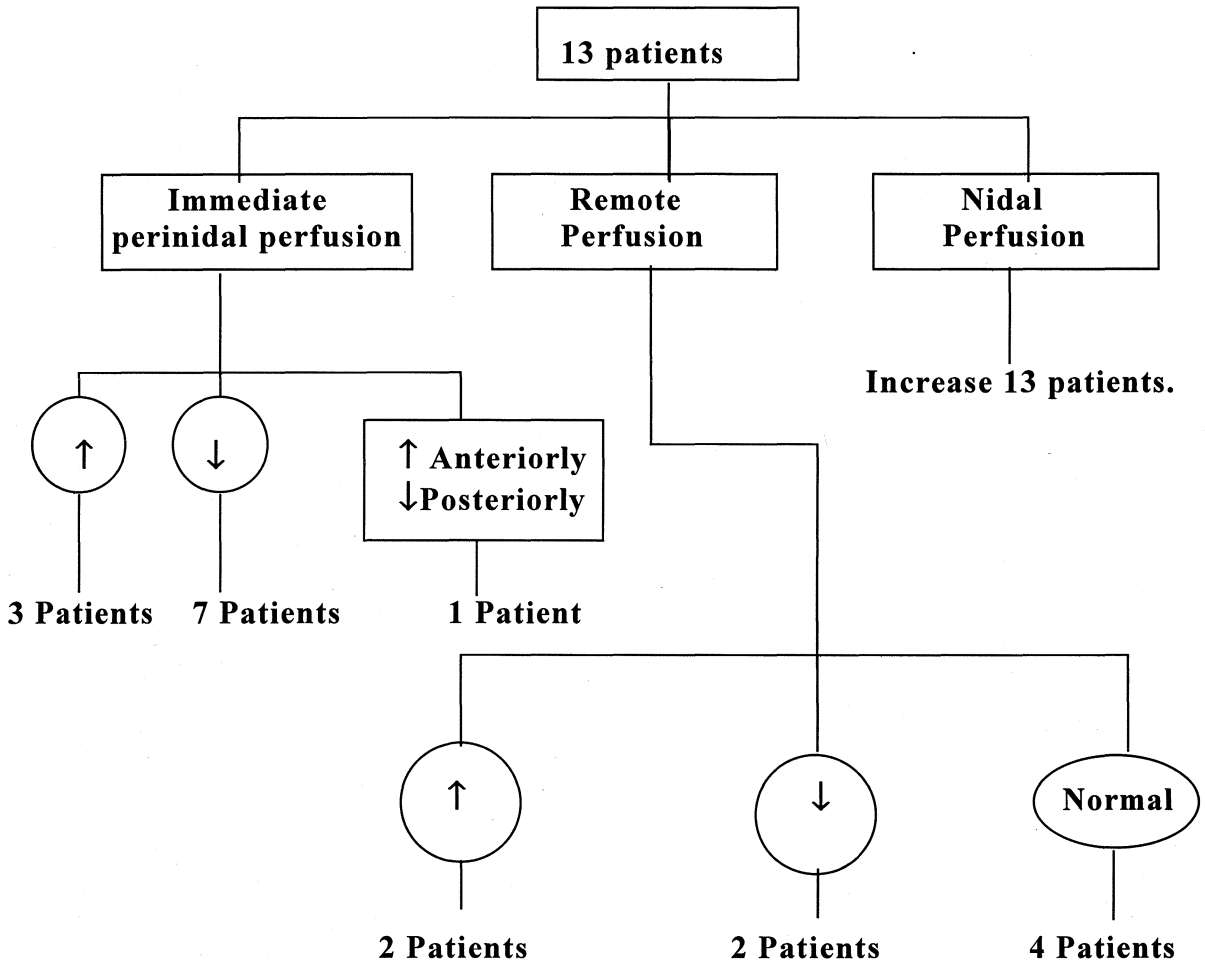
Pattern V: High perfusion in immediate perinidal region with normal perfusion in remote region.

Pattern VI: Heterogeneous or mixed immediate perinidal / remote perfusion.

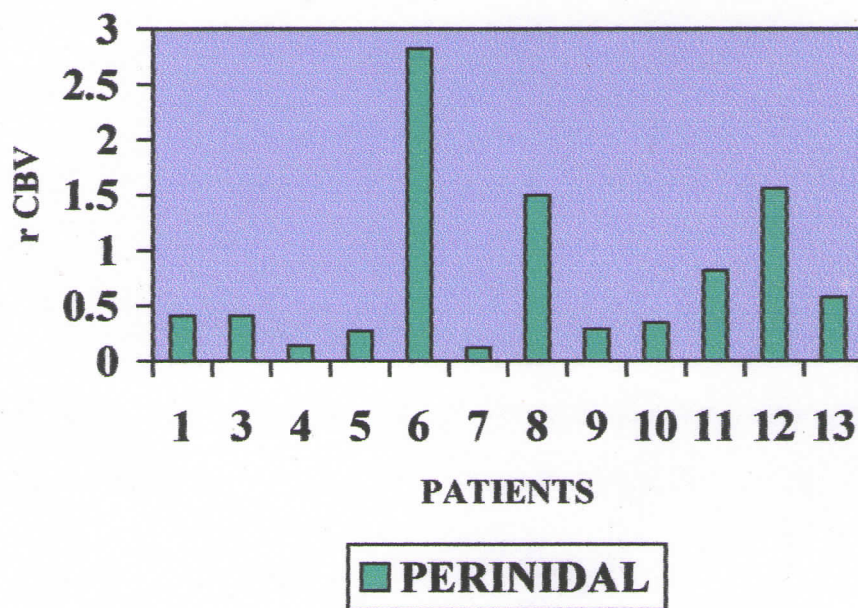
Perfusion Patterns**No. of Cases**

I	4 (Cases 3, 4, 5, 7)
II	2 (Cases 12, 14)
III	3 (Cases 1, 9, 13)
IV	1 (Case 6)
V	1 (Case 8)
VI	2 case 2, 10)

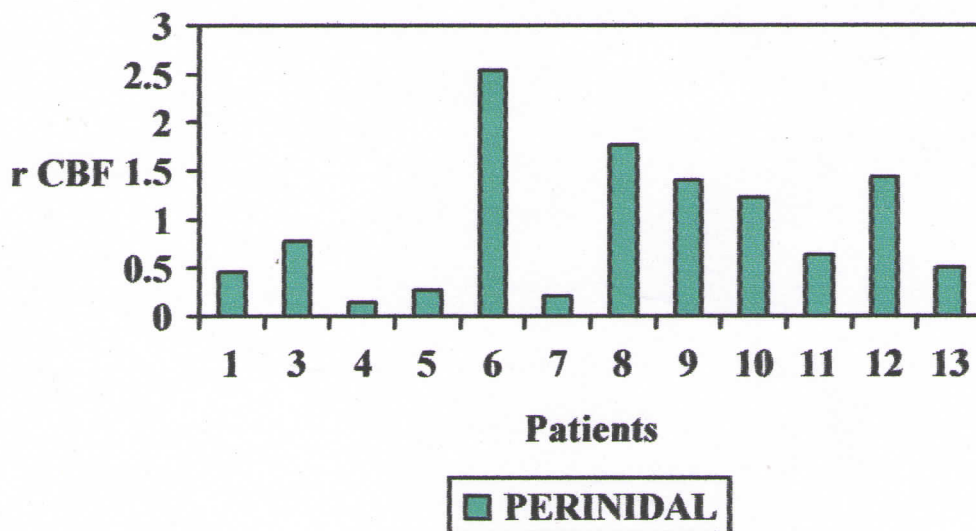
Baseline MR Perfusion Study



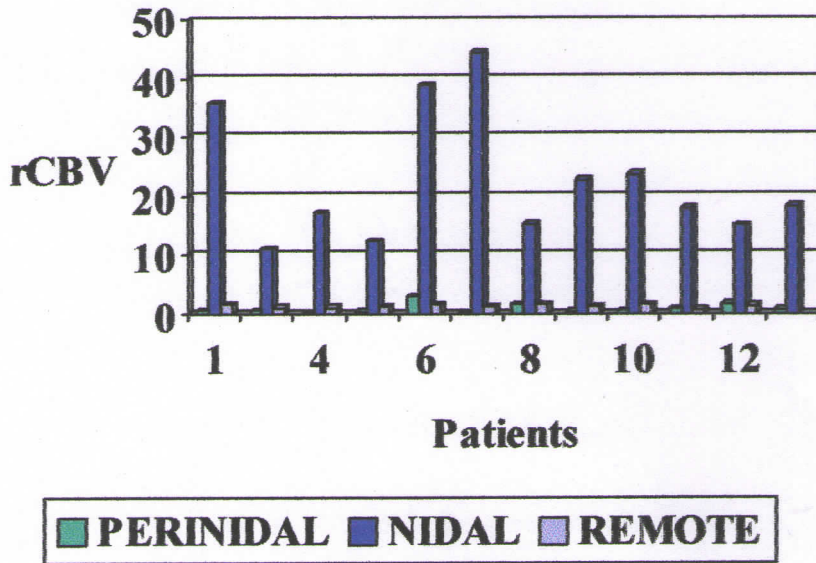
BASELINE PERINIDAL r CBV



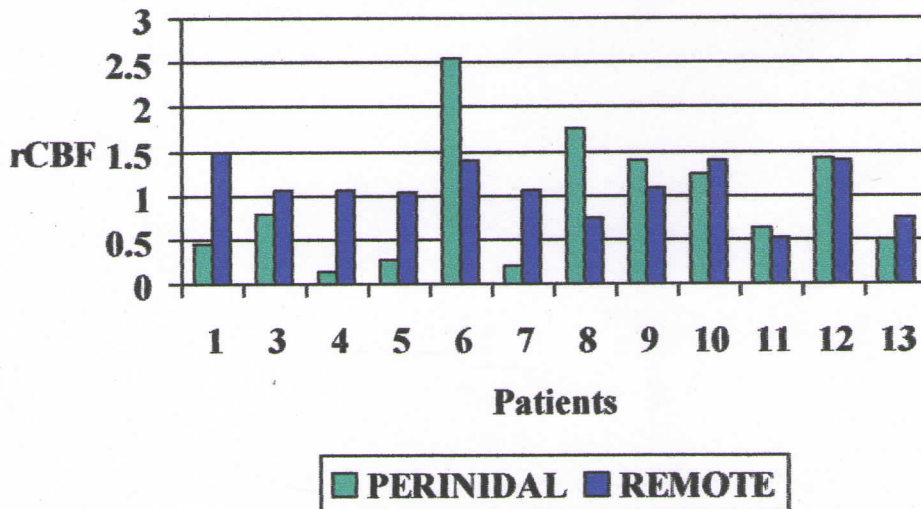
Baseline perinidal r CBF



Baseline rCBV



Baseline rCBF



POSTEMBOLISATION MR PERFUSION STUDY

Out of 13 cerebral AVM patients, 8 patients underwent follow up MR perfusion study. The time gap between embolization and MR study was from 2 days to 1 month.

Angiographically, significant nidus obliteration (40 to 90%) achieved in nearly all patients in one or multiple settings. Obliteration of macro-arteriovenous fistula achieved in 2 cases.

Pre- and post-embolization perfusion MR imaging and cerebral angiogram was correlated.

Perfusion defect within the embolized portion of the nidus was seen in most patients.

The final MR imaging revealed decreased AVM size and perfusion disturbances.

As a rule, postembolisation perfusion MR has shows decreased in nidal rCBV with return of intranidal rMTT towards 1 suggestive of decrease in intranidal arterio-venous shunting. Only exception being was case 3 in whom perfusion study has not shown any decrease in perfusion values (rCBV & rCBF) correlating with the final check angiogram which show only mild decrease in the arteriovenous shunt without any significant reduction of the nidus after 20 ml of absolute alcohol injection.

Furthermore, there was a trend of reversal of perfusion abnormality in mediate perinidal regions and remote brain parenchyma after the embolization. Five patients showed decreased immediate perinidal rCBV that increased to 1 after embolisation in 3 patients. Similarly, in 6 patients immediate perinidal rMTT was reduced and it increased to 1 in 3 patients after embolisation.

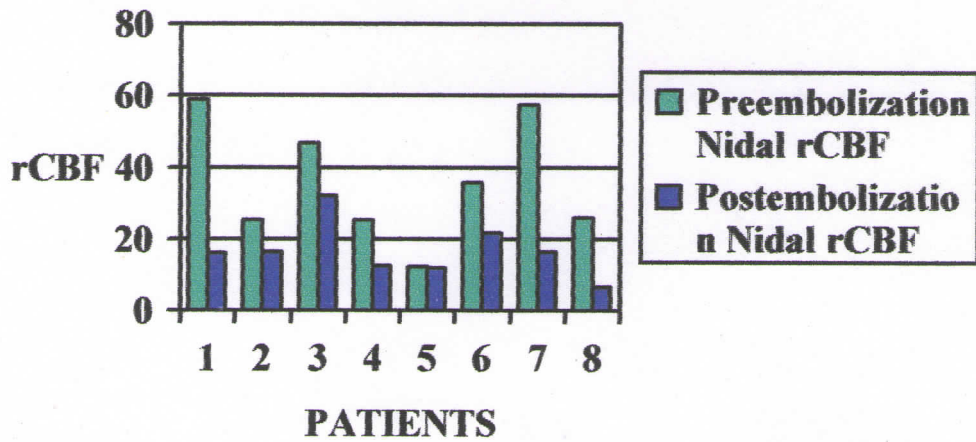
Table 6 : PRE AND POST EMBOLISATION MR PERFUSION

Case No	Pre embolisation			Post Embolisaton			
	rCBV	rCBF	rMTT	rCBV	rCBF	rMTT	
1	N	↑	↑	↓	↓	Normal	
	IPN	↓	↓	↓	→	→	
	R	↓	↓	Normal	↓	↓	Normal
2	N	↑	↑	↓	↓	Normal	
	IPN	A↑ / P↓	A↑ / P↓	↓	A↑ / P↓	A↑ / P↓	→
	R	↓	↓	Normal	↑	↑	Normal
3	N	↑	↑	↓	→	→	
	IPN	↓	↓	↓	↓↓	↓↓	↓
	R	Normal	Normal	Normal	Normal	Normal	Normal
4	N	↑	↑	↓	↓	↓	
	IPN	↓	↓	Normal	↓↓	↓↓	Normal
	R	Normal	Normal	Normal	Normal	Normal	Normal
5	N	↑	↑	Normal	↓	↓	↓
	IPN	↓	↓	Normal	↑	↑	Normal
	R	Normal	Normal	Normal	Normal	Normal	Normal
6	N	↑	↑	Normal	↓	↓	Normal
	IPN	↑	↑	Normal	↓	↓	Normal
	R	↑	↑	Normal	↓	↓	Normal
7	N	↑	↑	↓	↓	↑	
	IPN	↓	↓	↓	↑	↑	Normal
	R	Normal	Normal	Normal	Normal	Normal	Normal
8	N	↑	↑	↓	↓	Normal	
	IPN	↑	↑	↓	↓	↓	
	R	↑	↑	↓	↓	↓	→

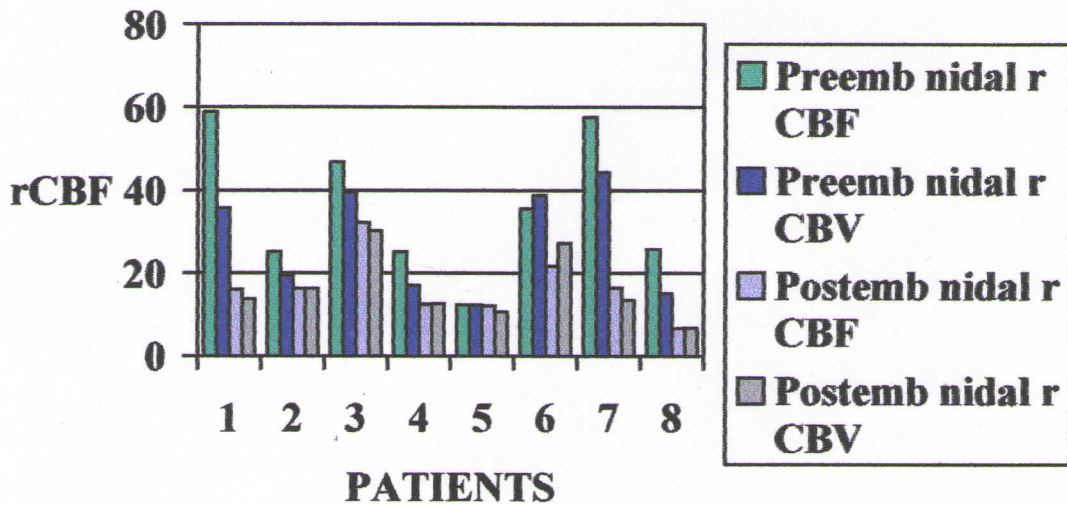
Table 7 : POST-EMBOLISATION MR PERFUSION

Cases	Nidal	Perinidal	Remote
1	↓	→	↓
2	↓	A↓ / P↑	↑
3	↓	↓	↓
4	↓	↓	Normal
5	↓	↑	Normal
6	↓	↓	↓
7	↓	↑	Normal
8	↓	↓	↓

PRE-AND POST-EMBOLIZATION NIDAL rCBF



PRE-AND POST-EMBOLIZATION NIDAL rCBF & rCBV



CASES ILLUSTRATION :

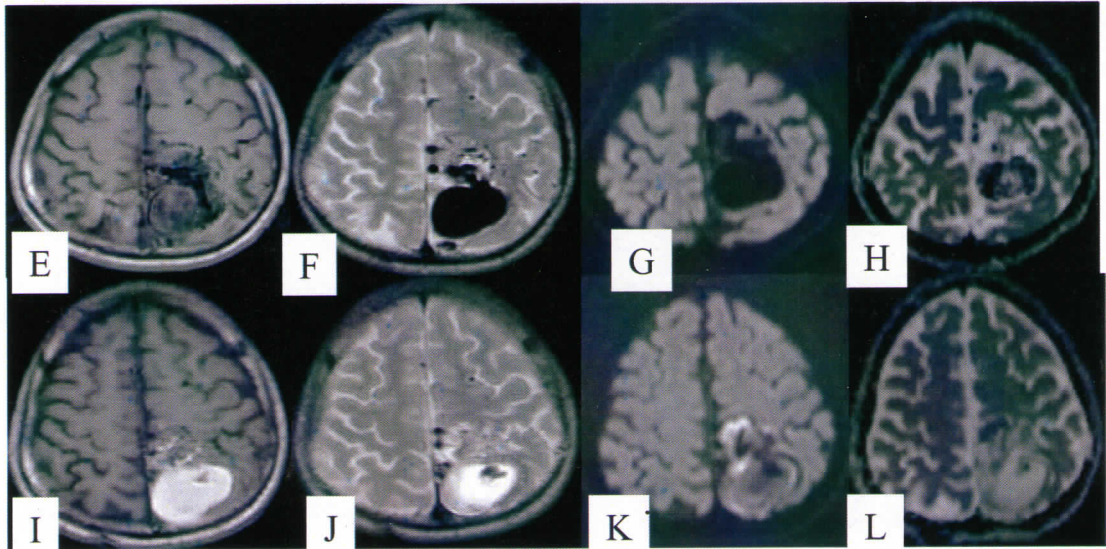
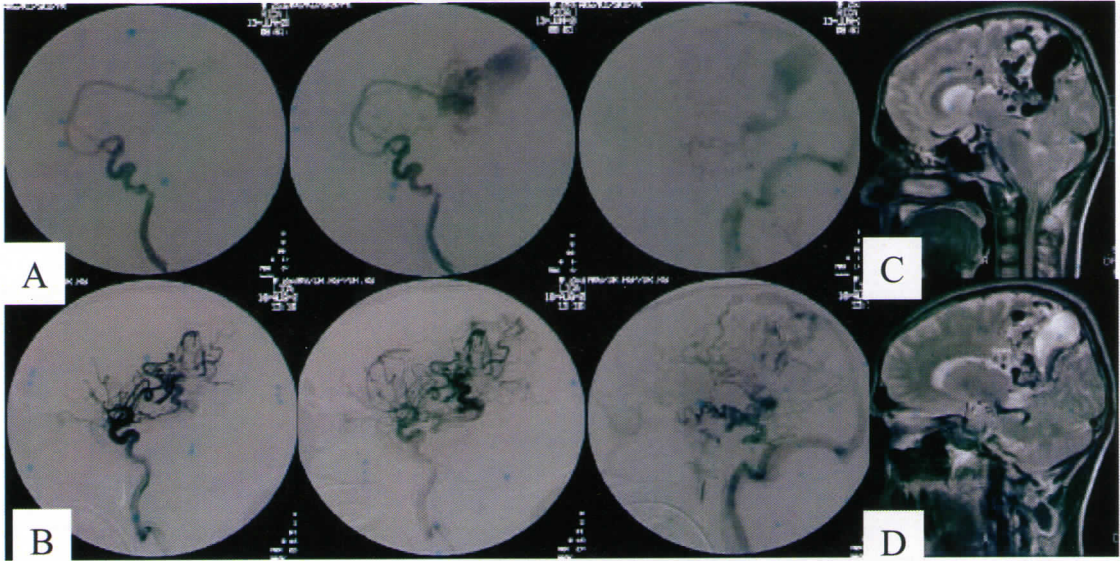
Case 1: This 37 year old male patient presented with history of chronic headache not associated with vomiting. CT scan was done to rule out any structural lesion, and found to have a large AVM in left parietal region. On examination, patient had no focal neurological deficit. Preprocedural diagnostic angiogram revealed left parietal high flow AVM with single hole AVF between the feeder artery and large draining venous sac. The patient underwent 2 setting of embolisation in 2-month period and was studied with MR imaging thrice, before and after each setting of embolisation. The two consecutive MRIs after each setting of embolisation revealed progressive thrombosis of the venous sac. The large venous sac was hypointense in all pulse sequence before the embolisation and after 2nd embolisation, the MR study display hyperintense signal intensity in all pulse sequences suggestive of subacute thrombus.

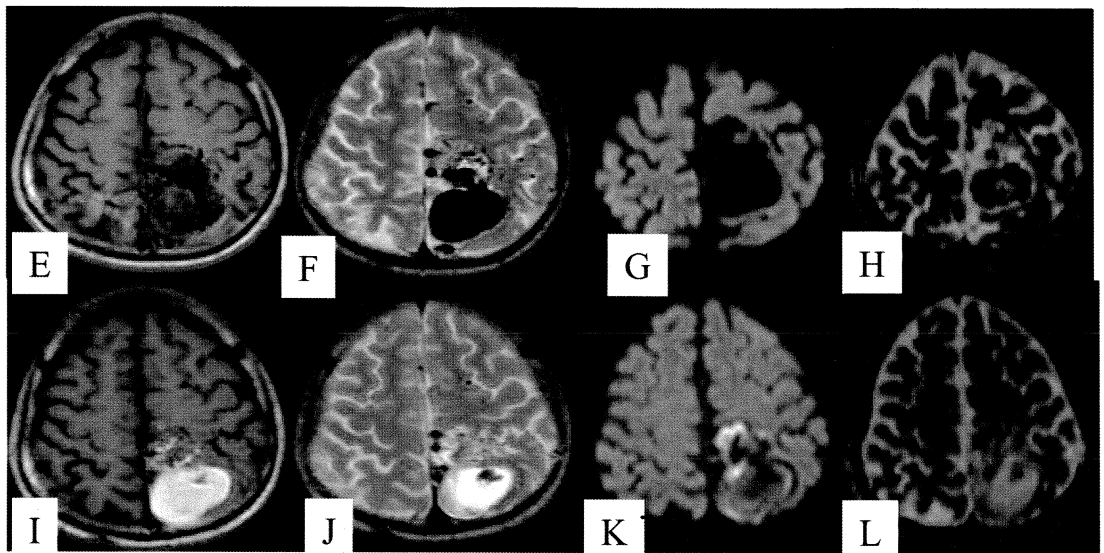
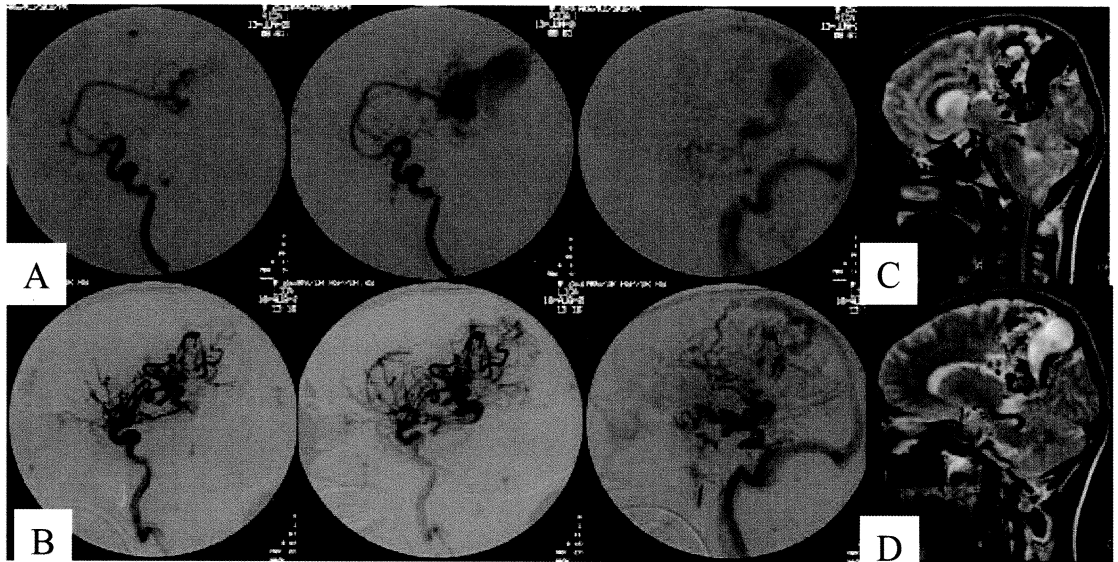
On DWI, the thrombosed venous sac shows restriction (hyperintense signal intensity) in the periphery and no restriction (hyperintense signal intensity) in the center.

Additional area of restriction is noted in immediate perinidal region on DWI on the final post embolisation MR study suggestive of perinidal ischaemic infarct. The nidus volume decreased from

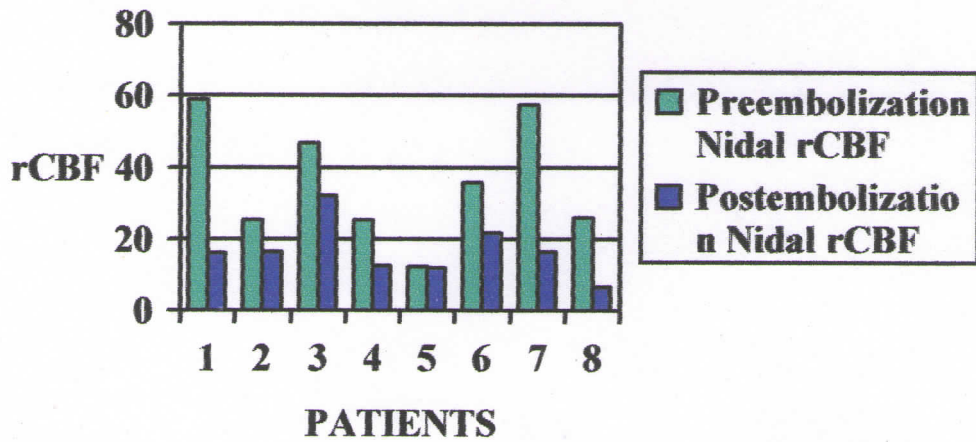
baseline 53.5ml (before embolization) to 37.7ml after 2nd embolisation.

Perfusion study demonstrates decreased nidal perfusion (rCBV & rCBF) and intranidal rMTT returns towards 1 (rMTT=0.33) suggestive of decrease intranidal arteriovenous shunting, which is well correlated with the post embolisation final angiogram. The patient had one simple hole macro-arteriovenous fistula which was embolised with 80% glue and rest of the nidus feeding from the proximal feeder artery was embolised with 22% glue achieving nearly 80-90% obliteration of the nidus. There was no change in immediate perinidal perfusion from the baseline perfusion, however, remote perfusion in frontal lobe decreased.





PRE-AND POST-EMBOLIZATION NIDAL rCBF



PRE-AND POST-EMBOLIZATION NIDAL rCBF & rCBV

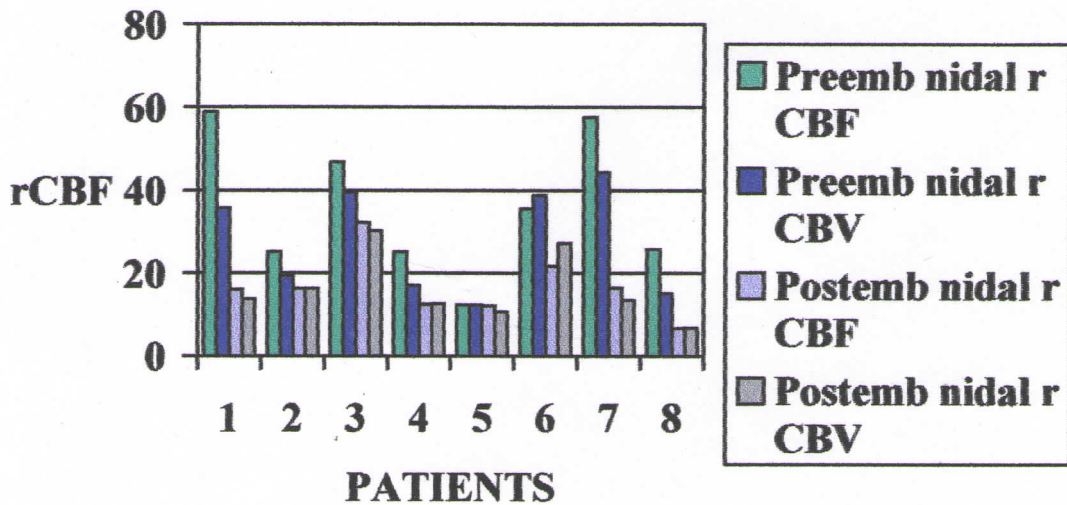
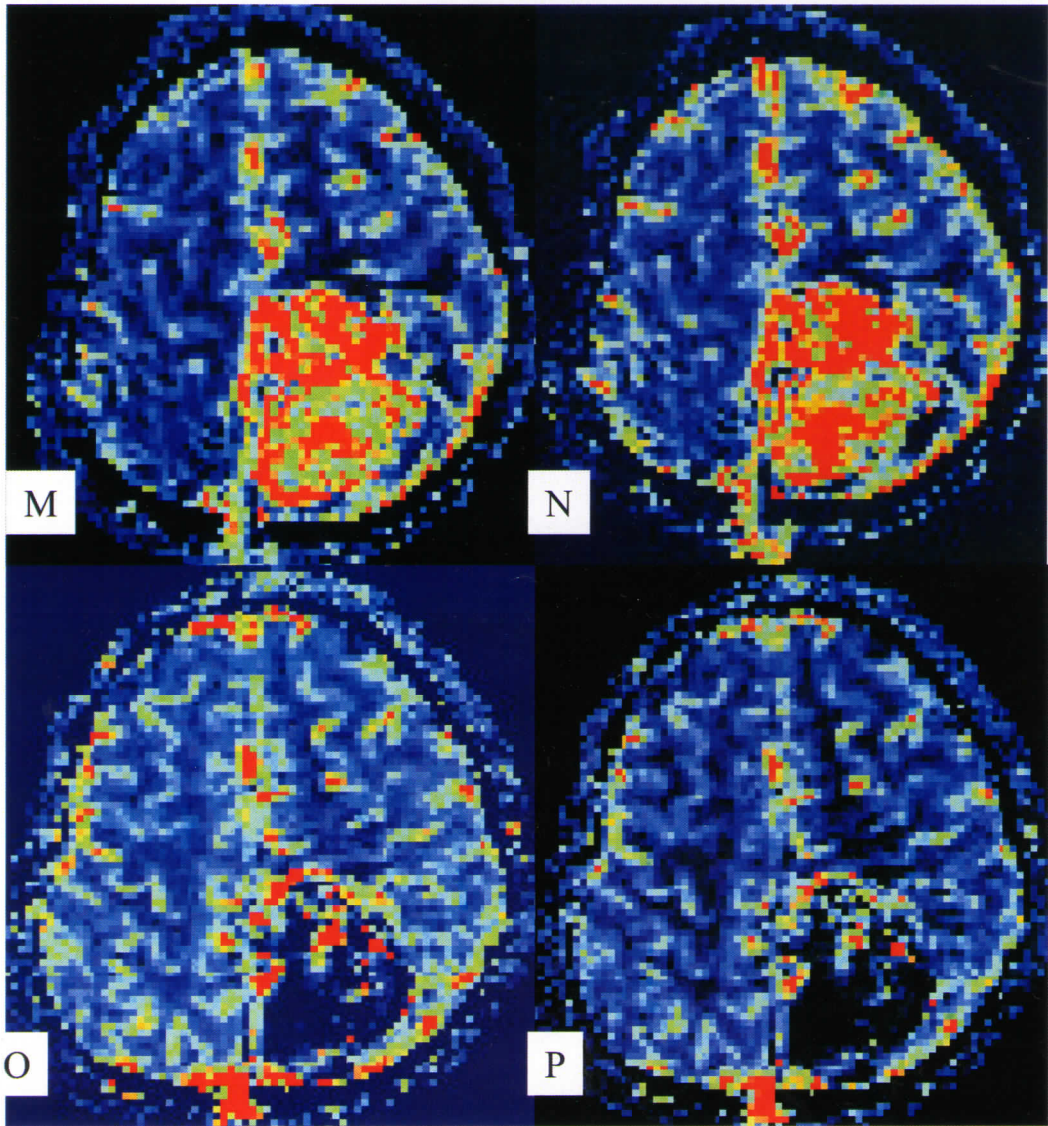


Fig. 1 :Case 1 : MR Perfusion study before and after embolisation

Preembolisation high nidal rCBV (M) and rCBF (N) .

Postembolisation perfusion study revealed no flow within the venous aneurysm and marked reduction of nidal rCBV(O) and rCBF (P) .



Case 2: This 29 year old female had presented with history of two episodes of LOC and one episode of speech arrest. At the time of presentation , her neurological status was normal. Cerebral angiogram revealed left insular large high flow compact nidus AVM . Multiple feeders were noted from sylvian branches of left MCA and venous drainage was to the superficial venous system. Patient underwent two setting of embolization ; second setting of embolization was done after 6 weeks of first embolization. Onyx was used in the first setting and n-BCA (20%) was used to embolize the feeders in the second setting.

Baseline perfusion study showed differential perfusion abnormality: the perfusion was increased in immediate anterior perinidal region and decrease in posterior perinidal region.

Postembolisation MR was done after 2 day of second setting. Thrombosis of draining vein of trolard is noted. Restriction on DWI was noted at immediate posterior perinidal region. ADC values were: 0.78 to 0.9.

The perfusion deficit was reversed after the 2 setting of the embolisation and rMTT returns to normal in immediate posterior perinidal region.

In the same patient, remote brain parenchyma showed decreased perfusion anteriorly as well as posteriorly which after the embolisation increased and rMTT returns to normal.

Fig. 2 : Case2 : Left insular AVM before and after embolisation

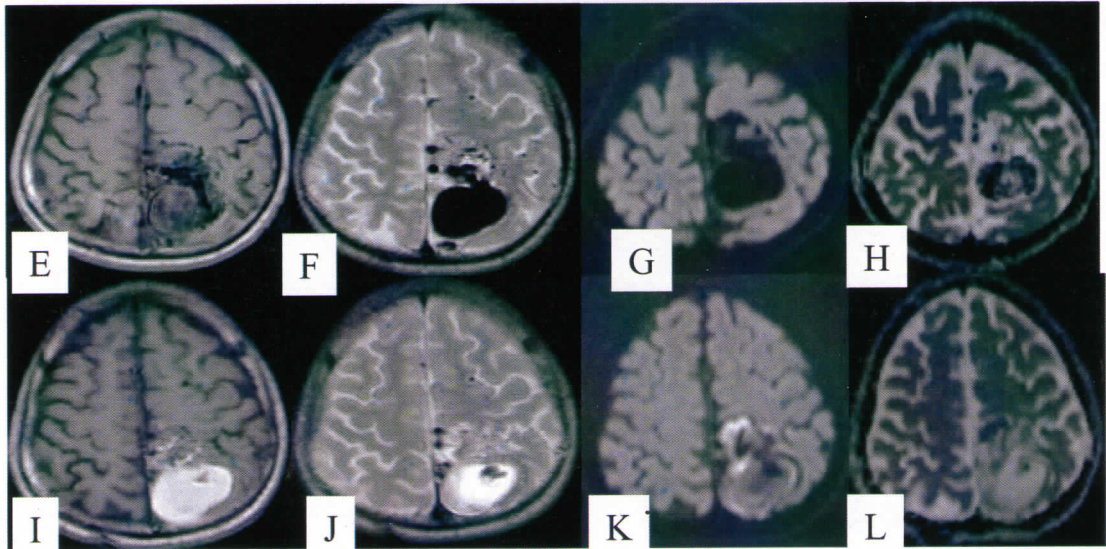
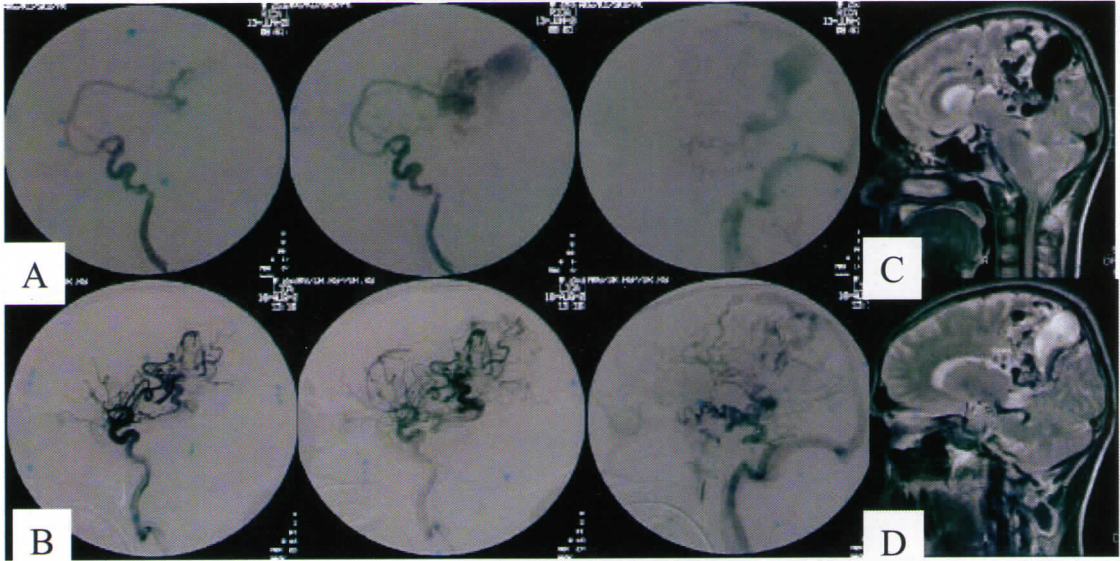
Diagnostic angiogram showed compact nidus, high flow AVM.

Final check angiogram after 2 setting of embolisation (Onyx & n-BCA) revealed 80 % reduction in nidus.

Pre embolisation FLAIR (C) and T1W (D), showed Left insular AVM nidus without any restriction on DWI (E) and ADC (F) .

Postembolisation FLAIR (G) and axial T1W (H) revealed nidal hyperintensity.

DWI (I) and ADC (J), revealed focal area of restriction in posterior perinidal region suggesting cytotoxic edema/infarct.



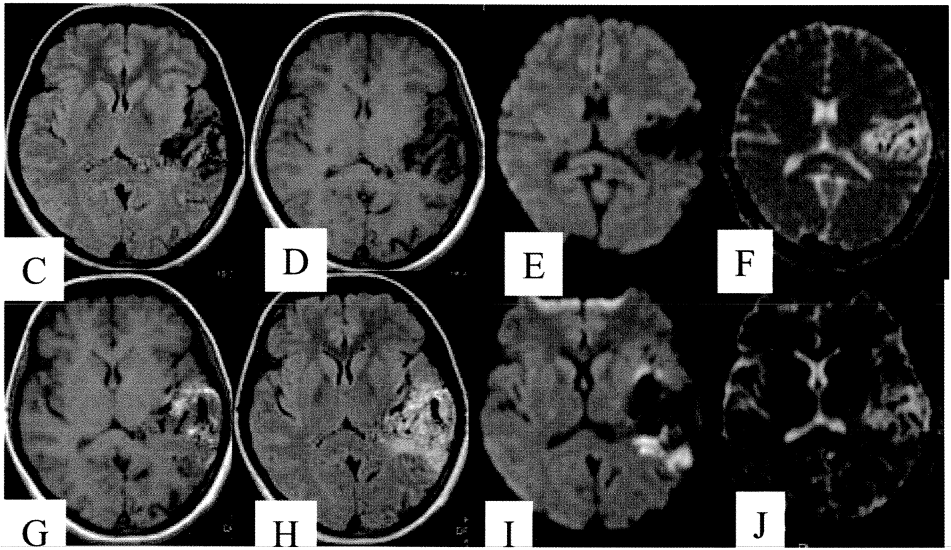
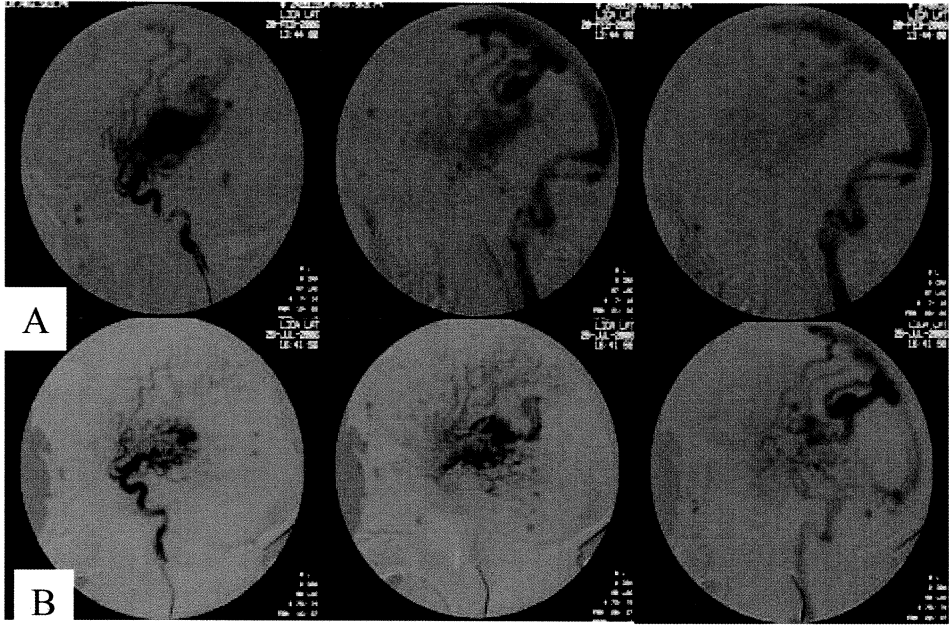
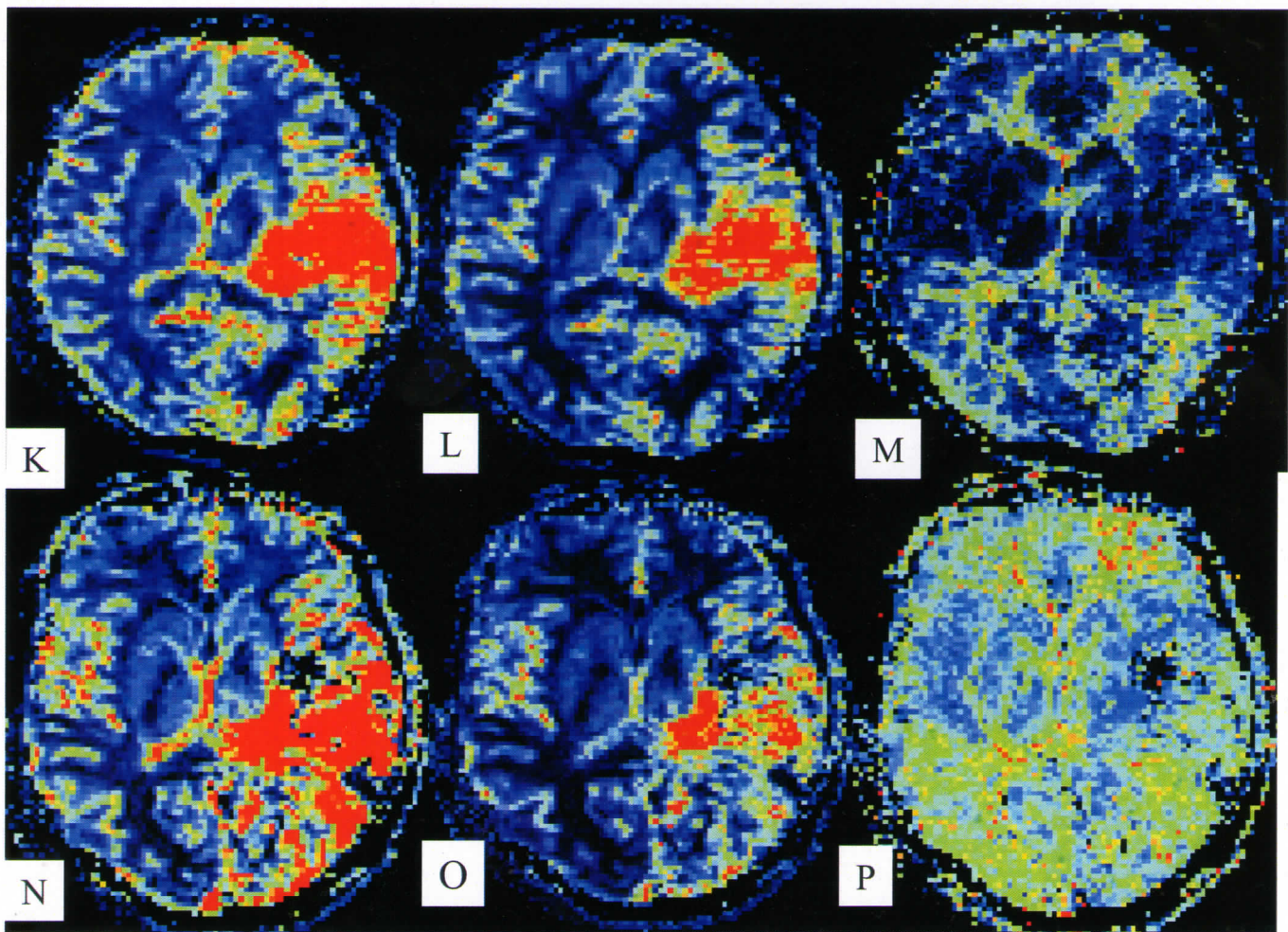


Fig. 2 :Case 2 : MR Perfusion study before and after embolisation

Preembolisation high nidal rCBV (K) and rCBF (L) and decreased nidal rMTT.

Postembolisation nidal rCBV (N) and rCBF (O) are markedly reduced and nidal rMTT increased to 1. rMTT pre- and post embolisation (M & P respectively).



Case 2: This 29 year old female had presented with history of two episodes of LOC and one episode of speech arrest. At the time of presentation , her neurological status was normal. Cerebral angiogram revealed left insular large high flow compact nidus AVM . Multiple feeders were noted from sylvian branches of left MCA and venous drainage was to the superficial venous system. Patient underwent two setting of embolization ; second setting of embolization was done after 6 weeks of first embolization. Onyx was used in the first setting and n-BCA (20%) was used to embolize the feeders in the second setting.

Baseline perfusion study showed differential perfusion abnormality: the perfusion was increased in immediate anterior perinidal region and decrease in posterior perinidal region.

Postembolisation MR was done after 2 day of second setting. Thrombosis of draining vein of trolard is noted. Restriction on DWI was noted at immediate posterior perinidal region. ADC values were: 0.78 to 0.9.

The perfusion deficit was reversed after the 2 setting of the embolisation and rMTT returns to normal in immediate posterior perinidal region.

In the same patient, remote brain parenchyma showed decreased perfusion anteriorly as well as posteriorly which after the embolisation increased and rMTT returns to normal.

Fig. 2 : Case2 : Left insular AVM before and after embolisation

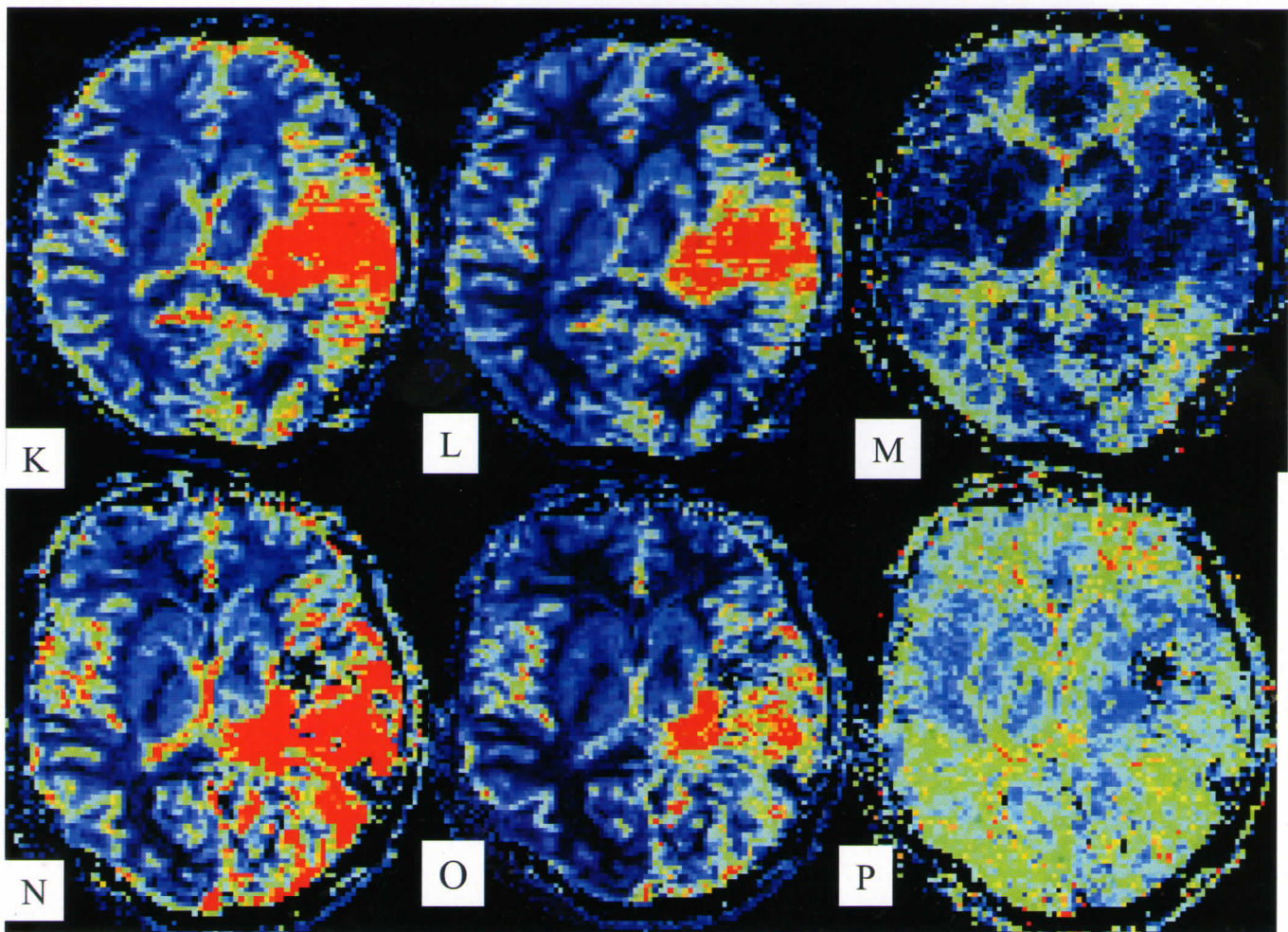
Diagnostic angiogram showed compact nidus, high flow AVM.

Final check angiogram after 2 setting of embolisation (Onyx & n-BCA) revealed 80 % reduction in nidus.

Pre embolisation FLAIR (C) and T1W (D) , showed Left insular AVM nidus without any restriction on DWI (E) and ADC (F) .

Postembolisation FLAIR (G) and axial T1W (H) revealed nidal hyperintensity.

DWI (I) and ADC (J), revealed focal area of restriction in posterior perinidal region suggesting cytotoxic edema/infarct.



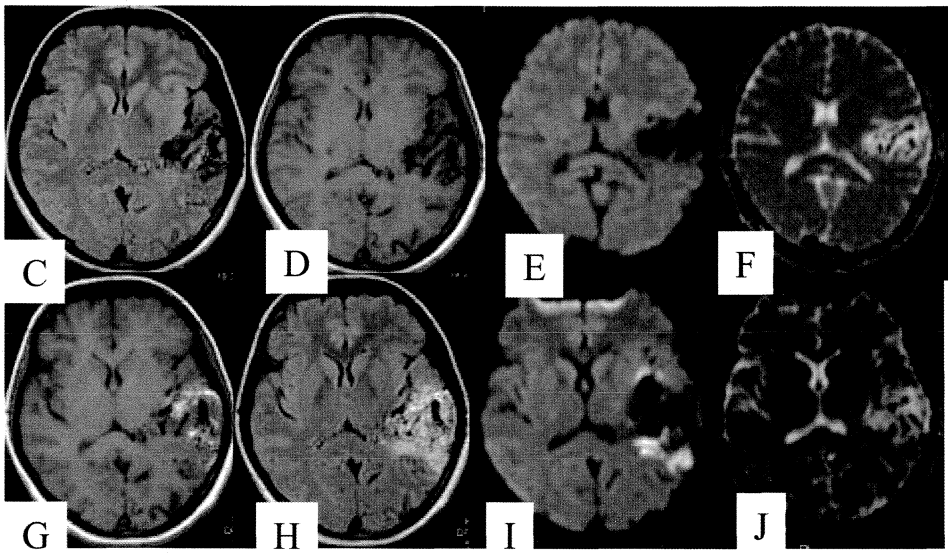
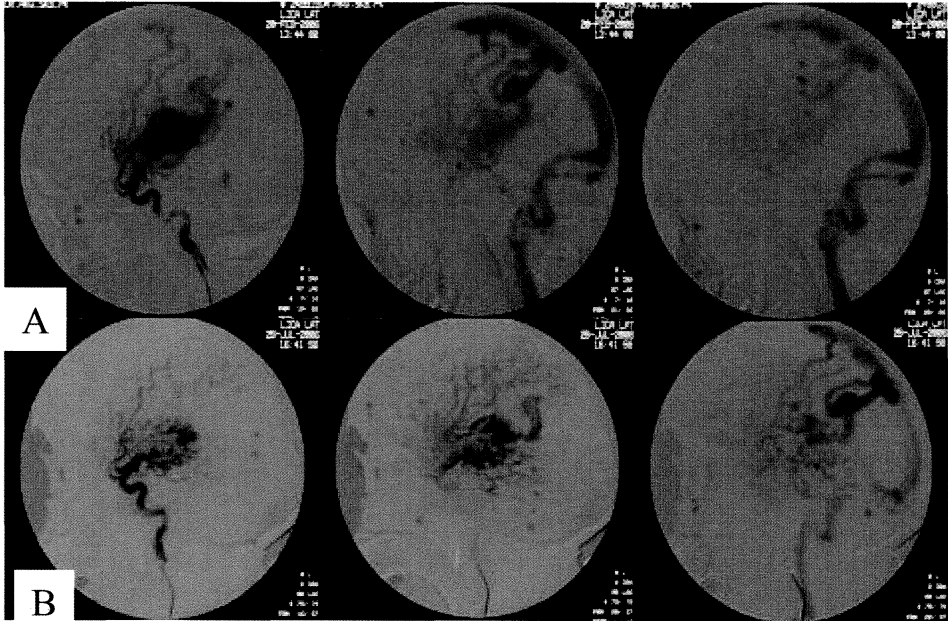


Fig. 2 :Case 2 : MR Perfusion study before and after embolisation

Preembolisation high nidal rCBV (K) and rCBF (L) and decreased nidal rMTT.

Postembolisation nidal rCBV (N) and rCBF (O) are markedly reduced and nidal rMTT increased to 1. rMTT pre- and post embolisation (M & P respectively).

Case 3: This 15 years female patient presented with history of sudden onset of severe headache with seizures followed by LOC, 8 months back. CT head showed left frontal hemorrhage with perilesional edema. MRI scan revealed serpiginous flow voids adjacent to the hematoma in left frontal lobe suggestive of AVM. Diagnostic angiogram showed left premotor cortex AVM fed by pre-rolandic and rolandic branch of left MCA and venous drainage was via superficial cortical vein to superior sagittal sinus. The patient underwent embolisation after 8 months. The pre-rolandic feeder was embolised using 20 ml of absolute alcohol. The patient had 3 episodes of focal seizures and had right UMN facial palsy with right hemiparesis within 24 hours of alcohol embolization. CT head after 24 hour revealed perinidal white matter edema. MR study done after 10 days of embolisation showed moderate perinidal vasogenic edema without any restriction on DWI and ADC maps.

The possible explanation for perinidal vasogenic edema are:

1. Postembolisation thrombosis of feeding artery, nidus as well as the draining veins, as the venous thrombosis most commonly cause vasogenic edema rather than cytotoxic edema.
2. Alcohol extravasation in the perinidal region causing cellular injury but as the imaging was done on the 10th day, vasogenic edema rather than cytotoxic edema was observed.

Focal subacute bleed is also noted anterior to the nidus, hyperintense on T1W, and iso to hypointense on T2W images.

Pre-embolization perfusion in immediate perinidal region were low and after the embolization, the perfusion decreased substantially and even in some of the ROI, the rCBV was 0 and rCBF was as low as 0.8. However, there was no decrease of intranidal perfusion suggesting no significant intranidal AV shunt reduction, as it was shown by the final angiogram. The patient was managed conservatively with antiedema measures and was recovered near-completely with except for finer movements of right hand and slight decrease in speech output.

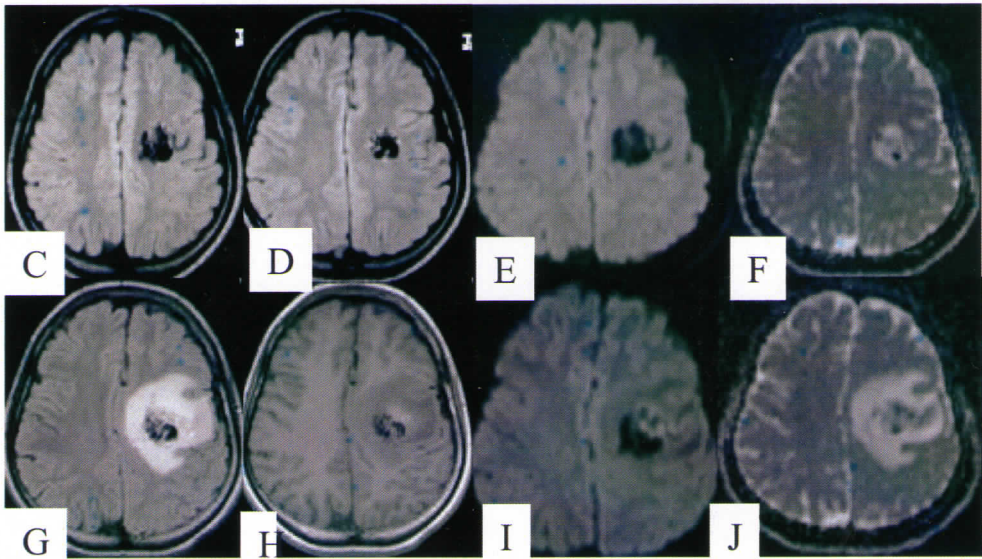
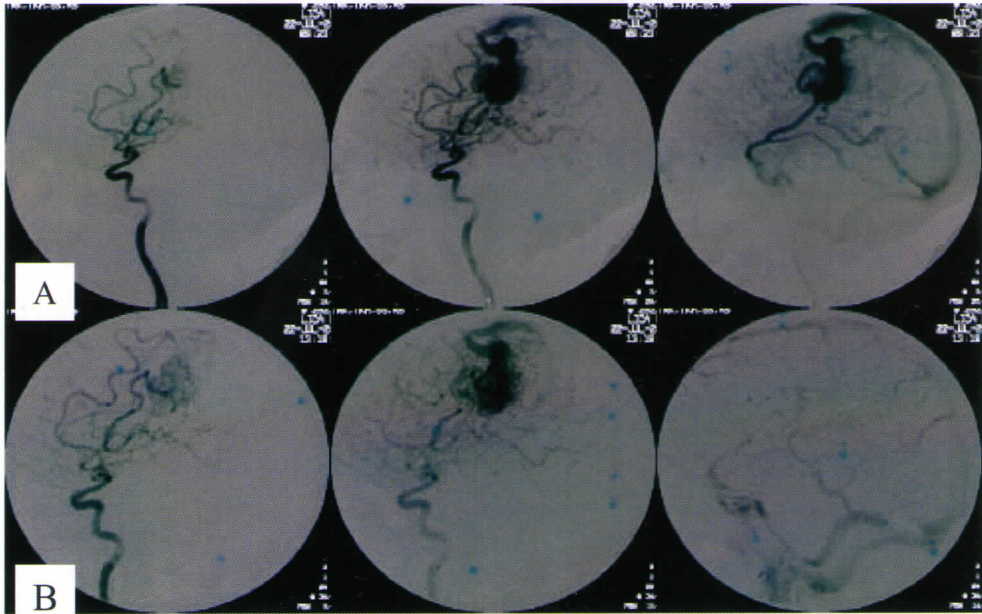
Fig. 3 : Case 3 : Premotor cortex AVM before and after embolisation

Diagnostic angiogram showed compact nidus, high flow AVM.

Final check angiogram after 20 ml of absolute alcohol, revealed marked reduction in arteriovenous shunting.

Pre embolisation FLAIR (C, D), DWI (E) and ADC (F) showed compact AVM nidus in corona radiata without any restriction.

Postembolisation FLAIR (G), axial T1W (H), DWI(I) and ADC (H), after 20 ml of absolute alcohol injection, revealed moderate perinidal edema and focal bleed in immediate anterior perinidal region. No restriction is noted in the perinidal edema on DWI suggesting vasogenic nature; focal area of restriction is noted in anterior perinidal region suggesting intraniadal thrombosis and/or bleed.



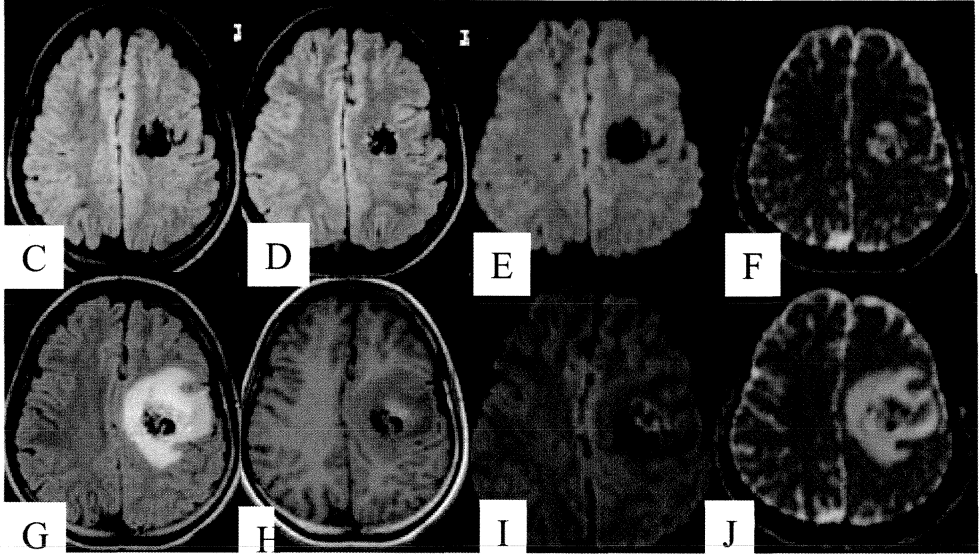
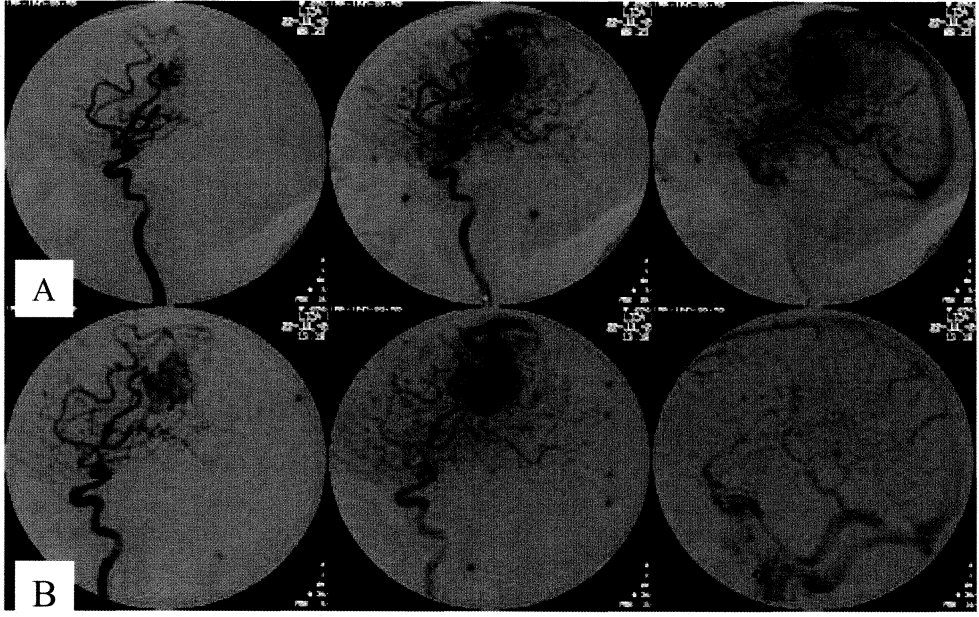


Fig. 3 : Case 3 : MR Perfusion study before and after embolisation

Preembolisation high nidal rCBV (K) and rCBF (L) .

Postembolisation nidal and perinidal rCBV (M) and rCBF (N) are markedly reduced .

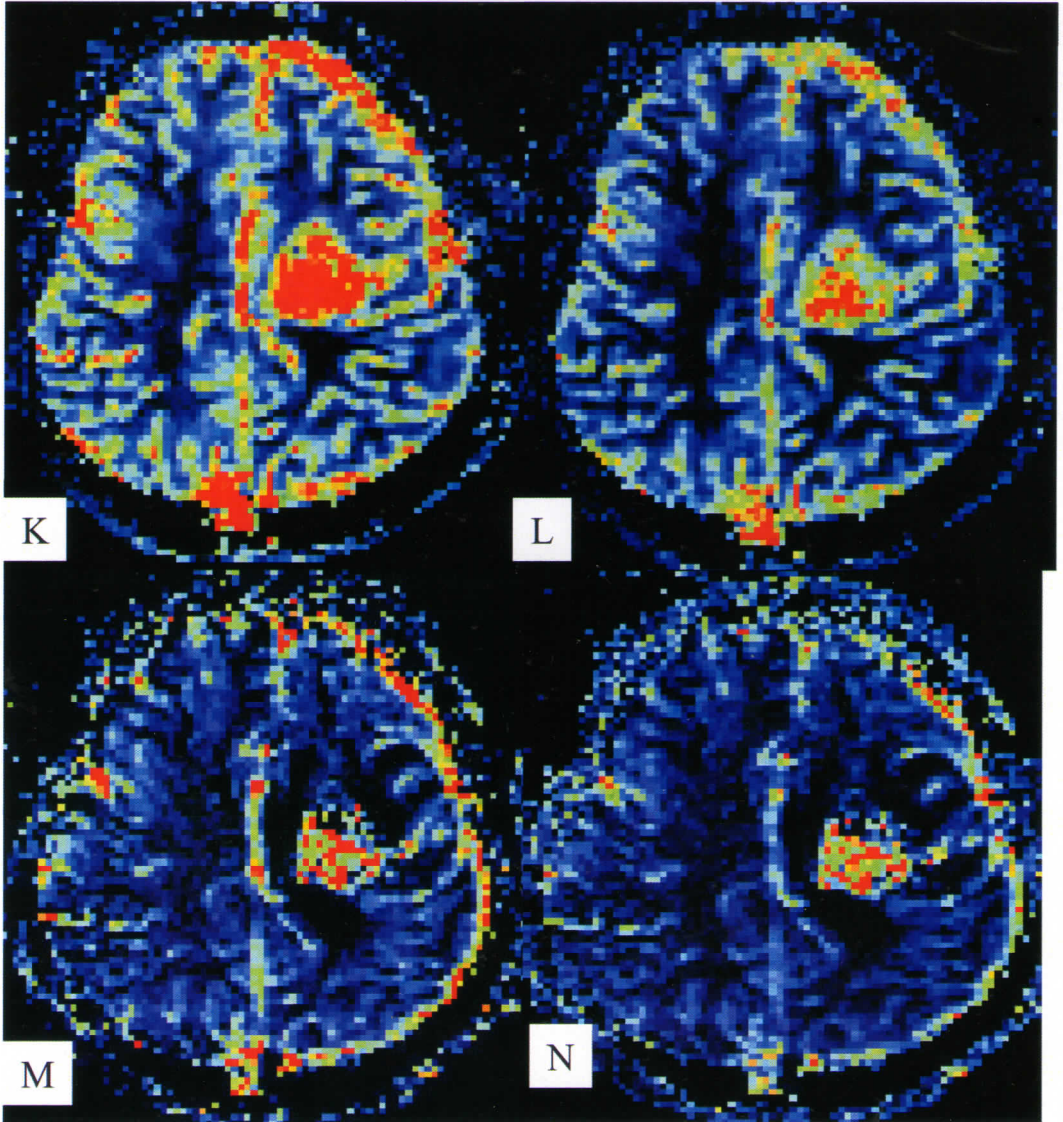
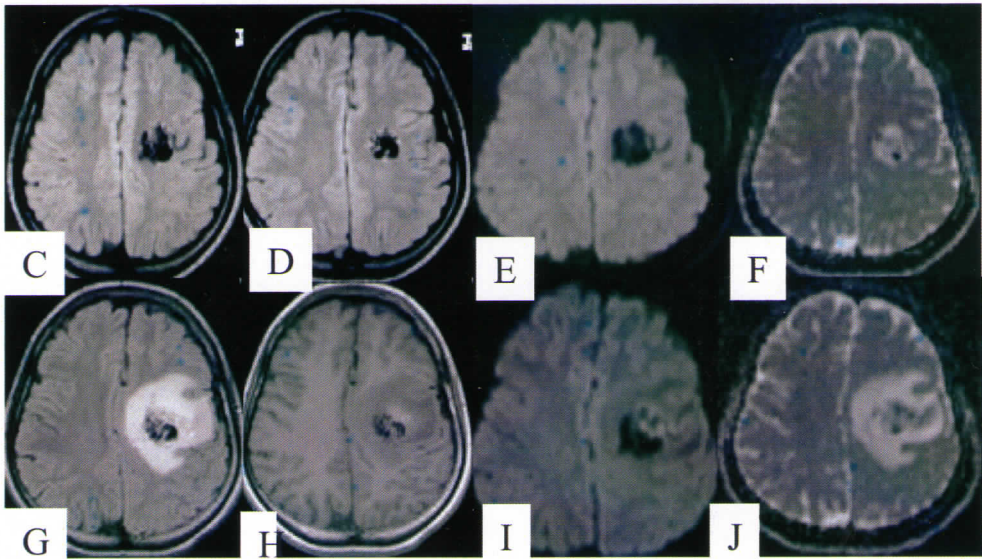
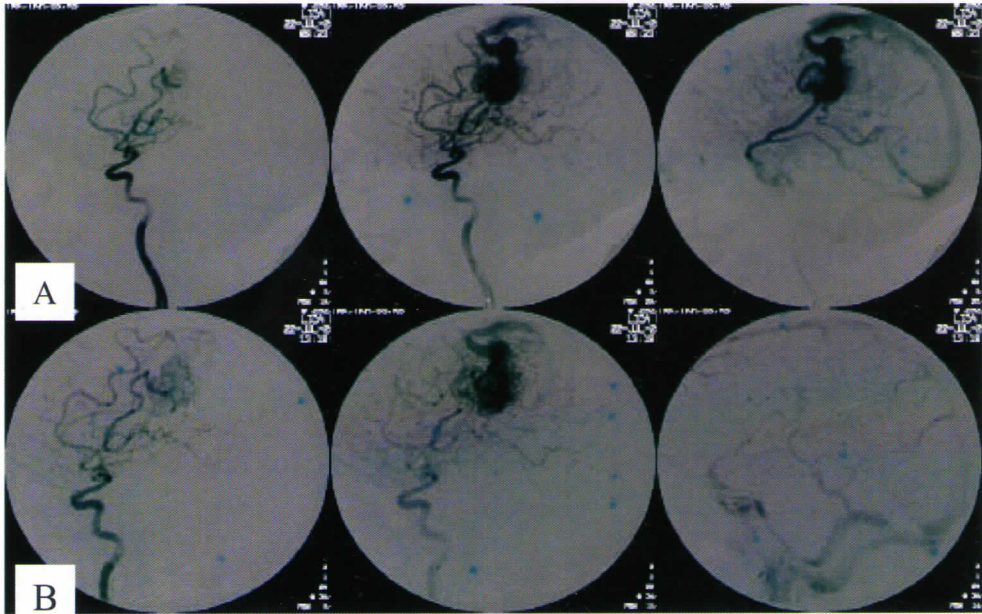


Fig. 4 : Case 4 : Left temporal AVM before and after embolisation

Diagnostic angiogram (A) showed left temporal, compact nidus high flow AVM, draining to deep venous system.

Final check angiogram (B) after 27 ml of absolute alcohol, revealed marked reduction in arteriovenous shunting.

Postembolisation DWI (C, D) and ADC (E, F), axial T2W (G,H) , T1W (I) and CT (J), after 27 ml of absolute alcohol injection, revealed moderate perinidal edema and focal bleeding immediate anterior perinidal region. Also noted is the cytotoxic edema in the left inferior gyrus.



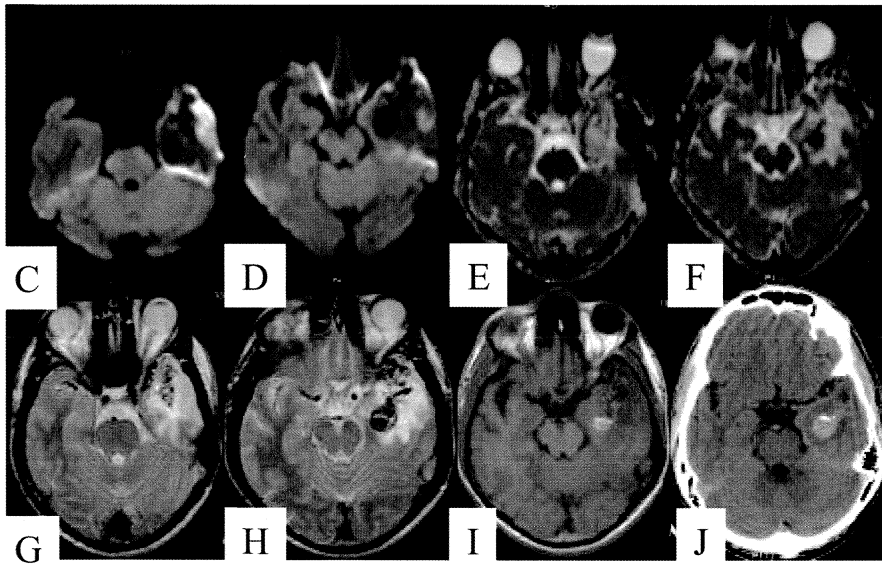
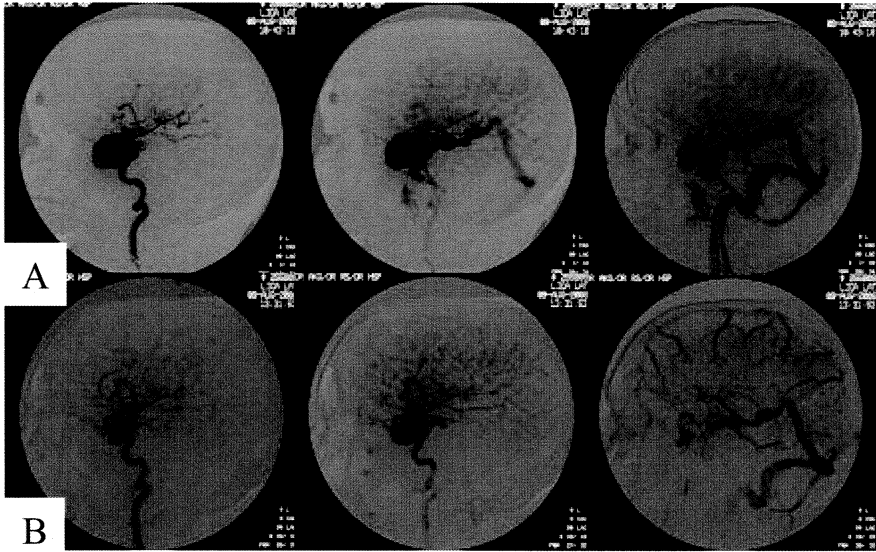
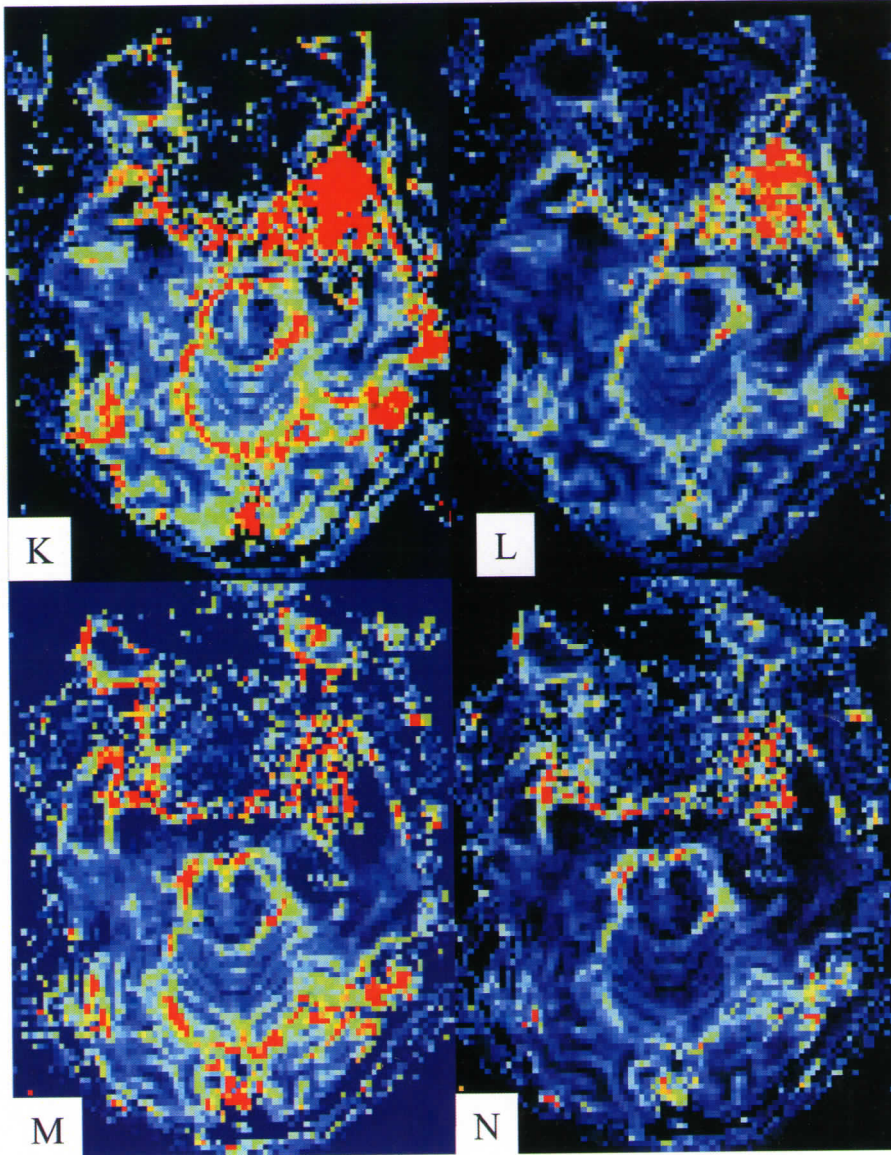


Fig. 4 : Case 4 : MR Perfusion study before and after embolisation

Preembolisation high nidal rCBV (K) and rCBF (L) .

Postembolisation nidal and perinidal rCBV (M) and rCBF (N) are markedly reduced .



Case 5 : This 20 year old male patient presented with severe headache with vomiting and LOC; CT head revealed left thalamic bleed. Cerebral angiogram revealed compact nidus AVM in left thalamic region fed by multiple thalamogeniculate perforators and feeders from left posterior choroidal artery. Posterior choroidal feeders were embolized with 3 ml of absolute alcohol followed by 20% glue.

Baseline MR study revealed no restriction within the nidus or perinidal region; the nidus appears hypointense on DWI and hyperintense on ADC maps. Baseline perfusion studies showed low perfusion in immediate perinidal region and normal perfusion in remote regions. Post embolisation MR imaging after 1 month showed T2 hyperintensity within left side of splenium of corpus callosum and was not showing any restriction on DWI suggestive of ischaemic infarct.

Fig. 5 : Case 5 : Left thalamic AVM before and after embolisation

Diagnostic angiogram (A) showed compact nidus, high flow AVM.

Final check angiogram (B) after 3 ml of alcohol and 22 % n-BCA injection, revealed no significant reduction in arteriovenous shunting.

Pre embolisation axial T1W (C), T2W (D) and FLAIR (E) showed compact AVM nidus .

Postembolisation axial T1W (F), T2W (G) and FLAIR (H) revealed no significant reduction in nidus size. Intranidal foci of linear foci of hyperintensity noted and FLAIR images suggestive of glue and /or nidal thrombosis.

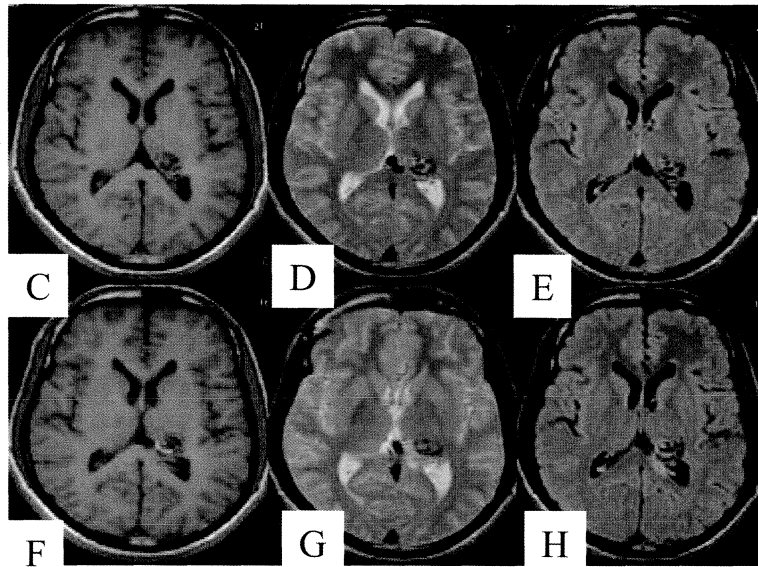
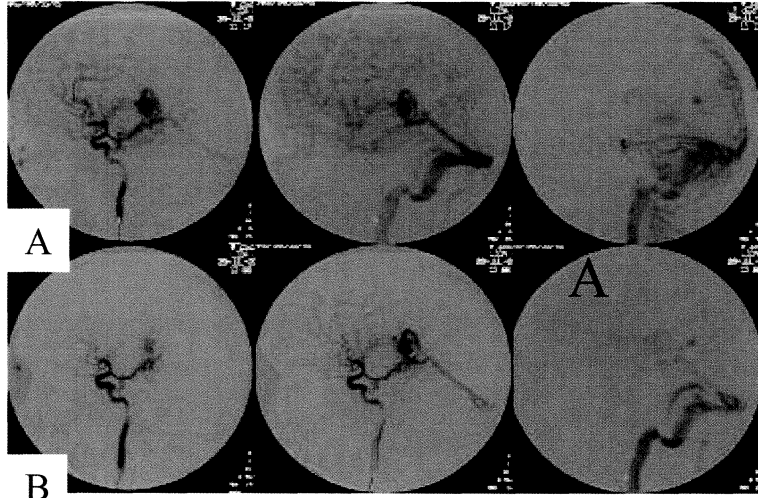
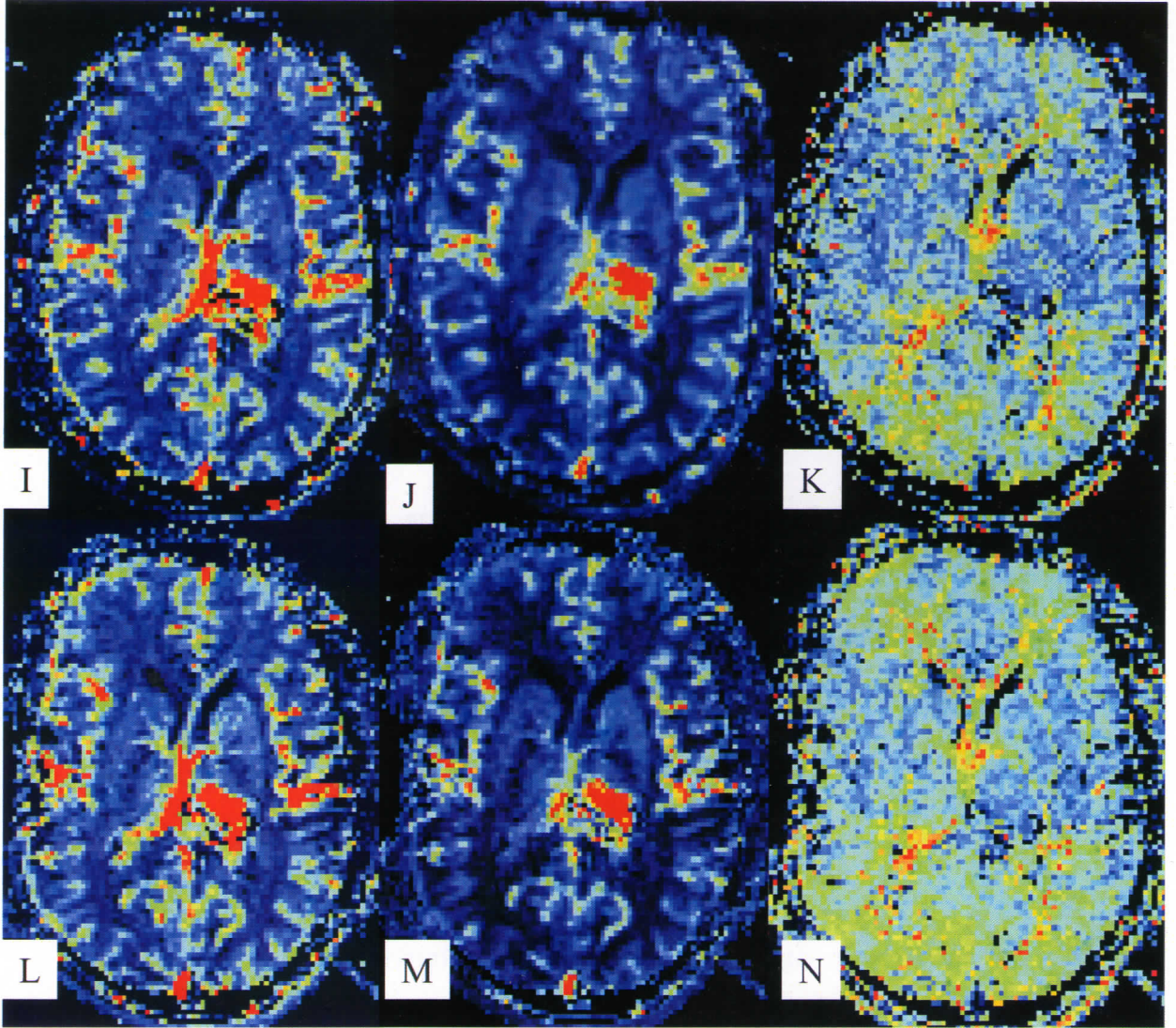


Fig. 5 : Case 5 : MR Perfusion study before and after embolisation

Preembolisation high nidal rCBV (I) and rCBF (J) .

Postembolization no significant change in nidal rCBV (L) and rCBF (M) .

rMTT pre and post embolisation (K & N respectively) .



Case 6: This 48 year male patient had left sided headache for past 15 years. No history of any reduced vision or seizure or LOC. Neurological examination was within normal limits. Cerebral angiogram revealed large AVM in left occipital lobe fed by multiple feeders from left PCA and MCA and dural feeders from left middle meningeal artery , left occipital artery. Venous drainage was to superior sagittal sinus. Embolisation was done at the same time and total 5 feeders were embolised. Absolute alcohol was used in the MCA and PCA feeders, PVA particles in the dural feeders and n-BCA (20 %) was used in left middle meningeal feeder.

Baseline MR study revealed neither perinidal gliotic changes nor restriction on DWI.

Postembolization MR imaging revealed focal areas of hyperintensities in nidus and perinidal region on DWI suggestive of thrombosis.

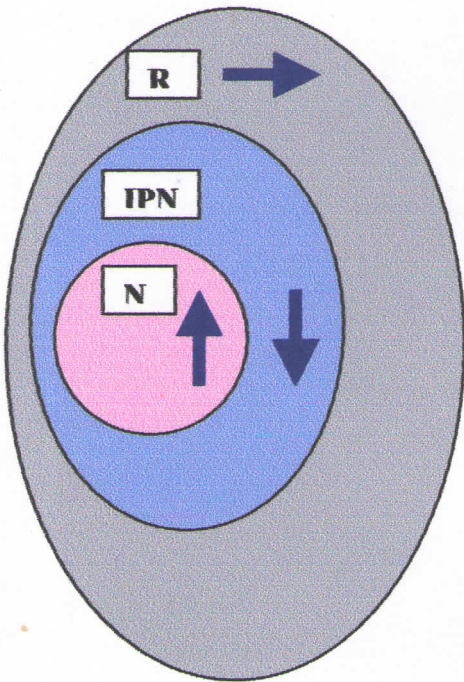
Baseline perfusion study revealed high perfusion in nidal, perinidal and remote areas. Postembolization , perfusion decreased in all three respective regions, however rMTT remain normal before and after the procedure.

Case 7. This 24 year old male patient presented with history of seizures for last 4 years. CT head showed irregular hyperdensity with mild perilesional edema in left basifrontal region. Cerebral angiogram revealed small AVM in left posterior basifrontal region with feeders from basifrontal and fronto-polar branches of left ACA. Venous drainage was via cortical vein to superficial venous sinus. Two feeders were embolised using a total of 12 ml of absolute alcohol. No postprocedure deficit noted.

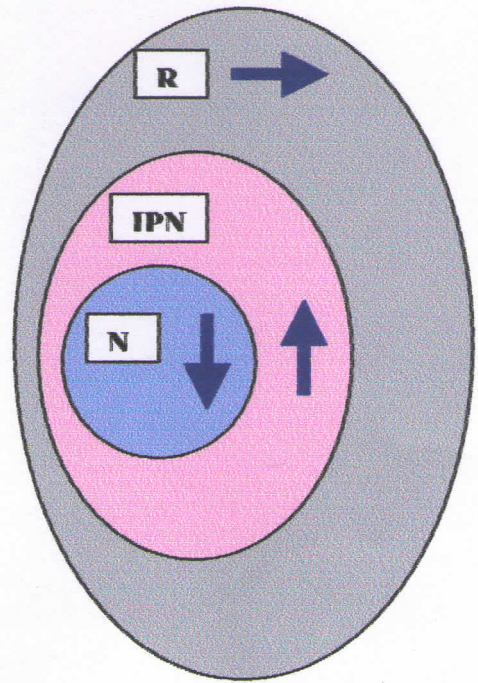
Postembolisation MR study after 2 days revealed focal areas of restriction in nidus and perinidal region in DWI suggestive of thrombosis. Postembolisation perfusion study revealed decreased intranidal as well as immediate perinidal perfusion suggesting decreased intranidal arteriovenous shunting.

CASE 5 AND CASE 7

PREEMBOLISATION

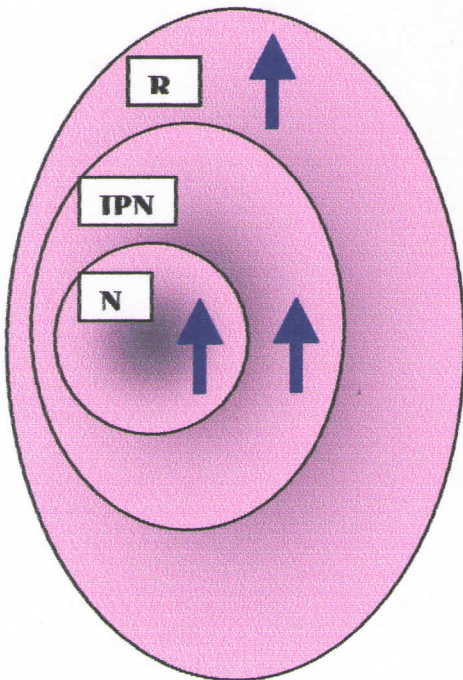


POSTEMBOLISATION

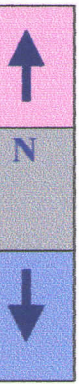
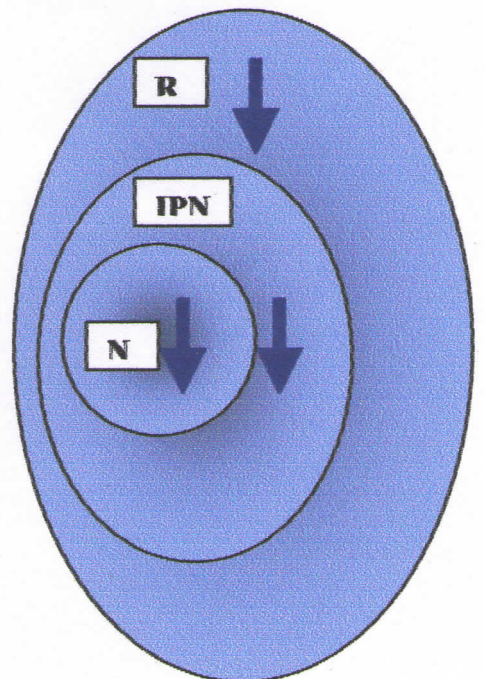


CASE 6

PREEMBOLISATION



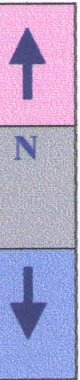
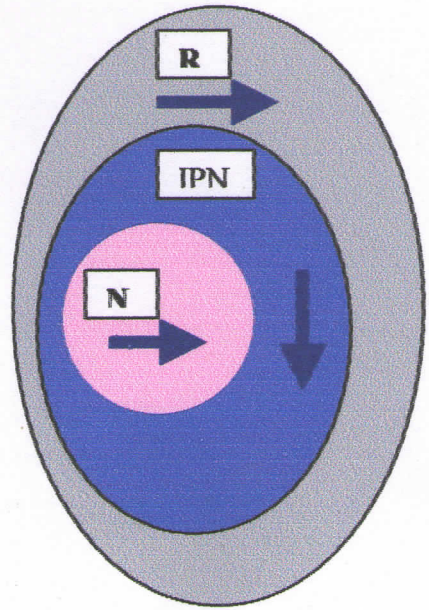
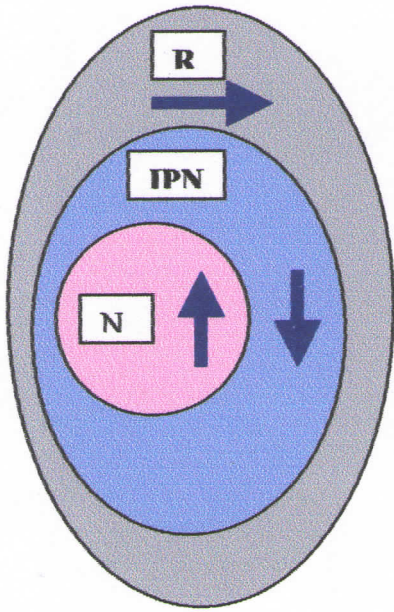
POSTEMBOLISATION



CASE 3

PREEMBOLISATION

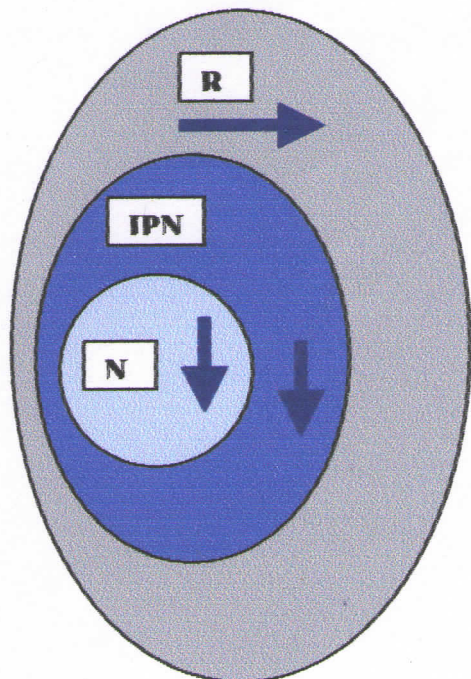
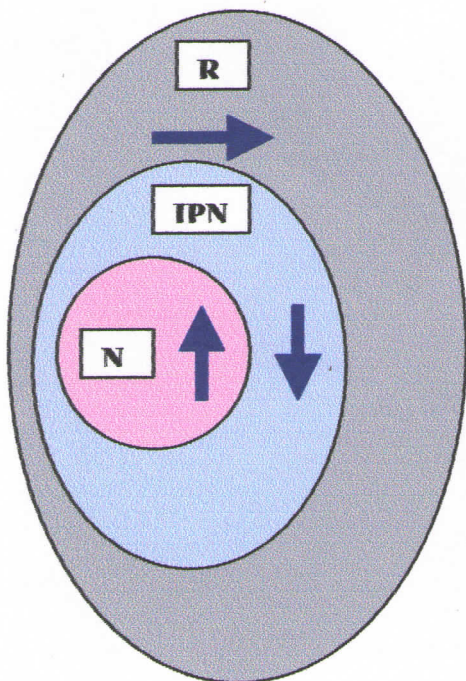
POSTEMBOLISATION



CASE 4

PREEMBOLISATION

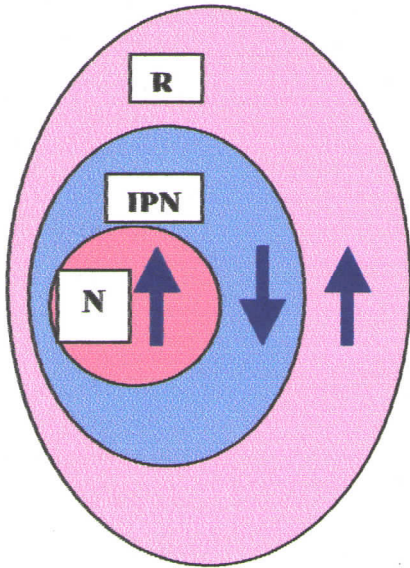
POSTEMBOLISATION



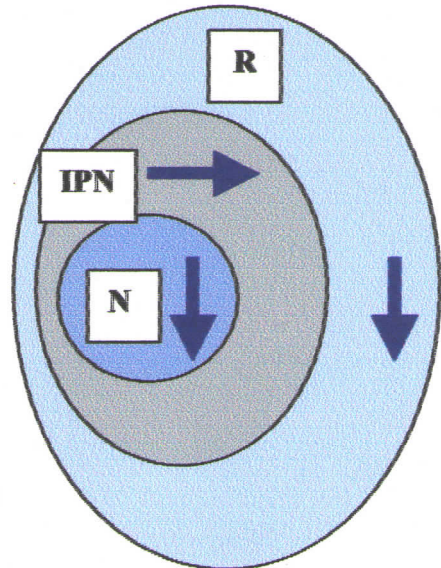
CASE ILLUSTRATIONS BEFORE AND AFTER THE EMBOLISATION

CASE1:

PREEMBOLISATION

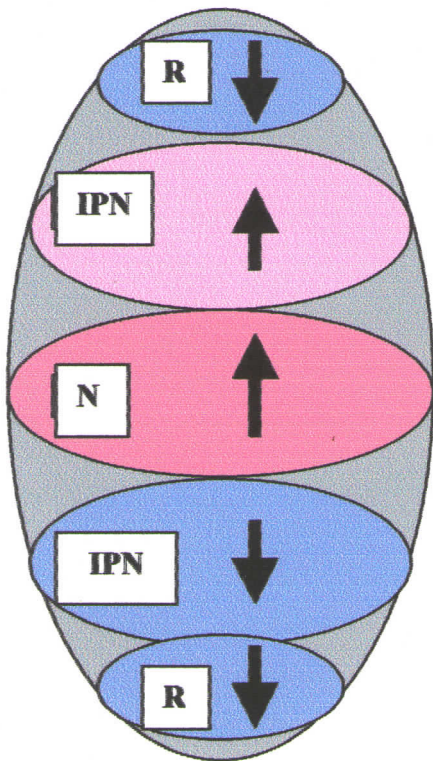


POSTEMBOLISATION

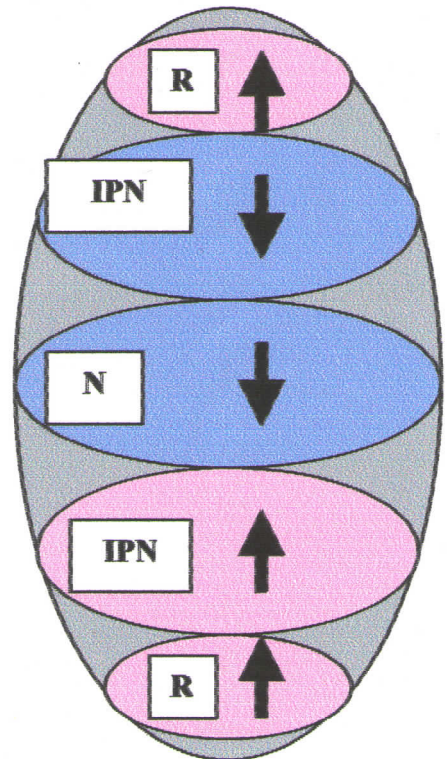


CASE 2

PREEMBOLISATION



POSTEMBOLISATION



Discussion

DISCUSSION

Thirteen patients of cerebral AVMs were studied with conventional and diffusion and perfusion MR imaging, before any intervention and 8 patients were studied after embolisation of AVM. All 8 patients show new findings on conventional MR imaging ; ischaemic lesions were noted in 4 cases (2 perinidal and 2 remote embolic infarcts), parenchymal hematoma in 3 patients, draining vein thrombosis in 2 patients and nidal hyperintensity in 5 patients.

Hemodynamic abnormalities were noted in AVM nidus as well as in immediate perinidal region in all patients. Postembolisation there was a tendency of reversal of baseline perfusion disturbance on MR imaging and was well correleating with the pre- and post-embolisation cerebral angiography.

CONVENTIONAL & DIFFUSION WEIGHTED MR

IMAGING :

1. : ISCHAEMIC EVENTS :

Ischemic events and perinidal venous thrombosis in conjunction with embolisation of intracerebral AVMs appear to be more frequent than previously understood. Neurointervention related

most ischemic episodes are asymptomatic or accompanied by transient symptoms and therefore not reported.

Because of their size and/or the concealing effect of extensive artifacts induced by the glue (*n*-BCA, Onyx), most small peripheral lesions and large perinidal ischemic lesions would have escaped detection by CT. DWI is known to be more sensitive to acute ischemia than CT and ordinary SE sequences.

The embolic agents (*n*-BCA and Onyx) caused virtually no artifacts on MR imaging and had signal intensities similar to that of fat on T1-weighted SE and T2-weighted turbo SE sequences.

Perinidal ischaemic lesions:

Ischaemic events were noted in in 4 out of 8 patients on postembolization MR study.

In two cases ischemic lesions were small and were located distally in the cortex and are may be due to diagnostic angiography. Data from recent DWI studies suggest that ischemic events occur in as many as 25% of patients during DSA (95).

In another 2 cases focal immediate perinidal restriction on DWI was noted suggestive of cytotoxic edema, which is most likely due to ischaemic infarct or rarely due to venous thrombosis. In both the

cases, nidal hyperintensity as well as draining vein thrombosis was noted after 2 days of glue (NBCA) embolization.

Perinidal ischaemic lesions were noted in two cases and it can be due to:

1. Adverse migration of glue/extravasation or reflux of alcohol.
2. Progressive thrombosis with subsequent ischemia.
3. Occlusion of small perforators and/or arteries arising from perforators close to the nidus, thus supplying the nidus as well as the surrounding parenchyma.

Cronqvist et al (35), performed 50 endovascular procedures in 21 patients of AVMs and studied with perfusion MR before and after embolization. After 22 procedures, 43 new abnormalities were found on MR imaging. An intracerebral hematoma was seen in 4 patients. Minor vasogenic edema was observed around the sites of embolization of the AVM in 4 patients; Procedural adverse events caused 6 new MR findings on 5 occasions (4 patients). Thirty-five hyperintense spots with corresponding decrease of ADC were found on DWI after 18 procedures. Twenty-three spots (66%) were regarded as true ischemic lesions, 8 (22%) represented stagnation of blood/clots within veins, and 4 (12%) were of uncertain origin (ischemic lesion or intravenous

clot). 26% ischemic lesions were considered to be associated with diagnostic angiographies performed immediately before and after the embolization procedure. The authors found new MR imaging abnormalities evolving between Procedures were noted between treatments in 3 patients. The authors noted that 40% of the ischemic lesions were found in close proximity to the AVM nidus, perinidally. These lesions were generally large (>10 mm diameter) and consistently associated with the superselective injection of glue.

Venous Thrombosis and Related Hemorrhage:

In the present study, moderate perinidal vasogenic edema with focal asymptomatic bleed is noted only with use of absolute alcohol as an embolic agent. Two of the 3 patients, whom absolute alcohol was solely used as the only embolic agent, show moderate perinidal vasogenic edema. Vasogenic edema may be caused by venous congestion or venous thrombosis. Delayed venous thrombosis is a potential complication to endovascular treatment of AVMs.

The probable explanation is alcohol reflux into the proximal branches or the feeder might be supplying the normal territory (Enpassent feeder), or could be due to progressive nidal and draining vein thrombosis venous thrombosis rarely can cause cytotoxic edema instead of vasogenic edema. In two cases multiple focal

hyperintensities were noted within the nidus in DWI suggestive of intranidal thrombosis.

Venous clots, whether acute or subacute, may show DWI (and ADC) signal intensity patterns that were barely distinguishable from those seen with ischemic lesions.

Correlating the DWI findings with the corresponding morphologic MR imaging (subacute clots are hyperintense on T1-weighted images) and DSA might suggest the location of these lesions. Clots were generally thinner and more tubular in appearance than ischemic lesions. The process of "normalization" differed significantly between the true ischemic lesions and the clots. The ischemic lesions seen on DWI consistently disappeared between examinations, whereas the diffusion pattern (high signal intensity on DWI and low on ADC maps) tended to remain unchanged for prolonged periods of time when representing a hematoma or clot in a draining vein. "Normalization" occurred especially late in clots and remained unchanged for several months in some veins.

In the study by **Cronquist et al** (35), venous clotting was recognized intra- or perinidally on posttreatment MR imaging on 8 occasions. Vasogenic edema appeared around the nidus on MR imaging immediately after treatment in 4 patients and between

treatments in one patient with a progressive venous occlusion . Perfusion was decreased in the area of edema. In all 5 patients, a minimal volume of glue had entered into the draining veins of the AVM. Two patients with venous thrombosis progressing between the treatments showed impaired perfusion. In the patient with extensive vasogenic edema, perfusion was decreased (both rCBF and rCBV). Following treatment, however, the edema was almost totally reabsorbed and the perfusion abnormality reversed.

Vasogenic edema may be caused by venous congestion with or without venous thrombosis. Possibly, the edema was caused by locally increased perfusion pressure, induced by the venous outflow obstruction that was eliminated instantly with the reduction of the AVM shunt.

PERFUSION MR STUDY :

The study provided a noninvasive and in vivo model with high spatial and temporal contrast by employing DSC-MR imaging to demonstrate the increased focal rCBV and rCBF in AVMs. In the current study, hemisphere with AVM contains higher flow and volume as revealed by significantly higher rCBV and rCBF ratios. The results supported the prevailing hypotheses that perinidal arteries become dilated to adapt to the low-resistance and high-flow transnidial shunts that occur in AVMs.

The increases in rCBF and rCBV were similar and correlated more to the distribution of the draining veins than to the feeding arteries. Whenever the cortical and draining veins were multiple and diverging toward a long extension of the draining dural sinus, the area of increased perfusion tended to be larger than the size of the AVM (ie, overestimated). Hence, it was almost impossible to evaluate the perfusion pattern in the parenchyma located in close proximity to the nidus or between the draining veins. To make an exact definition of the nidus on the PI proved to be extremely difficult, in part because the perfusion disturbances almost invariably exceeded the size of the AVM.

Image quality was reduced in regions with susceptibility artifacts at bone-air interfaces; geometric distortion and signal voids were noted in case 7 with left basifrontal AVM.

At places rCBV values were 0.

All of the cerebral AVMs show hemodynamic alterations adjacent to the nidus (immediate perinidal region). The most common hemodynamic alteration in immediate perinidal region was decrease perfusion (Low rCBV and rCBF), occurring in nearly 70% of the cases (9/13 patients). In 3 patients, immediate perfusion (rCBV and rCBF) was high, whereas one patient had increase perfusion in

immediate perinidal region and decrease in posterior perinidal region.

rMTT did not reveal any obvious hemodynamic disturbances in immediate perinidal region in 7 patients (68%).

In 4 patients, rCBV, r CBF and r MTT all were decreased in immediate perinidal region; which could be due to steal effect rather than due to permanent changes like gliosis in the perinidal brain tissue.

On the other hand, 38 % of the patients (5 out of 13 patients) show no perfusion abnormality in remote brain parenchyma, all of them had smaller AVM nidus (< 3cm) with only mild to moderate arterio-venous shunting. Three patients had low perfusion and 4 patients had increased perfusion in remote areas.

These types of perfusion disturbance suggest that an AVM may steal blood from immediate surrounding and remote areas, from the contralateral hemisphere via communicating arteries, or even from the other branches of the carotid artery extracranially (35).

Following six patterns of perfusion abnormality noted in the hemisphere ipsilateral to the AVM:

- ❖ **Pattern I:** Low perfusion in immediate & normal perfusion in remote perinidal regions.
- ❖ **Pattern II:** Low perfusion in immediate as well as in remote perinidal region.
- ❖ **Pattern III:** Low perfusion in immediate perinidal region & high perfusion in remote areas.
- ❖ **Pattern IV:** High perfusion in immediate perinidal region with high perfusion in remote region.
- ❖ **Pattern V:** High perfusion in immediate perinidal region with normal perfusion in remote region.
- ❖ **Pattern VI:** Heterogeneous or mixed immediate perinidal / remote perfusion.

Most common pattern of perfusion disturbance noted in present study is low perfusion in immediate perinidal region & normal perfusion in remote perinidal regions (Type I) occurring in 30% (4/13) of patients. This is followed by type II perfusion disturbance occurring in 23% (3/13) of patients. The least common type of

perfusion disturbance was type IV and V, where immediate perinidal region show high perfusion and remote brain parenchyma revealed normal or low perfusion; both of these pattern occurs in one patient each (7%).

Two AVMs involved more than one type of perfusion disturbance. This was similar to the so-called patchy hypoperfusion in brain tissue surrounding AVMs that was previously reported (34, 36-38).

The baseline (pre-embolisation) perfusion patterns are in contradiction to the study recently reported by Wan-Yuo Guo et al (34); they studied 19 AVM patients with DSC- MR perfusion imaging, before and after radiosurgery. They observed three pattern of perfusion disturbances in their patients and classified it into three types. In type 1, cerebral blood flow (CBF) and volume (CBV) increase in both immediate and remote perinidal regions. In type 2, the immediate perinidal rCBV and rCBF ratios increased and the remote perinidal regions decreased. In type 3, rCBV and rCBF ratios of both immediate and remote perinidal regions decreased. Four AVMs involved more than one type of perfusion disturbance in their study. They have reported high perfusion in the immediate perinidal region and decreased remote perinidal region as the most common

pattern, unlike present study where the most common pattern was decreased perfusion in immediate perinidal region and normal unaffected remote perfusion.

The decreased immediate perinidal perfusion could be due to steal from nidus arterio-venous shunting or could be due to perinidal gliosis. Both are possible explanation for decreased perfusion in the perinidal region in the present patients as in some cases this perinidal low perfusion has reversed and in others, it remain more or less same.

The AVM nidus as well as the perinidal brain parenchyma reveals a continuous hemodynamic changes after embolisation. Perfusion defect within the embolised portion of the nidus was seen in most patients after embolization. The most constant effect was on the nidus perfusion and least effect was observed in ipsilateral and contralateral remote brain parenchyma. rMTT was the most constant parameters before and after embolisation.

No major disturbances of rCBF/rCBV or MTT were found in the parenchyma distally or contralaterally to the AVM before or immediately after treatment.

Postembolization decrease of rCBV and rCBF close to the AVM was seen in 68% of the cases, mostly following total or near-total AVM occlusion and reduction of the shunt. Five patients show

decreased immediate perinidal rCBV that increased to 1 after embolization in 3 patients. Similarly, in 6 patients immediate perinidal rMTT was reduced before embolization and it increased to 1 in three patients after embolization.

Reduction in postembolisation nidial rCBV and rCBF ratios to 1.0 and elevation of nidial rMTT ratio to 1.0 indicated declining transnidial shunts. The trend of changes in perinidal ratios to 1.0 after embolisation indicated reversal of the steal.

Reversal of rCBV and rCBF ratios to less than 1.0 was indicative of impaired local perfusion due to vasogenic edema.

This findings are well consistent with those of previously reported by **Wan-Yuo Guo** et al (34), who studied 19 AVM patients before and after radiotherapy with MR perfusion imaging. They demonstrated that the nidial rCBV and rCBF ratios gradually decreased to 1.0 after radiosurgery, whereas rMTT ratios gradually increased to 1.0; anterior and posterior immediate perinidal rCBV and rCBF ratios decreased, indicating reversal of steal toward normal perfusion. AVM nidial volumes were observed to be decreasing after radiotherapy on follow up imaging.

In the current study, it was observed that the rMTT ratios were least sensitive compared with rCBV and rCBF ratios in demonstrating

AVM perfusion. This is explained by the fact that rMTT is derived from rCBV and rCBF. These steal and adaptation mechanisms may result in different patterns of perfusion disturbance.

In well concordance with our study, **Cronquist et al.** (35), also had reported abnormal perfusion in 85% of their patients, with increased rCBF and rCBV at the site of the AVM before embolisation. No major differences were noted between rCBF and rCBV patterns in other areas of the ipsilateral parenchyma versus the contralateral hemisphere, with 2 exceptions. MTT did not reveal any obvious hemodynamic disturbances in 90% of MR imagings. After embolisation, immediate decrease of rCBV and rCBF close to the AVM was seen in only 48% of the procedures, mostly following total or near-total AVM occlusion and reduction of the shunt. In another 48%, no immediate change was noted. This is not surprising, in light of the partial reduction of the nidus and the regular patency of the veins without instant adaptation (lumen reduction) to the reduced flow.

All patterns of perfusion disturbance was noted in the brain parenchyma adjacent to the AVM and no generalization can be made, however a preferential pattern of perfusion disturbance was noted in the present study; The most common hemodynamic

disturbance noted was low perfusion in immediate perinidal region and normal perfusion in remote brain parenchyma. Both the short- and long-term postoperative regional cerebral blood flow studies indicate that the hypoperfusion does not resolve immediately with removal of the AVM and may be, at least in part, permanent. This could be due to permanent damage to the brain tissue rather than functional steal. Zones of ischaemic neuronal changes with glial proliferation have commonly been observed during neuropathological examinations of brain tissue adjacent to cerebral AVMs as well as hemorrhagic cysts with hemosiderin deposits. Pathological changes of this nature probably account for regions of cerebral atrophy and hypodensity frequently reported adjacent to the AVMs on CT scanning.

In the present study cerebral steal was demonstrated in immediate and remote perinidal region which was reversed to normal suggesting a dynamic changes in the cerebral blood flow with treatment. The present perfusion MR study can provide a pathophysiological basis of normal perfusion pressure breakthrough (NPPB) and pre-embolisation MR perfusion study may predict the patients with certain pattern of perfusion disturbance which can predict the clinical outcome after embolisation.

Conclusion

CONCLUSION

1. MR Perfusion imaging provides a non invasive method to understand the hemodynamics of AVMs and adjacent brain parenchyma. It provides an simple and fast objective method to demonstrate intracerebral steal in the adjacent brain parenchyma, therefore, can be added as imaging protocol to the routine structural evaluation by conventional imaging.
2. DWI and PWI may be useful for the evaluation of treatment results and complications of endovascular treatment as well as in follow up for demonstrating the progressive nidal thrombosis and occlusion.
3. Initial high transnidal flow and perinidal steal were noninvasively and objectively demonstrated in brain AVM. After embolization reduction of transnidal perfusion (rCBV & rCBF) and increase of nidal rMTT towards 1 suggest reduction of arteriovenous shunting and increase in perfusion in previously hypoperfused areas were suggestive of reversal of cerebral steal with improved circulation in remote areas.
4. Clinically, the effects of embolization on AVM and adjacent hemodynamics may reflect the therapeutic effects of treatment on brain perfusion and contribute significantly to understanding of transient and permanent neurologic deficits following AVM treatment.

References

REFERENCES

1. Karhunen PJ, Pentilla A, Erkinjuntti T. Arteriovenous malformations of the brain: imaging by postmortem angiography. *Forensic Sci Int* 1990;48:9–19
2. Jellinger K. Vascular malformation of the central nervous system: a morphological overview. *Neurosurg Rev* 1986;9: 177–216
3. Stapf C, Mast H, Sciacca, et al. The New York Island AVM study: design, study progress and initial results. *Stroke* 2003;34:e29–e33
4. Crawford PM, West CR, Chadwick DW, et al. Arteriovenous malformation of the brain: natural history in unoperated patients. *J Neurosurg Psychiatr* 1986;49:1–10
5. Ondra SL, Troupp H, George ED, et al. The natural history of symptomatic arteriovenous malformations of the brain: a 24 year follow-up assessment. *J Neurosurg* 1990;73:387–91
6. Hofmeister C, Stapf C, Hartmann A, et al. Demographic, morphological and clinical characteristics of 1289 patients with brain arteriovenous malformation. *Stroke* 2000;31:1307–10

7. Ostergaard L, Weisskoff RM, Chesler DA, Gyldensted C, Rosen BR. High resolution measurement of cerebral blood flow using intravascular tracer bolus passages: part I. mathematical approach and statistical analysis. *Magn Reson Med* 1996; 36 :715 –725
8. Meier P, Zierler KL. On the theory of the indicator-dilution method for measurement of blood flow and volume. *J Appl Physiol* 1954;6:731–744
9. Zierler KL. Theoretical basis of indicator-dilution methods for measuring flow and volume. *Circ Res* 1962;10:393–407
10. Ostergaard L, Weisskoff RM, Chesler DA, Gyldensted C, Rosen B. High resolution measurement of cerebral blood flow using intravascular tracer bolus passages. I: Mathematical approach and statistical analysis. *Magn Reson Med* 1996;36:715–725
11. Rempp KA, Brix G, Wenz F, Becker CR, Guckel F, Lorenz WJ. Quantification of regional cerebral blood flow and volume with dynamic susceptibility contrast-enhanced MR imaging. *Radiology* 1994;193:637–641
12. Rosen BR, Belliveau JW, Vevea JM, Brady TJ. Perfusion imaging with NMR contrast agents. *Magn Reson Med* 1990;14:249–265

13. Haggendal E, Ingvar DH, Lassen NA, et al. Pre- and postoperative measurements of regional cerebral blood flow in three cases of intracranial arteriovenous aneurysms. *J Neurosurgery* 1965;22: 1- 6
14. Lassen NA, Munck O. Cerebral blood flow in arteriovenous anomalies of the brain determined by the use of radioactive krypton 85. *Acta Psychiatr Scand* 1956;31:71-80
15. Menon D, Weir B. Evaluation of cerebral blood flow in AVM by Xe-133 inhalation method. *Can J Neurol Sci.* 1979;6:411 - 416
16. Feindel W, Yamamoto YL, Hodge CP. Red cerebral veins and the cerebral steal syndrome. Evidence from fluorescein angiography and microregional blood flow by radioisotope during excision of an angioma. *J Neurosurgery*, 1971;35:167-179
17. Homan RW, Devous MD, Sokely EM, Bonte FJ. Quantification of intracerebral steal in patients with AVM. *Arch Neurol* 1986;43:779-785
18. Marks MP, Donahue JO, Fabricant J I, Frankel KA, Phillips MH, Delapaz RL, Enzmann DR. CBF evaluation of AVM with stable xenon CT. *AJNR* 1988;9:1169-1175

19. Okabe T, Meyer J S, Okayasu H, Harper R, Rose J, Grossmann RG, Centeno R, Tachibana H, Lee Y. Xenon enhanced CT CBF measurements in cerebral AVMs before and after excision. *J Neurosurgery* 1983;59: 21-31
20. Hauper AM. Autoregulation of CBF: influence of the arterial blood pressure on the flow through the cerebral cortex. *JNNP* 1966;29:398-404
21. Murphy JP. Cerebrovascular disease. Chicago: Year Book Medical, 1954
22. Barnett GH, Little JR, Ebrahim ZY, et al. Cerebral circulation during AVM operation. *Neurosurgery* 1987;20:836-842
23. Yonas H, Good WF, et al. Clinical experience with the use of xenon-enhanced CT blood flow mapping in cerebral vascular disease. *Stroke* 1984;15:443-450
24. Tarr RW, Johnson DW, et al. Use of Acetazolamide-Challenge Xenon CT in the Assessment of CBF dynamics in patients with AVMs. *AJNR* 1990;11:441-448.
25. Nornes H, Gap A. Hemodynamic aspects of cerebral arteriovenous malformation. *J Neurosurgery* 1980;53:456-464

26. Mast H, Mohr JP, Osipov A, et al. 'Steal' is an unestablished mechanism for the clinical presentation of cerebral arteriovenous malformations. *Stroke* 1995;26:1215–1220
27. Young WL, Kader A, Ornstein E, et al. Cerebral hyperemia after arteriovenous malformation resection is related to "breakthrough" complications but not to feeding artery pressure. *Neurosurgery* 1996;38:1085–1095
28. Meyer B, Schaller C, Frenkel C, Ebeling B, Schramm J. Distributions of local oxygen saturation and its response to changes of mean arterial blood pressure in the cerebral cortex adjacent to arteriovenous malformations. *Stroke* 1999;30:2623–2630
29. Fogarty-Mack P, Pile-Spellman J, Hacein-Bey L, et al. Superselective intraarterial papaverine administration: effect on regional cerebral blood flow in patients with arteriovenous malformations. *J Neurosurg* 1996;85:395–402
30. Sekhon LHS, Morgan MK, Spence I. Normal perfusion pressure breakthrough: the role of capillaries. *J Neurosurg* 1997;86: 519–524
31. Kuschinsky W, Paulson OB. Capillary circulation in the brain. *Cerebrovasc Brain Metab Rev* 1992;4:261–286

32. Fink GR. Effects of cerebral angioma on perifocal and remote tissue: A multivariate PET study. *Stroke* 1992;23:1099-1105
33. Spetzler RF, Wilson CB, Weinstein P, et al: Normal perfusion pressure breakthrough theory. *Clin Neurosurgery* 1978;25:651-672.
34. Guo WY, Wu YT, Wu HM, Chung WY et al. Towards Normal Pressure After Radiosurgery : Perfusion MRI with Independent Component Analysis of brain AVMs. *AJNR* 2004;25:1636-1664
35. M. Cronqvist, R. Wirestam, B. Ramgren, L. Brandt, B. Romner, O. Nilsson, H. Säveland, S. Holtås and E.-M. Larsson. Endovascular Treatment of Intracerebral Arteriovenous Malformations: Procedural Safety, Complications, and Results Evaluated by MR Imaging, Including Diffusion and Perfusion Imaging. *American Journal of Neuroradiology* 27:162-176, 2006
36. Pertuiset B, Ancri D, Clergue F. Preoperative evaluation of hemodynamic factors in cerebral AVMs for selection of a radical surgery tactic with special reference to vascular autoregulation disorders. *Neurol Res* 4:209-233, 1982

37. Yamada S, Cojocararu T. Arteriovascular Malformation In. : Wood JH (ed) CBF. Physiologic and clinical aspects. McGraw Hill, New York, pp 580-590.
38. Hassler W, Steinmetz H. Cerebral Hemodynamics in angioma patients: An intraoperative study. J Neurosurgery 67: 822-831, 1987.
39. Deruty R, Pelissou Guyotat I, Mottolese C, Amat D, et al. Therapeutic risk in multidisciplinary approach of cerebral AVMs. Neurochirurgie 42 : 35-43, 1996.
40. Folkow B, Gurevich M, Hallbach M, Lundgreen Y, et al. The hemodynamic consequence of regional hypotension in spontaneously hypertensive & normotensive rats. Acta Physiol Scand 83 : 532-541, 1977.
41. Norlen G. Arteriovenous aneurysm of brain: Report of 10 cases of total removal of the lesion. J Neurosurgery 6 : 475, 1949.
42. Mohr J P . Neurological manifestations and factors related to therapeutic decisions. In.: Wilson CB, Stein BM (eds) Intracranial AVMs. Williams and Wilkins; Baltimore, pp 12-23.
43. Luessenhop AS, Rossa L. Cerebral AVMs: Indication for and results of surgery, and the role of intravascular techniques. J Neurosurgery 60: 14-22, 1984.

44. Feindel W, Perot P. Red cerebral veins : A report on arteriovenous shunts in tumors and cerebral scars. J Neurosurgery 22: 315-325, 1965.
45. Al-Rodhen NRF, Sundt TM Jr, Piepgras DJ, et al : Occlusive hyperemia : A theory for the hemodynamic complications following resection of intracerebral AVMs. J Neurosurgery 78: 167-175, 1993.
46. Chin LS, Raffel C, Gonazalez-Gomez I, Giannoth SL, Mc Comb JG. Diffuse AVM :A clinical, radiological an pathological description. Neurosurgery 31:863-867, 1992.
47. Jellinger K. Vascular malformation of the ventral nervous system: A morphological overview. Neurosurgery Rev 9 : 177-216, 1986.
48. Mandybur TI, Nazek M. Cerebral AVMs : A detailed morphological and immunohistochemical study using actin. Arch Pathol Lab Med 114: 970-973, 1990.
49. McCormic WF. The pathology of vascular arteriovascular malformation. J Neurosurgery 24 : 807-816, 1996.
50. Rustam Al-Shahi and Charles Warlow.A. Systematic review of the frequency and prognosis of arteriovenous malformations of the brain in adults Brain Vol. 124, No. 10, 1900-1926, October 2001.

51. Miyachi S, Negoro M, Handa T, Sugita K. Contribution of meningeal arteries to cerebral arteriovenous malformations. *Neuroradiology* 1993; 35: 205–9.
52. Pile-Spellman JM, Baker KF, Liszczak TM, Sandrew BB, Oot RF, Debrun G, et al. High-flow angiopathy: cerebral blood vessel changes in experimental chronic arteriovenous fistula. *AJNR Am J Neuroradiol* 1986; 7: 811–5
53. Montanera W, Marotta TR, terBrugge KG, Lasjaunias P, Willinsky R, Wallace MC. Cerebral arteriovenous malformations associated with moyamoya phenomenon. *AJNR Am J Neuroradiol* 1990; 11: 1153–6
54. Viñuela F, Nombela L, Roach MR, Fox AJ, Pelz DM. Stenotic and occlusive disease of the venous drainage system of deep brain AVM's. *J Neurosurg* 1985; 63: 180–4.
55. Michelson WJ. Natural history and pathophysiology of arteriovenous alformations. *Clin Neurosurg.* 1978;26:307–313.
56. McCormick WF, Schochet SS Jr. *Atlas of Cerebrovascular Disease*. Philadelphia, Pa: WB Saunders Co; 1976:422.
57. Hofmeister C, Stapf C, Hartmann A, et al. Demographic, morphological, and clinical characteristics of 1289 patients with brain AVM. *Stroke* 31:1307, 2000.

58. Christopher S. O, Chair; Philip E. Stieg, Issam A et al. Recommendations for the Management of Intracranial Arteriovenous Malformations: A Statement for Healthcare Professionals From a Special Writing Group of the Stroke Council, American Stroke Association . *Stroke*. 2001;32:1458.
59. Hartmann A, Mast H, Mohr JP, et al. Morbidity of intracranial hemorrhage in patients with cerebral arteriovenous malformation. *Stroke*. 1998;29:931–934
60. Mast H, Mohr JP, Osipov A, et al. "Steal" is an unestablished mechanism for the clinical presentation of cerebral arteriovenous malformations. *Stroke*. 1995;26:1215–1220
61. Miyasaka Y, Yada K, Ohwada T, et al. An analysis of the venous drainage system as a factor in hemorrhage from arteriovenous malformations. *J Neurosurg*. 1992;76:239–243.
62. Brown RD, Wiebers DO, Forbes G, et al. The natural history of unruptured intracranial arteriovenous malformations. *J Neurosurg*. 1988;68:352–357
63. Wilkins RH. Natural history of intracranial vascular malformations: a review. *Neurosurgery*. 1985;16:421–430.
64. Mast H, Mohr JP, Osipov A, et al. "Steal" is an unestablished mechanism for the clinical presentation of cerebral arteriovenous malformations. *Stroke*. 1995;26:1215–1220.

65. Furlan AJ, Whisnant JP, Elveback LR. The decreasing incidence of primary intracerebral hemorrhage: a population study. *Ann Neurol.* 1979;5:367-373.
66. Graf CJ, Perret GE, Torner JC. Bleeding from cerebral arteriovenous malformations as part of their natural history. *J Neurosurg.* 1983;58:331-337.
67. Fults D, Kelly DL. Natural history of arteriovenous malformations of the brain: a clinical study. *Neurosurgery.* 1984;15:658-662.
68. Crawford PM, West CR, Chadwick DW, et al. Arteriovenous malformations of the brain: the natural history in unoperated patients. *J Neurol Neurosurg Psychiatry.* 1986;49:1-10.
69. Forster DM, Steiner L, Hakanson S. Arteriovenous malformations of the brain: a long-term clinical study. *J Neurosurg.* 1972;37:562-570.
70. Ondra SL, Troupp H, George ED, et al. The natural history of symptomatic arteriovenous malformations of the brain: a 24 year follow-up assessment. *J Neurosurg.* 1990;73:387-39.
71. Graf CJ, Perret GE, Torner JC. Bleeding from cerebral arteriovenous malformations as part of their natural history. *J Neurosurg.* 1983;58:331-337.

72. Kondziolka D, McLaughlin MR, Kestle JR. Simple risk predictions for arteriovenous malformation hemorrhage. *Neurosurgery*. 1995;37:851–855.
73. Brown RD. Simple risk predictions for arteriovenous malformation hemorrhage. *Neurosurgery*. 2000;46:1024. Letter.
74. Forster DM, Steiner L, Hakanson S. Arteriovenous malformations of the brain: a long-term clinical study. *J Neurosurg*. 1972;37:562–570
75. Frizzel RT, Fisher WS: Cure, morbidity, and mortality associated with embolization of brain arteriovenous malformations: a review of 1246 patients in 32 series over a 35-year period. *Neurosurgery* 37:1031–1040, 1995
76. Valavanis A, Yasargil MG: The endovascular treatment of brain arteriovenous malformations. *Adv Tech Stand Neurosurg* 24:131–214, 1998
77. Yu SCH, Chan MSY, Lam JMK, Tam PHT, Poon WS: Complete obliteration of intracranial arteriovenous malformation with endovascular cyanoacrylate embolization: initial success and rate of permanent cure. *AJNR Am J Neuroradiol* 25:1139–1143, 2004

78. Vinuela F, Dion JE, Duckwiler G, et al. Combined endovascular embolisation and surgery in the management of cerebral arteriovenous malformations: experience with 101 cases. *J Neurosurg.* 1991;75:856–864.
79. Cromwell LD, Harris AB. Treatment of cerebral arteriovenous malformations: combined neurosurgical and neuroradiologic approach. *AJNR Am J Neuroradiol.* 1983;4:366–368.
80. Yakes WF, Luethke JM, Parker SH, et al. Ethanol embolization of vascular malformations. *Radiographics.* 1990;10:787–796
81. Purdy PD, Samson D, Batjer HH, et al. Preoperative embolization of cerebral arteriovenous malformations with polyvinyl alcohol particles: experience in 51 adults. *AJNR Am J Neuroradiol.* 1990;11:501–510.
82. Spetzler RF, Martin NA, Carter LP, et al. Surgical management of large AVM's by staged embolization and operative excision. *J Neurosurg.* 1987;67:17–28.
83. Ogilvy CS. Radiation therapy for arteriovenous malformations: a review. *Neurosurgery.* 1990;26:725–735.
84. Lunsford LD, Kondziolka D, Flickinger JC, et al. Stereotactic radiosurgery for arteriovenous malformations of the brain. *J Neurosurg.* 1991;75:512–524.

85. Steiner L, Lindquist C, Adler JR, et al. Clinical outcome of radiosurgery for cerebral arteriovenous malformations. *J Neurosurg.* 1992;77:1-8.
86. Dawson RC III, Tarr RW, Hecht ST, et al. Treatment of arteriovenous malformations of the brain with combined embolization and stereotactic radiosurgery: results after 1 and 2 years. *AJNR Am J Neuroradiol.* 1990;11:857-864.
87. Dion JE, Mathis JM. Cranial arteriovenous malformations: the role of embolization and stereotactic surgery. *Neurosurg Clin N Am.* 1994;5:459-474.
88. Gobin YP, Laurent A, Merienne L, et al. Treatment of brain arteriovenous malformations by embolization and radiosurgery. *J Neurosurg.* 1996;85:19-28.
89. Colombo F, Pozza F, Chiarego G, et al. Linear accelerator radiosurgery of cerebral arteriovenous malformations: an update. *Neurosurgery.* 1994;34:14-20; discussion 20-21.
90. Han PP, Ponce FA, Spetzler RF: Intention-to-treat analysis of Spetzler-Martin Grades IV and V arteriovenous malformations:natural history and treatment paradigm. *J Neurosurg* 98:3-7,2003

91. Kwon O, Han DH, Han MH, Chung YS: Palliatively treated cerebral arteriovenous malformations: follow-up results. *J Clin Neurosci* 7:69–72, 2000
92. Berenstein A, Lasjaunias P. *Surgical Neuroangiography*. Vol 4. New York, NY: Springer-Verlag; 1987.
93. Fox AJ, Girvin JP, Vinuela F, et al. Rolandic arteriovenous malformations: improvement in limb function by IBC embolization. *AJNR Am J Neuroradiol*. 1985;6:575–582.
94. Vinuela FV, Debrun GM, Fox AJ, et al. Dominant-hemisphere arteriovenous malformations: therapeutic embolization with isobutyl-2-cyanoacrylate. *AJNR Am J Neuroradiol*. 1983;4:959–966.
95. Bendszus M, Koltzenburg M, Burger R, et al. Silent embolism in diagnostic cerebral angiography and neurointerventional procedures : a prospective study. *Lancet* 1999;354:1594-97
96. Spetzler RF, Martin NA. A proposed grading system for arteriovenous malformations. *J Neurosurg*. 1986;65:476–483.
97. Picard L, Costa EDA, Anxionnat R, et al . Acute spontaneous hemorrhage after embolization of cerebral AVMs with n-BCA. *J Neuroradiology* 28 :147-165, 2001.

98. Fournier D, TerBrugge KG, Willinsky R, et al. Endovascular treatment of intracerebral arteriovenous malformations: experience in 49 cases. *J Neurosurg.* 1991;75:228–233.
99. Wallace RC, Flom RA, Khayata MH, et al. The safety and effectiveness of brain arteriovenous malformation embolization using acrylic and particles: the experiences of a single institution. *Neurosurgery.* 1995;37:606–615; discussion 615–618.

APPENDIX I

MATERIALS		MANUFACTURERS
1	7F Short Sheath (11cm)	Avanti + Cordis corporation, Miami FL 33102-5700, USA
2	7F Brite tip long sheath (55cm)	Cordis corporation, Miami FL 33102-5700, USA
3	6F Vistabrite tip guiding Catheter (55cm)	Cordis Corporation P. O. Box 025700 Miami, FL 33102-5700, USA
4	5F Angiographic Catheter (Infiniti)	Cordis Europa. N.V Oosteinde 8, NL 9301 LJ Roden, Netherlands
5	5F Vertebral Glide	Terumo Corporation, Tokyo, 151-0072, Japan
6	5F Mulipurpose	Terumo Corporation, Tokyo, 151-0072, Japan
7	5F SIM 2	Cordis Corporation, P.O Box 025700 Miami, FL 33102-5700, USA
8	7F Launcher Guiding Catheter	Medtronic, Inc Minneapolis, MH USA – 55432
9	Medtronic PTFE guidewire, J tip 0.035	Medtronic vascular Danverse, MA-0192 31, 1-800-225-0898 USA

	MATERIALS	MANUFACTURERS
10	Angled Terumo Guidewire 0.035''	Terumo Corporation, Tokyo 151-0072, Japan
11	Agility 10	Cordis Neurovascular, Inc. Miami, FL 33102-5700, USA
12	Transend 0.010''	8600 NW 41 st Street, Miami, FL 33166-6202, USA
13	Elite 1.5 or 1.8 F (S, L, XL)	Business and Technology park, Model Farm Road, Cork, Ireland
14	Magic 1.2F M	- 10, rue Croix Vigneron 95160 Montmorency, France.
15	Nectacryl (n-Butyl Cyanoacrylate)	Nectar Laboratories limited PLOT # 54A and 54B Anrich Industrial estate Bollalram, Medak AP-502 325
16	Lipidol Ultra fluid	Guerbet BP 50400 F-95443- Roissy CDG Cedex- 16 rue J. Chaptal F 93600- Aulnay-Sous-Bois France
17	Onyx 18	Microtherapeutics, Inc. Irvine, CA 92618 USA
18	MTI Ultraflow Micro-catheter	Micro therapeutics, Inc. Irvine, CA – 92618, USA

APPENDIX II

ABBREVIATIONS :

1. ACA : Anterior cerebral artery
2. Acom : Anterior communicating artery
3. ADC : Apperent diffusion coefficient
4. APEH : Acute postemolizatrion Hemorrhage
5. APTT: Activated plasmin thromboplastin time
6. AVM : Arteriovenous malformation
7. AVF : Arteriovenous fistula
8. CBF : Cerebral blood flow
9. CBV : Cerebral blood volume
10. CMRGlc : Cerebral metabolic rate of glucose
11. CMRO2 : Cerebral metabolic rate of oxygen
12. CT : Computed Tomography
13. CMR : Cerebral metabolic rate
14. DAVF : Dural arteriovenous malformation

15. DSA : Digital subtraction angiogram
16. DWI : Diffusion weighted imaging
17. EPI : Echo planner imaging
18. FOV: Field of view
19. GEF : Glucose extraction fraction
20. IPN : Immediate perinidal
21. LOC : Loss of consiousness
22. MCA: Middle cerebral artery
23. MR : Magnetic resonance
24. MTT: Mean transient time
25. N : Nidal
26. NEX : Number of Excitation
27. NPPB : Normal Perfusion Presurre Breakthrough
28. NTG : Nitrotriglycerine
29. OEF : Oxygen extraction fraction
30. rCBF : Relative Cerebral blood flow

31. rCBV: Relative Cerebral blood volume
32. rMTT: Relative Mean transient time
33. R : Remote
34. ROI : Region of interest
35. Kr-85 : Krypton-85
36. PET : Positron emission tomograph
37. SPECT : Single Photon Emission Computed
Tomogram
38. TR : Time of Relaxation
39. TE : Time of Echo
40. Xe-133 : Xenon-133

